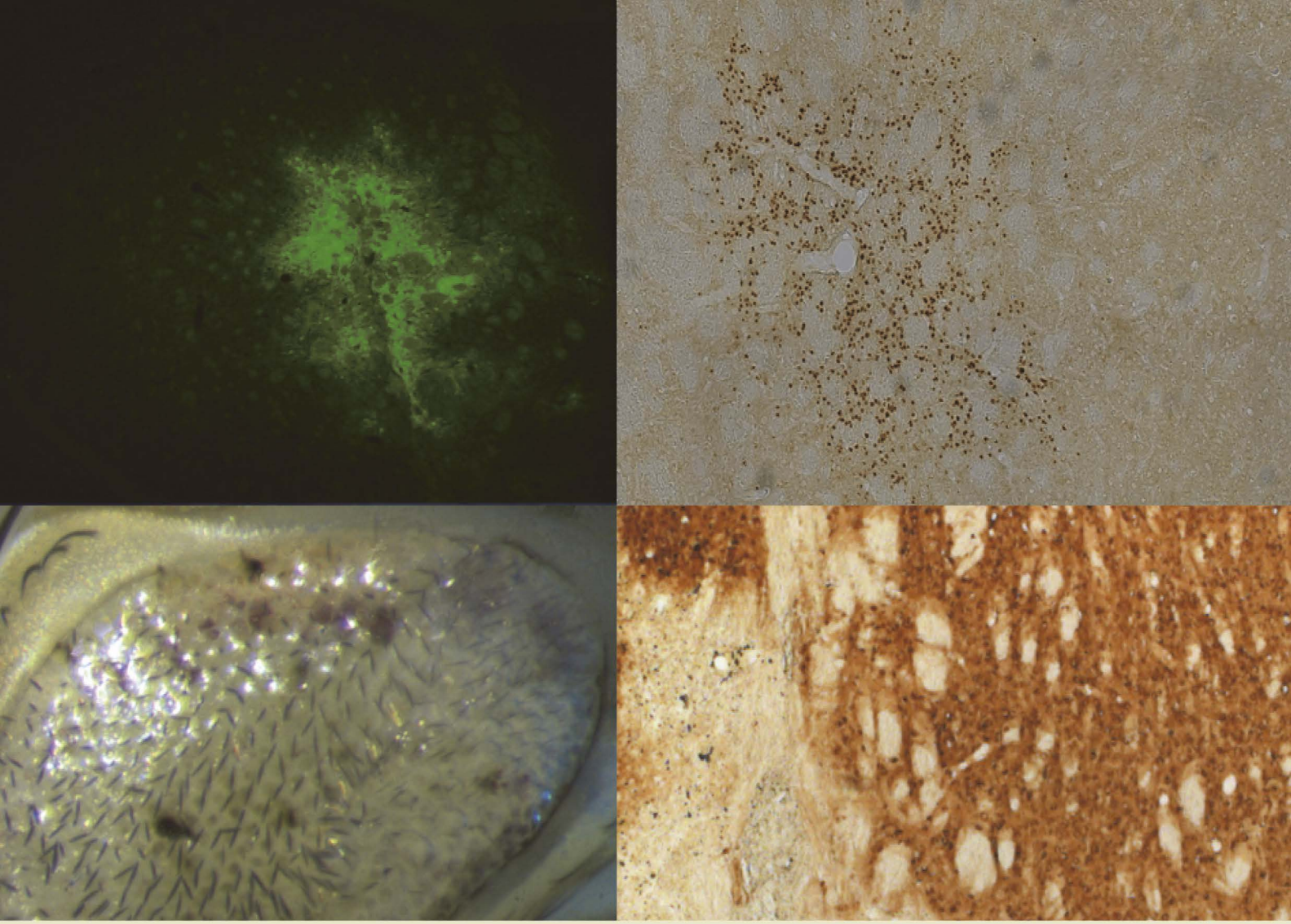

Udaya Geetha Vijayakumar

ROLE OF MICRORNA DEREGULATION IN THE PATHOGENESIS OF MACHADO-JOSEPH DISEASE

Tese de doutoramento em Biologia Experimental e Biomedicina, ramo de Neurociências e Doença,
orientada pelo Professor Doutor Luís Pereira de Almeida
e apresentada ao Instituto de Investigação Interdisciplinar da Universidade de Coimbra.

Setembro 2016

· U C ·

UNIVERSIDADE DE COIMBRA

Role of microRNA deregulation in the pathogenesis of Machado-Joseph disease

Udaya Geetha Vijayakumar

Thesis submitted to the Institute for Interdisciplinary Research of the University of Coimbra to apply for the degree of Doctor in Philosophy in the area of Experimental Biology and Biomedicine, specialization in Neurosciences and Disease

Tese submetida ao Instituto de Investigação Interdisciplinar da Universidade de Coimbra para obtenção do grau de doutor na área de Biologia Experimental e Biomedicina, especialização em Neurociências e Doença

September 2016

UNIVERSIDADE DE COIMBRA

Front cover:

Top left: Microscope images of the GFP expression in the striatal MJD mouse sections treated with miR-10b inhibitor. **Top right**: Ubiquitin-positive inclusions.

Bottom left: In-vivo image of the eye of a male MJD *D. melanogaster* crossed with a miR-control inhibitor. **Bottom right**: DARPP-32 staining.

Role of microRNA deregulation in the pathogenesis of Machado-Joseph disease

The research work presented in this thesis was performed at the Center for Neuroscience and Cell Biology of the University of Coimbra, Portugal, under the supervision of Prof. Luís Pereira de Almeida. Part of this work was performed at Paris Diderot University, France, under the supervision of Dr. Herve Tricoire.

O trabalho experimental apresentado nesta tese foi elaborado no Centro de Neurociências e Biologia Celular da Universidade de Coimbra, Portugal, sob a supervisão do Professor Luís Pereira de Almeida. Parte deste trabalho foi elaborado na Universidade Diderot de Paris, França, sob a supervisão do Doutor Herve Tricoire.

This work was supported by funds FEDER and the Competitive Factors Operational Program – COMPETE 2020 and by national funds through the Portuguese Foundation for Science and Technology UID/NEU/04539/2013, PTDC/SAU-NMC/116512/2010 and E-Rare4/0003/2012; by the Richard Chin and Lily Lock Machado Joseph Disease Research Fund; the National Ataxia Foundation and by the Marie Curie ITN –Treat PolyQ network. Udaya Geetha Vijayakumar was the recipient of a Marie Curie Action Initial Training network within the Seventh Framework Programme of the European Union, Research Executive Agency-FP7-PEOPLE-2010-ITN with the Grant Agreement Number 264508 TreatPolyQ.

Este trabalho foi financiado por fundos FEDER através do Programa Operacional Factores de Competitividade – COMPETE 2020, por fundos nacionais, através da Fundação Portuguesa para a Ciência e Tecnologia (FCT) no âmbito do projecto Estratégico UID/NEU/04539/2013, PTDC/SAU-NMC/116512/2010 e E-Rare4/0003/2012; pelo Richard Chin and Lily Lock Machado-Joseph Research Fund; pela National Ataxia Foundation e pela rede Marie Curie ITN –Treat PolyQ. Udaya Geetha Vijayakumar foi suportada por uma bolsa de doutoramento da rede de formação inicial Marie Curie no âmbito do Sétimo Programa Estrutural da União Europeia, Agência Executiva de Investigação - FP7-PEOPLE-2010-ITN com o acordo de subvenção número 264508 TreatPolyQ.


CNC
CENTER FOR NEUROSCIENCE AND CELL BIOLOGY
UNIVERSITY OF COIMBRA, PORTUGAL

IIIUC
INSTITUTO DE INVESTIGAÇÃO
INTERDISCIPLINAR
UNIVERSIDADE DE COIMBRA

MARIE CURIE
ACTIONS

QUALIFICAR É CRESCER.

QUADRO
DE REFERÊNCIA
ESTRATÉGICO
NACIONAL
PORTUGAL 2007.2013

GOVERNO DA REPÚBLICA
PORTUGUESA

E-Rare

COMPETE
2020

PORTUGAL
2020

UNIÃO EUROPEIA
Fundo Europeu
de Desenvolvimento Regional

FCT
Fundação para a Ciência e a Tecnologia
MINISTÉRIO DA CIÊNCIA, TECNOLOGIA E ENSINO SUPERIOR

Acknowledgements

I would like to express my sincere gratitude to my advisor Prof. Luis Pereira de Almeida for his patience, motivation and continuous support in my Ph.D research. His guidance and technical discussions helped me throughout my PhD research and thesis writing.

My sincere thanks to Dr. Herve Tricoire for giving me an opportunity to join his team for doing my secondment at Paris Diderot University, Paris and also for giving access to the laboratory and research facilities.

Besides my advisor, I would like to thank my colleagues Dr. Clevio Nobrega, Vitor Carmona, Janete Cunha Santos and Dr. Ligia Ferreira for all the help in doing this research work. Especially, I am indebted to Vitor Carmona for proof reading my Thesis. My friends have a big part in my last four and half years living in Portugal and took every care to make me feel at home. Very special thanks to my best friend Dr. Mariana who has been helping me from day one since I landed in Portugal. Also, I thank my close friends Sara Lopes, Patricia Rosado, Dina Pereira and Ana Cristina who made me feel very comfortable, sharing my personal things in life, enjoyed our evening walk back home, helping me with the Portuguese language, being great companions during the weekends in the lab and for accompanying me patiently for a whole day in the hospital and in the academic services.

I would like to thank my family members. Special thanks to my husband Dr. Murali krishnan Hari, for his constant care and affection, particularly in supporting me throughout my times of despair. Special thanks to my mother Nirmala Devi Vijayakumar for the moral support during my PhD and my brothers Vijayadharsan and Udaya Suray for being my pillars of support, particularly when my dad passed away.

I also want to thank my best friends Preethi, Kavitha and Priyanka for their encouragement. Special thanks to Preethi for always highlighting my strength, motivating me during the presentation and laboratory work in the last 4 years.

Finally I wish to dedicate my PhD to my father Vijayakumar Nagasamy, whom I miss

at many moments in my life, and he has always been a source of motivation and strength in my life. Although he is no longer with us, yet his eternal love and presence will be with me.

TABLE OF CONTENTS

Abbreviations

AAV	Adeno-associated virus
AD	Alzheimer’s disease
AGO	Argonaute
AKT3	AKT serine/threonine kinase 3
ATP	Adenosine Tri Phosphate
Aβ peptide	Amyloid beta peptide
BCL2L1	B-cell lymphoma-2 -like protein 1
BDNF	Brain-derived neurotrophic factor
CAG	Cytosine-adenine-guanine
cDNA	Complementary DNA
CELF2	CUGBP, Elav-like family member 2
CMV	Cytomegalovirus
CSF	Cerebrospinal fluid
DARPP-32	Dopamine- and cyclic AMP-regulated phosphoprotein of 32 kDa
DMEM	Dulbecco's Modified Eagle's medium
EAT3	Expanded ataxin 3
EXP5	Exportin 5
FLUC	Firefly luciferase
GBM	Glioblastoma
HD	Huntington’s disease

HEK293T	Human Embryonic Kidney 293T cells
HIP-1	Huntingtin interacting protein
HPRT	Hypoxanthinephophoribosyltransferase
HTT	Huntingtin
LTR	Long terminal repeat
MBNL1-3	Muscleblind like splicing regulator 1-3
miR	microRNA
miRNA	microRNA
MJD	Machado-Joseph disease
MRI	Magnetic resonance imaging
mRNA	Messenger RNA
Mut atxn3	Mutant ataxin-3
PEI	Polyethylenimine
PFA	Paraformaldehyde
PGC-1α	Peroxisome proliferator-activated receptor-gamma coactivator
PGK	Phosphoglycerate kinase 1
PolyQ	Polyglutamine
Pre-miRNAs	Precursor-microRNAs
pri-miRNAs	Primary-microRNAs
qRT-PCR	Quantitative real-time PCR
RISC	RNA-induced silencing complex

RLUC	Renilla luciferase
RNAi	RNA interference
RSRC1	Arginine/Serine-Rich Coiled-Coil 1
SART3	Squamous Cell Carcinoma Antigen Recognized By T-Cells 3
SBMA	Spinal and bulbar muscular atrophy
SCA1	Spinocerebellar ataxia type 1
SCA3	Spinocerebellar ataxia type 3
SCA7	Spinocerebellar ataxia type 7
s.e.m	Standard error of the means
Seq	Sequence
SNOR202	Small nucleolar RNA 202
SOX9	Sex determining Region of Y-Chromosome-homeobOX9
SP-1	Specificity protein-1
TFAP2C	Transcription Factor AP-2 Gamma
TTR	Transthyretin
TuD	Tough Decoy RNAs
UAS	Upstream activation sequence
UTR	Untranslated region
VEGFA	Vascular Endothelial Growth Factor alpha.
Wt	Wild type

Summary

Machado-Joseph disease (MJD) / Spinocerebellar ataxia type 3 (SCA3) is an autosomal dominant neurodegenerative disorder caused by the over-repetition of the CAG trinucleotide in the coding region of MJD1 gene which translates into an expanded polyglutamine tract within the affected protein ataxin-3. The toxic mutant ataxin-3 protein results in neuronal dysfunction and neurodegeneration in many brain regions. Until now, there is no therapy to prevent or delay the disease progression in MJD.

Recent evidence suggests transcriptional dysregulation may play a crucial role in MJD. Even though different transcripts have been shown to contribute to the pathogenesis of MJD, in recent years the evidence regarding dysregulation of microRNAs in other neurodegenerative disorders was suggestive of a potential role in MJD. Therefore, the aim of this project to study the role of microRNA dysregulation in MJD and to develop a microRNA based therapeutic strategy towards MJD.

In the first part of this project, described in chapter 2, using a miRNA microarray we identified numerous miRNAs that are differentially expressed in a lentiviral MJD mouse model. Notably, of all the differentially expressed miRs, miR-10b expression levels were robustly up-regulated. miR-10b expression levels were also evaluated in other MJD models and found to be significantly up-regulated in a transgenic mouse model of MJD and to show a trend towards upregulation in human post-mortem brain tissue. Our results suggest that microRNAs are dysregulated in MJD potentially contributing to the pathogenesis of the disease.

We next investigated whether a miR-10 inhibitor would modify disease progression in a small organism, *D. melanogaster*. MJD *D. melanogaster* treated with a miR-10b repressor resulted in the elongation of the life-span of MJD flies. Our results suggest miR-10b dysregulation could contribute to the pathogenesis of MJD and that re-establishing the normal levels of miR-10b may be protective in MJD.

In chapter 3, taking advantage of lentiviral based delivery of a miR-10b tough-decoy inhibitor, we re-established the normal levels of miR-10b in the striatal lentiviral MJD mouse model. Notably, our study identifies transthyretin as a target of miR-10b. Importantly, neuronal dysfunction, ubiquitin-positive inclusions and ataxin-3 positive inclusions were reduced upon miR-10b TuD inhibitor treatment in the striatal lentiviral MJD mouse model.

In summary, the present thesis provides evidence for a dysregulation of microRNAs in MJD, showing, for the first time, that miR-10b is upregulated in MJD. Moreover, we have validated a novel target gene for miR-10b, transthyretin, a gene previously implicated in other neurodegenerative diseases. Importantly, inhibition of mir-10b *in vivo* in a MJD mouse model was effective in ameliorating the disease manifestations. Altogether, we believe our study identifies a novel disease pathway in MJD and, at the same time, opens a new door for the development of a miR-based therapeutic strategy towards MJD.

Resumo

A doença de Machado-Joseph (DMJ), também conhecida como ataxia espinocerebelosa do tipo 3, é uma doença neurodegenerativa autossómica dominante causada por uma expansão no número de repetições do trinucleótido CAG na região codificante do gene MJD1, a qual é traduzida num trato poliglutamínico expandido na proteína ataxina-3. Esta proteína mutada resulta em disfunção neuronal e neurodegenerescência em diferentes regiões do cérebro. Até à data, não foi ainda desenvolvida nenhuma terapia capaz de bloquear ou atrasar a progressão da DMJ.

Estudos recentes sugerem que a desregulação transcripcional desempenha um papel importante na DMJ. Apesar de diferentes transcritos terem sido implicados na patogénese da DMJ, nos últimos anos a desregulação de microRNAs observada em outras doenças neurodegenerativas sugeriu um potencial papel destas moléculas na DMJ. Assim sendo, o objectivo deste projecto foi estudar o papel da desregulação de microRNAs na DMJ e simultaneamente desenvolver e avaliar o potencial de uma nova estratégia terapêutica baseada em microRNAs recorrendo para isso a um modelo lentiviral da DMJ em murganho.

Na primeira parte deste projecto, descrita no capítulo 2, recorrendo à tecnologia de microarray de miRNAs identificámos diversos miRNAs cuja expressão se encontra alterada num modelo lentiviral estriatal da DMJ em murganho. De entre o conjunto de miRNAs com expressão alterada, os níveis do miRNA miR-10b encontravam-se particularmente elevados. Para além disso, os níveis de expressão do miR-10b foram também avaliados em outros modelos de DMJ, verificando-se um aumento significativo nos níveis deste miRNA no cerebelo de murganhos transgénicos DMJ observando-se também uma tendência para aumento em tecido humano post-mortem de cerebelo de doentes DMJ.
Assim sendo, focámo-nos neste miRNA (miR-10b) para avaliar os efeitos terapêuticos da sua modulação no contexto da DMJ. Antes de avançar para um modelo em murganho da DMJ, começámos por avaliar o efeito de um inibidor do miR-10b num organismo mais simples, a *D. melanogaster*. A inibição do miR-10b

em *D. melanogaster*s DMJ resultou numa extensão do seu período de vida. Estes resultados sugerem assim que os miRNAs desregulados no modelo lentiviral de DMJ poderão contribuir para a patogénese da doença e que a reposição dos seus níveis, em *D. melanogaster*, leva a um aumento do seu tempo de vida implicando assim este miRNA no processo patológico da DMJ.

No capítulo 3, recorrendo à utilização de lentivírus codificantes para um inibidor do miR-10b baseado na tecologia *tough-decoy,* conseguimos re-estabelecer os níveis normais de miR-10b no estriado de um modelo lentiviral DMJ em murganho. Para além disso, identificámos a transtirretina como um alvo do miR-10b. A inibição do miR-10b no modelo lentiviral DMJ levou a uma redução do número de inclusões de positivas para ataxina-3 e ubiquitina ao mesmo tempo que levou a uma diminuição da disfunção neuronal associada a este modelo.

Em conclusão, esta tese reúne evidências que demonstram que a desregulação de miRNAs é uma componente da DMJ, identificando pela primeira vez o miRNA miR-10b como estando sobrexpresso no contexto da doença. Para além disso, foi validado um novo alvo deste miRNA, a transtirretina, um gene previamente associado ao desenvolvimento de outras doenças neurodegenerativas. Simultaneamente, a inibição do miR-10b, num modelo de murganho da DMJ levou a uma melhoria das manifestações da doença. Em suma, este estudo não só identificou uma nova via patógenica na DMJ como também gerou uma nova oportunidade para o desenvolvimento de uma estratégia terapêutica baseada em miRNAs para o tratamento da DMJ.

CHAPTER 1

General Introduction

1.1. Polyglutamine disorders (PolyQ) overview

Polyglutamine diseases are fatal neurological disorders. At least nine neurodegenerative disorders are caused due to the expansion of CAG repeats in the coding regions of the respective genes that translate into polyglutamine tracts within the affected proteins. With the exception of SBMA, which is an X-linked recessive disorder, all other polyglutamine disorders are autosomal dominant (Zoghbi 2000). Polyglutamine disorders include spinobulbar muscular atrophy (SBMA), Dentatorubral-pallidoluysian atrophy (DRPLA), Huntington disease (HD), and 6 spinocerebellar ataxias (SCAs 1, 2, 3, 6, 7, and 17) (van de Warrenburg et al. 2002).

1.1.1. Machado-Joseph disease/Spinocerebellar ataxia type 3 (MJD/SCA3)

Machado-Joseph disease (MJD) also known as Spinocerebellar ataxia type 3 (SCA3), was initially identified in the Northern American families of Azorean ancestry (Nakano *et al*. 1972). Few years later, Rosenberg and his colleagues identified another family from the Azorean ancestry with hereditary ataxia (Rosenberg *et al*. 1976). Finally, Portuguese researchers by studying 15 families from the Azores confirmed both the reports from Nakona and Rosenberg and proposed that all the reports corresponded to one same disorder: Machado-Joseph disease with variable phenotypic expression (Coutinho and Andrade 1978).

Many years later, Kawaguchi et al identified the CAG expansion in the novel gene and mapped it to chromosome 14q32.1 for Machado-Joseph (Takiyama *et al*. 1993, Kawaguchi *et al*. 1994). MJD is inherited in an autosomal dominant manner and is the most common spinocerebellar ataxia (Haberhausen *et al*. 1995, Ranum *et al*. 1995, Silveira *et al*. 1996). It has been identified as the 8th inherited disorder known to have an association with trinucleotide repeat expansion (Kawaguchi *et al*. 1994). MJD is caused by the abnormal expansion of CAG repeats in the coding region of MJD1 gene, which translates into a polyglutamine tract within ataxin-3 (Coutinho and Andrade 1978). The expanded allele carrying 61-87 CAG repeats and the normal allele with 12-44 CAG repeats was described (Maciel *et al*. 2001).

1.1.2. Clinical symptoms and prevalence

Symptoms develop in MJD patients from early to mid-age. Ataxia and Rigidity, pyramidal and extra pyramidal, dystonia and peripheral neuropathy, external ophthalmoplegia, bulging eyes, parkinsonism, facial and lingual fasciculation are the most common symptoms. MJD patients first experience unsteadiness while turning, followed by imbalance and finally suffer from ataxia ending up using the wheelchair (Lima and Coutinho 1980, D'Abreu *et al*. 2010).

The proportion of MJD/SCA3 among the dominantly inherited ataxia varies based on population. Even though MJD was initially identified in a Portuguese Azorean family, a few years later non-Portuguese families have also been reported with the same disorder. Regardless of the fact that MJD is the most common autosomal dominant ataxia in many populations followed by SCA1, SCA2, SCA6 and SCA7 (Figure 1.1), the overall occurrence of this dominantly inherited ataxia is 1-5: 100,000 (van de Warrenburg e*t al*. 2002, Ruano *et al*. 2014)

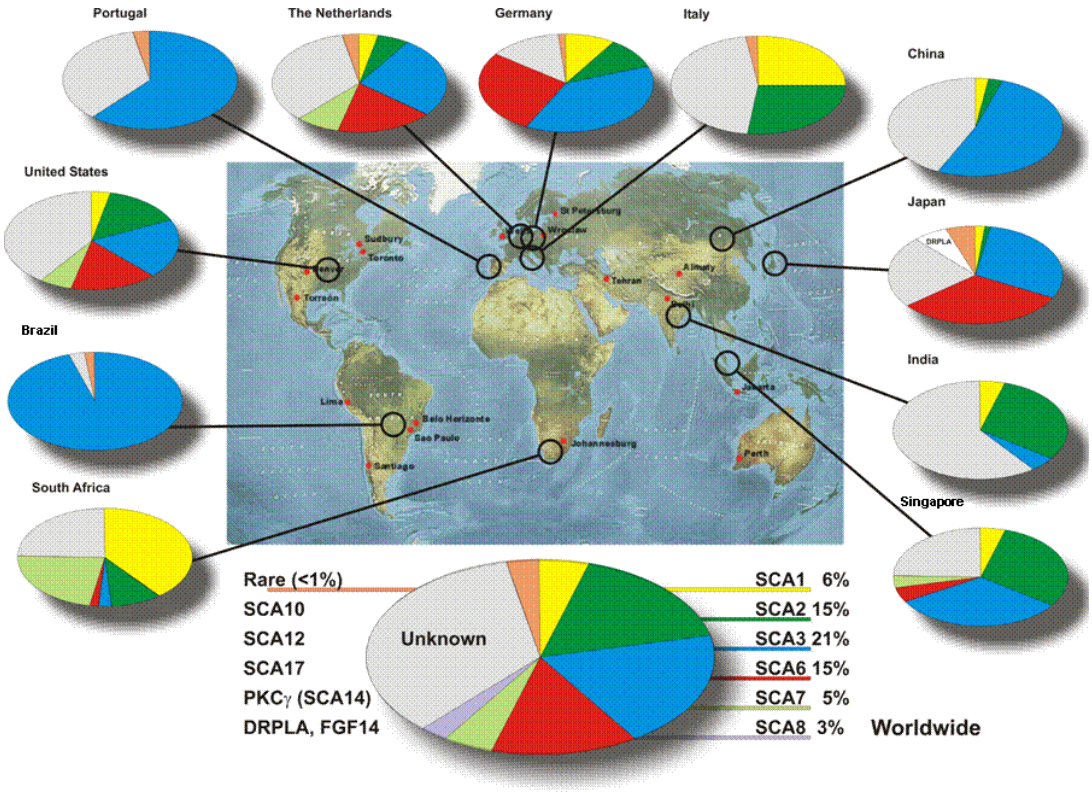

Figure 1.1. Worldwide distribution of SCA subtypes (Schöls *et al* 1997, Moseley *et al* 1998, Saleem *et al* 2000, Storey *et al* 2000, Tang *et al* 2000, Maruyama *et al* 2002, Silveira *et al* 2002, van de Warrenburg *et al* 2002, Dryer *et al* 2003, Brusco *et al* 2004, Schöls *et al* 2004, Shimizu *et al* 2004, Zortea *et al* 2004, Jiang *et al* 2005).

Figure published courtesy of L Schols, P Bauer, T Schmidt, T Schulte, O Reiss of University of Tübingen and Ruhr-University Bochum, Germany. Adapted from (Bird 1993).

1.1.3. Neuropathology

Many brain regions are affected in MJD. Using computed tomographic scanning Yuasa and col. analyzed different brain regions of 4 MJD patients from a Japanese family and found atrophy in pons and cerebellum in all 4 patients. In one of the MJD patients of this Japanese family, some brain regions such as the dentatorubral and pallidoluysian system, Clarke's column and spinocerebellar tracts, anterior horn cells, pontecerebellar system and substantia nigra were affected. Authors also reported that other regions such as thalamus, cerebral cortex, purkinje and granule cells in the cerebellum and the striatum remained preserved in MJD patients (Yuasa *et al*. 1986). Nevertheless, many years later, Yamada et al identified that brain

regions such as striatum, cerebral cortex and thalamus that had been previously reported to be preserved were also affected in MJD, in addition to other brain regions that were shown to be involved (Yamada *et al*. 2004).

Even though many brain regions are subjected to degeneration in MJD, the main lesions in MJD are located in the cerebellar dentate nucleus and spinocerebellar system. A recent study from Reetz et al using MRI data analysis of 19 MJD patients at baseline, and after a follow up study of 2 years, has not shown the very expected brain regions like cerebellum, to significantly change of size in the neuroimaging analysis. The strongest change of volume loss was found in the caudate and putamen, followed by the brain stem, while moderate effects were seen in the cerebellum. Secondly, voxel-based morphometry analysis was performed and found that grey matter changes in the putamen and pallidum were significant when compared with the control subjects after a two years follow up study. Overall, MRI analysis revealed that after disease onset, the striatum is the region most sensitive to change over time in MJD (Reetz *et al*. 2013).

1.1.4. Pathogenesis

The mechanism by which CAG repeat mutation leads to disease remains largely unknown. Nevertheless, the wide variety of research that has been carried out in the last 20 years led to a greater understanding of the disease reducing the gap towards treatment of MJD.

1.1.4.1. Expanded CAG repeats

Research on the mechanism through which neurodegeneration occurs in polyglutamine diseases including MJD, has first focused on the CAG repeats it selves (Mangiarini *et al*. 1996, Perutz 1996). In MJD the expanded allele has been reported to span from 61 to 87 CAG repeats, while the normal allele from 12 to 44 CAG repeats (Maciel *et al*. 2001). Importantly, all the disease-causing proteins in polyglutamine disorders encode for CAG repeats but are entirely different from one another other than the polyglutamine tract. Moreover, longer CAG repeats lead to

increase in severity of all the polyglutamine diseases. Furthermore, many transgenic mouse models encoding full length or truncated forms of the disease proteins, resulted in neurodegenerative phenotypes (Ikeda *et al*. 1996, Mangiarini *et al*. 1996). These results were consistent with different mouse models in different polyQ diseases showing pathological protein conformations upon the expansion of the CAG repeats (Trottier *et al*. 1995), which could lead to the aggregation of the disease protein (Ikeda *et al*. 1996).

1.1.4.2. Protein sub-cellular localization and neuronal intranuclear inclusions

The subcellular localization and amyloidogenic features differ greatly between wild type ataxin-3 and mutant ataxin-3 (Marsh *et al*. 2009). Ataxin-3 is located in the cytoplasm in healthy control brains, whereas in the case of MJD patient brains, ataxin-3 is localized in the nucleus. In the nucleus, mutant ataxin-3 accumulates and aggregates into neuronal intranuclear inclusions (Paulson *et al*. 1997, Schmidt *et al*. 1998).

Protein aggregation is the hallmark of polyQ diseases and therefore a logical therapeutic target. Although aggregates were found in cell models, transgenic mouse models and in human postmortem brain tissue, the exact role of aggregation is largely unknown (Paulson *et a*l. 1997, Skinner *et al*. 1997, Becher and Ross 1998). These intranuclear inclusions contain mutant ataxin-3, wild type ataxin-3, ubiquitin, polyQ proteins, proteosomal subunits, heat shock molecular chaperones and transcriptional factors suggesting that not only mutant ataxin-3, but also many other proteins were sequestered into the nucleus leading to the deposition of aggregated proteins (Paulson *et al*. 1997, Chai *et al*. 1999, Chai *et al*. 2001). The presence of ubiquitin-interacting motifs in the ataxin-3 protein could be the reason for the co-localization with ubiquitin and can also be linked to an ubiquitination mechanism to tag the misfolded protein to the proteosomal chamber for degradation, which has been reported in other polyQ proteins (Becher and Ross 1998, de Almeida *et al*. 2002).

1.1.4.3. Quality control system failure

The quality control system is a tightly regulated process important for normal cellular function. In the case of MJD and other polyQ disorders, expanded CAG repeats cause misfolding and aggregation (Scherzinger *et al*. 1997). One important pathway involved in protein folding and degradation of misfolded proteins is the chaperone-mediated control system involving heat shock proteins belonging to the family of chaperones and widely-studied in polyQ disorders for refolding and promoting the degradation of misfolded proteins (Jana *et al*. 2005, Miller *et al*. 2005, Al-Ramahi *et al*. 2006). When the protein fails to fold properly despite the effective chaperone mediated control system, the ubiquitin-proteosome system often degrades it. Disturbances in the ubiquitin-proteosome system have been reported in MJD (Schmidt *et al*. 2002). Another major pathway involved in the degradation of the misfolded protein is lysosome-mediated autophagy. Our group has previously shown that the autophagy pathway is impaired in the brain of MJD patients and that overexpression of the autophagy-associated protein beclin-1 mitigates motor and neuropathological deficits and stimulates the autophagic flux resulting in a clearance of mutant ataxin-3 (Nascimento-Ferreira *et al*. 2011, Nascimento-Ferreira *et al*. 2013).

1.1.4.4. Proteolytic cleavage

Early studies reported that small fragments of the ataxin-3 protein with the expanded polyglutamine tract had cytotoxic properties, in accordance with observations in other polyQ disorders (Ikeda *et al*. 1996, Mangiarini *et al*. 1996). Such fragments of ataxin-3 were identified as resulting from proteolysis of the full length protein by proteases, specifically calpains, and caspases. Even though, several caspase cleavage sites are predicted for ataxin-3, caspase 1 and caspase 3 mediated cleavage resulted in a modest cleavage of ataxin-3 (Wellington *et al*. 1998). Findings from Haacke et al. suggest that proteolytic cleavage is required to initiate the aggregation and the aggregation formation is strictly dependent on the CAG stretch (Haacke *et al*. 2006). Furthermore, aggregation formation was not reduced using caspase 1 and caspase 3 inhibitors in a SCA3 neuronal cell line (Koch *et al*. 2011).

Our group has shown that inhibition of calpains via calpastatin and an orally administered calpain inhibitor, BDA-410, prevents mutant ataxin-3 proteolysis, nuclear localization, aggregation and neuronal dysfunction in the striatal and cerebellum lentiviral MJD mouse brain. In addition to this, the calpain inhibitor BDA-410 also alleviated the motor deficits in a cerebellar lentiviral MJD mouse model (Simoes *et al*. 2012, Simoes *et al*. 2014). In support to the previously described paper, another group demonstrated that the knock out of calpastatin in MJD transgenic mice resulted in an increased number of aggregates, endogenous ataxin-3 cleavage, neurodegeneration and mutant ataxin-3 fragmentation upon calcium stimulation (Hubener *et al*. 2012).

1.1.4.5. Mitochondrial dysfunction

It has been reported that oxidative stress and inability to protect against free radicals with age could result in mitochondrial damage and dysfunction in polyQ diseases (Kim *et al*. 2003, Goswami *et al*. 2006, Miyata *et al*. 2008, Ajayi *et al*. 2012). Hsieh and colleagues were first to show decreased antioxidant enzymes levels of glutathione reductase, catalase and superoxide dismutase and reduced mitochondrial DNA copy number in the SK-N-SH cells expressing mutant ataxin-3 with 78 CAGs (Yu *et al*. 2009). In concordance with the findings in cells expressing mutant ataxin-3, mitochondrial DNA copy number was also reduced in the MJD human blood samples compared to the healthy controls (Yu *et al*. 2009). A few years later, HEK cell lines, PC6-3 cells expressing expanded CAG repeats and cerebellar granule cells from MJD transgenic mice showed increased susceptibility to 3-nitropropionic acid, which is an irreversible inhibitor of mitochondrial complex II. A significant decrease in the mitochondrial complex II activity was observed in PC6-3 cells differentiated into a neuronal-like phenotype with nerve growth factor (NGF). Moreover, mitochondria from MJD transgenic mouse model and lymphoblast cell lines derived from MJD patients also showed a similar trend towards decreased complex II activity (Laco *et al*. 2012). Recent evidence suggests a decrease in the pattern of mitochondrial DNA copy number with age and accumulation of 3,867 bp deletions that relates with the early stages of the transgenic mouse and concludes that 3,867 bp deletions may be used as a biomarker to detect early stages of the disease (Kazachkova *et al*. 2013).

1.1.4.6 Transcriptional dysregulation

Recent evidence suggests transcriptional dysregulation may play a crucial role in MJD. Early studies reported that the transcription factor (TATA-binding protein) and transcription co-factor (CREB binding protein) are incorporated into nuclear inclusions of polyQ-expanded ataxin-3 (Steffan *et al*. 2000, Li *et al*. 2002). Complete mRNA expression profile in the MJD transgenic mice with 10-11 months old revealed reduced expression levels of genes involved in cell signaling, transcription factors that regulate neuronal survival and differentiation, glutamatergic neurotransmission, heat shock proteins and increased expression in the cyclin D1, Bax and CDK5-p39 that could mediate neuronal death. Similarly, transgenic mice with 4 to 5 months old with no neurological phenotype been displayed also showed decreased expression in the mRNA expression levels of the genes involved in signal transduction and glutamergic signalling (Chou *et al*. 2008).

The balance between histone acetylation and deacetylation is well-regulated in normal condition but reported to be disturbed in polyQ diseases (Kim and Bae 2011). Yi and colleagues found that valproic acid, a histone deacetylase inhibitor, prevented the pigmentation loss, extended the lifespan and mitigated climbing disability in a transgenic MJD *Drosophila melanogaster*. For simplicity *Drosophila melanogaster* will be referred as *D. melanogaster* in the following part of this thesis. Moreover, authors reported an increase in the acetylation levels of histone H3 and H4 and a reduction in the early apoptotic cells in the MJD cell line (Yi *et al*. 2013).

Bringing the dysregulated mRNA transcripts back to the steady state level using valproic acid in the *D. melanogaster* MJD (Yi, Zhang et al. 2013), T1-11 (adenosine A_{2A} receptor agonist) and JMF1907 (synthetic analog of T1-11) in the transgenic mouse model was able to mitigate the neurodegeneration induced by mutant ataxin-3 (Chou *et al*. 2015).

Even though different transcripts have been shown to contribute to the pathogenesis of MJD, in recent years the evidence regarding dysregulation of microRNAs in other neurodegenerative disorders was suggestive of a potential role in MJD. Therefore, this thesis focuses on the study of microRNA dysregulation in MJD and its correction

to alleviate neuropathological deficits. Therefore, studies exploring microRNA as a potential tool for the treatment of MJD will be discussed in section 1.2

1.2 MicroRNAs

MicroRNAs are small endogenous non-coding RNA molecules composed of 18-22 nucleotides in length. MicroRNAs act as regulators of gene expression at post-transcriptional level by binding to 3'untranslated regions (3'UTR), coding sequences or 5´UTR of target messenger RNAs (mRNAs) and resulting in mRNA degradation or inhibition of the translation (Ambros 2004, Bartel 2004).

1.2.1 Discovery of microRNAs

Victor Ambros and colleagues Rosalind Lee and Rhonda Feinbaumin discovered the first microRNA in 1993. A genetic screen in the *Caenorhabditis elegans* revealed the the first miRNA termed as lin-4, did not encode a protein but instead a novel 22-nucleotides small RNA (Lee *et al*. 1993). Followed by lin-4, let-7 was identified seven years later as a small RNA of 22 nucleotides by Reinhart et al (Reinhart *et al*. 2000). The discovery of small RNA molecules were particularly exciting for two reasons. Firstly, small RNA molecules were conserved in many different species including *D. melanogaster* and humans. Secondly, the RNA interference (RNAi) mechanism was discovered and it became clear that small RNA was linked with the RNAi mechanism. Few years later, more than 100 small RNA molecules had been identified in different species including *D. melanogaster*, mice and humans and named microRNAs (Reinhart *et al*. 2000). Until now, 2588 mature miRNAs have been identified in humans, as inferred from the recently updated miRbase database.

1.2.2 Biogenesis of miRNAs

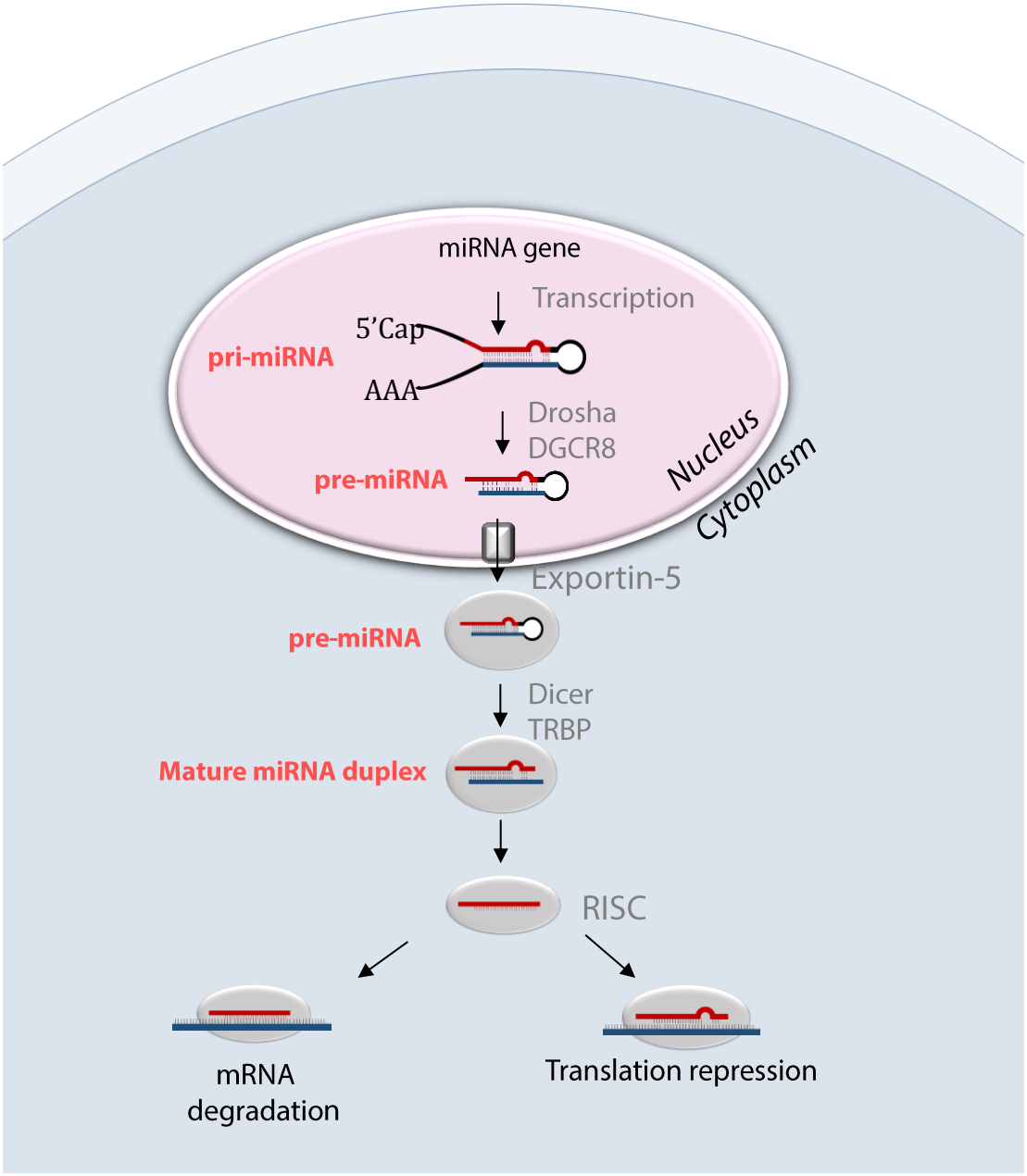

Figure 1.2. miRNA biogenesis. MiRNAs are transcribed from DNA by RNA polymerase II to form Primary miRNAs (Pri-miRNAs). Pri-miRNA is converted in to pre-cursor miRNA by cleavage enzymes such as Drosha. This Precursor miRNA is then transferred from the nucleus to the cytoplasm by Exportin 5. In the cytoplasm, Dicer cleaves the pre-miRNA to form a 5' and 3' miRNA duplex. The Argonaute protein (part of the RNA-induced silencing complex (RISC) selects one strand of miRNA and degrades the other one. The selected miRNA strand will become incorporated into the RISC complex, recognize its target and bind to 3' UTR of the target mRNA. mRNA degradation occurs if there is a perfect complementarity between the miRNA and the target. Imperfect complementarity results in translational repression.

MicroRNAs are encoded in the genome and transcribed by RNA polymerase II (Pol II) as long primary transcripts (named as pri-miRNAs). Pri-miRNAs include a hairpin structure where miRNA sequences are embedded. The pri-miRNA has a cap structure at 5'end and a poly-adenylated tail at the 3'end (Cai *et al*. 2004, Lee *et al*. 2004, Parizotto *et al*. 2004). Pri-miRNAs are processed into 60-110 nt miRNA precursors (Pre-miRNAs) by RNase III enzyme Drosha which initiates the maturation process by cropping the stem-loop to release a small hairpin shaped RNA. Drosha together with the essential cofactor DiGeorge syndrome chromosomal region 8 (DGCR8) (also known as PASH-1 in C. elegans and Pasha in D. melanogaster), which is a double-stranded RNA-binding domain protein (dsRBD), form a complex called microprocessor (Lee *et al*. 2002, Lee *et al*. 2003, Denli *et al*. 2004, Gregory *et al*. 2004, Han *et al*. 2004). As Drosha cleavage defines the terminus of a miRNA, microprocessor recognizes and cleaves a pri-miRNA.

Pre-miRNAs are then transferred from the nucleus to the cytoplasm by Exportin-5, which forms a transport complex with GTP-binding nuclear protein RAN-GTP and a pre-miRNA. Following translocation through the nuclear pore complex, GTP is hydrolysed, resulting in the disassembly of the complex and the release of the pre-miRNA into the cytosol (Yi *et al*. 2003, Bohnsack *et al*. 2004, Lund *et al*. 2004). Exonucleolytic digestion of the pre-miRNA in vitro was inhibited by the RAN-GTP, EXP5 and a pre-miRNA Complex formation. Exp5 binding not only allows the transfer of pre-miRNAs from nucleus to cytoplasm but also prevents nuclear pre-miRNAs degradation (Zeng and Cullen 2004).

Dicer which is another RNase III enzyme cleaves pre-miRNAs to form 20 nt long miRNA duplexes, together with trans-activation response RNA-binding protein (TRBP) and Protein activator of PKR (PACT), which are dsRBD proteins (Bernstein *et al*. 2001, Grishok *et al*. 2001, Hutvagner *et al*. 2001, Ketting *et al*. 2001, Chendrimada *et al*. 2005, Jiang *et al*. 2005, Saito *et al*. 2005). Following dicer processing, miRNA duplexes are loaded onto particular types of Argonaute proteins (AGO) to form an RNA-induced silencing complex (RISC or miRISC) (Hammond *et al*. 2001).

RISC involves two steps, loading of the miRNA duplex on the AGO protein followed by unwinding (Kawamata and Tomari 2010). In flies, miRNA duplexes are loaded

onto an AGO1 protein (Forstemann *et al*. 2007), whereas in C.elegans, miRNA duplexes interact with ALG-1 and ALG-2 proteins (Jannot *et al*. 2008). Central mismatches at positions 9-10 in the guide strand direct the miRNA duplex to incorporate into AGO1 protein and prevent it from entering AGO2 (Okamura *et al*. 2009). The identity of the 5' nucleotide of the guide miRNA strand also contributes to the loading of small RNAs into AGO proteins, as AGO1 preferably binds to miRNAs with a 5' U (Ghildiyal *et al*. 2010). In humans, miRNA duplexes can be loaded into all the four AGO proteins AGO1, AGO2, AGO3 and AGO4 with a preference for small RNA duplexes with central mismatches at position 8-11 (Yoda *et al*. 2010).

Further to the loading of miRNA duplexes, the passenger strand is removed by pre-RISC (where miRNA duplexes associate with AGO proteins) only when the duplex is matched at the centre to generate a mature RISC (Diederichs and Haber 2007). Removal of the passenger strand is facilitated by the endonuclease C3PO (Liu *et al*. 2009). The more general process is miRNA duplex unwinding without cleavage. Mismatches in the guide strand at nucleotide positions 2–8 and 12–15 promote unwinding of miRNA duplexes (Yoda *et al*. 2010). AGO proteins can be modulated by numerous modifications. Epidermal growth factor receptor phosphorylates human AGO2 protein under hypoxia condition, which results in the separation of human AGO2 from Dicer and the reduction of pre-miRNA processing for some miRNAs (Shen *et al*. 2013).

Prolyl 4-hydroxylation of human AGO2 by type I collagen prolyl 4-hydroxylase increases the stability of AGO2 or localization within processing bodies (Qi *et al*. 2008, Wu *et al*. 2011). AKT3 or MAPK-activated protein kinase 2 phosphorylates human AGO2 at Ser387 leading to translational repression or its localization to P-bodies respectively (Zeng *et al.* 2008, Horman *et al*. 2013)**.**

1.2.3 miRNA-mRNA interaction

miRNAs interact with mRNA by base pairing. The seed region, which represents 2-8 nucleotides at the 5’ end of miRNA, is critical for the base pairing. Usually miRNAs bind to the 3’ untranslated region (UTR) of target messenger RNAs (Huang *et al*. 2014), but it can also bind to the 5’ UTR or to coding sequences (Duursma *et al*.

2008, Tsai *et al*. 2009). Target sites of animal microRNA's are not distributed evenly within the 3'UTR. Large number of mRNAs have multiple binding sites for the same miRNA and this strengthens the degree of down-regulation (Lai 2004, Brennecke *et al*. 2005, Grimson *et al*. 2007). The classification of miRNA target sites is based on complementarity between the 5' seed region of miRNAs and the 3' mRNA. Target sites are classified into 3 different types:

1) Canonical sites refer to the complete base pairing with the seed regions, which is critical for the interactions, and most of the known targets represent this type.
2) 3'-supplementary: additional base pairing occurs at position 13-16 of miRNA seed and 5' target mRNA. At least 3-4 nucleotides paired consecutively contribute to the increased efficiency.
3) 3'-compensatory sites: Mismatch occurs in the seed regions of 3'miRNA in compensatory sites but additional base pairing at position 13-16 compensates the mismatch in the seed region (Bartel 2009).

The intricacy of miRNA-mRNA interactions makes it difficult to rely completely on the algorithms based on the sequence matching to predict miRNA-mRNA interactions and to look for the need for additional parameters such as orthologous sequence alignment (Bartel 2009).

1.2.4 Function of microRNA gene regulation

miRNAs regulate the target genes either by direct cleavage of their target mRNA or translational inhibition. In plants, the majority of miRNAs have perfect complementarity with the target mRNA (Rhoades *et al*. 2002). Upon binding to the target mRNA, miRNA-containing RISC cleaves the mRNA (Llave *et al*. 2002, Tang *et al*. 2003). In animals, the complementarity between miRNAs and the target mRNA has been restricted to the seed region. A seed region consists of 2-8 nucleotides, which is at the 5'end of the miRNA (Lai 2004, Brennecke *et al*. 2005, Lewis *et al*. 2005, Xie *et al*. 2005). Since the seed region of the miRNA is very short, it is predicted to target many genes. When the miRNA has complete complementarity, it will result in the direct degradation of mRNA, while when there is an imperfect complementarity it will prevent the translation. There is evidence that miRNAs may

regulate around one third of the protein coding genes (Lewis *et al*. 2005, Xie *et al*. 2005, Baek *et al*. 2008).

To investigate the function of microRNAs, the enzyme Dicer that is required for the synthesis of microRNAs was inactivated in the zebra fish. Interestingly, this resulted in developmental arrest at day 10 suggesting that Dicer and the miRNA pathway are critical for vertebrate development (Wienholds *et al*. 2003) and also for physiological processes in immune system (Muljo *et al*. 2005). Later, further evidence have shown the importance of dicer in the pathogenesis of many diseases including cancer and neurodegenerative diseases (Bilen *et al*. 2006).

MicroRNAs have been shown to have differential expression in different tissues. A recent study focused on 24 different body regions such a heart, liver, lungs, bone, stomach etc. from two male human bodies to characterize the microRNA expression of different tissues. Most of the microRNAs were neither stable nor specific for a single tissue. Nevertheless, different microRNAs were predominately expressed in certain tissues. Furthermore, significantly smaller variation between the organisms, as compared to the inter-organs, was observed using lung and prostate biopsies. A different storage interval (1-14 days at 4°C) of heart and lung tissues from biopsies had limited influence on the miRNA expression pattern. Interestingly, tissue specificity index values of miRNAs from human tissues were significantly correlated to the miRNAs previously published in rats (Ludwig *et al*. 2016).

1.2.5 miRNAs implicated in polyglutamine Disorders

miRNAs are involved in several pathological conditions including PolyQ disorders as described in the following sections and summarized in Table 1.1.

Table 1.1 miRs involved in polyQ diseases

PolyQ	miR	Source	Targets	References
HD	miR-9 and miR-9*	Postmortem human brain samples	REST& CoREST	(Packer *et al*. 2008)
HD	miR-34b	NT2 cells, Plasma samples from pre-manifest HD patients		(Gaughwina *et al*. 2011)
HD	miR-196a	huntingtin	Mut-Htt	(Cheng *et al*. 2013)
HD	miR-128a	Striatum	HIP-1, HTT, SP-1	(Kocerha *et al*. 2014)
HD	miR-10b-5p	Human brain striatum	brain-derived neuro-trophic factor (BDNF)	(Hoss *et al*. 2015)
HD	miR-124	Transgenic R6/2 HD mouse model	PGC-1α and BDNF and SOX9	(Liu *et al*. 2015)
HD	miR-214	Knock in HD striatal cell model	Beta catenin	(Ghatak and Raha 2015)
SCA1	miR-19, miR-101 and miR-130	HEK293T	Ataxin-1	(Lee *et al*. 2008)
SCA1	miR-144	Cortex and cerebellum from humans, chimpanzees and rhesus macaques on a genome-wide scale	Ataxin-1	(Persengiev *et al*. 2011)
SCA1	miR-150	Transgenic SCA1 mouse	Vegfa	(Rodriguez-Lebron *et al*. 2013)
SCA3	Ban	*D. melanogaster*, HeLa cell line		(Bilen *et al*. 2006)
SCA3	miR-148	Transgenic mice	Ataxin-3	(Rodriguez-Lebron *et al*. 2013)
SCA3	miR-34b, miR-29a, miR-25 and miR-125b	Serum samples from MJD/SCA3 patients		(Shi *et al*. 2014)

SCA3	miR-25	HEK293T cells, SH-SY5Y cells	Ataxin-3	(Huang *et al*. 2014)
SCA3	No evidence for significantly differential expression. Trend for mir-33, and mir-92a overexpression	MJD *D. melanogaster* model		(Reinhardt *et al*. 2012)
SCA7	miR-124		Long non-coding RNA (lnc-SCA7) and ataxin-7	(Tan *et al*. 2014)
SBMA	miR-196a	HEK293T, Transgenic mouse, Human fibroblast	CELF2	(Miyazakii *et al*. 2012)

1.2.5.1 miRs dysregulated in Huntington's disease (HD)

In HD, miR-9/miR-9* was found to be down regulated in postmortem brain samples and predicted to target RE1-silencing transcription factor (REST) and CoREST which was further confirmed using luciferase assay. Moreover, suppression of REST expression in HEK 293 and NT2 cells led to an enhanced miR-9 expression levels suggesting that the interaction between miR-9 and the target REST is direct (Packer *et al*. 2008). More recently, miR-34b expression was found to be dysregulated and upregulated in NT2 cells and in the plasma samples from the pre-manifest HD patients suggesting that it might be used as a biomarker (Gaughwin *et al*. 2011).

Intranuclear aggregates, mRNA and the protein levels of mutant huntingtin were reduced upon miR-196a-mimic treatment by indirect interaction with huntingtin (Cheng *et al*. 2013). Other researchers found down-regulation of miR-128a in HD transgenic monkeys. miR128 targets are HD-associated genes including SP1, HIP1 as well as HTT itself (Kocerha *et al*. 2014).

Ghatak and col. reported low beta-catenin levels due to the overexpression of miR-

214 (Ghatak and Raha 2015). Furthermore, it was recently shown that miR-124 injection improved behavior phenotypes and elevated neurogenesis in cortex and the striatum of R6/2 HD mice model by targeting PGC-1α, BDNF and SOX9 (Liu *et al*. 2015). Another recent study conducted using postmortem brain tissues revealed miR-10b-5p was differentially expressed, which relates to striatal involvement and age of onset (Hoss *et al*. 2015).

1.2.5.2 miRs involved in Spinocerebellar ataxia type 1 (SCA1)

Lee et al focused on miRs whose target is ataxin-1 and identified miR-19, miR-101 and miR-130 as direct targets of ataxin-1. miR-19, miR-101 and miR-130-mimics treatment in cells resulted in a significant decrease in ATXN1 levels (Lee *et al*. 2008). More recently, miR-144, miR-101 and miR-130 were found upregulated in cerebellum and cortex of SCA1 patients and were identified as directly targeting ataxin-1. Furthermore, miR-144 was also involved in the ageing progression (Persengiev *et al*. 2011). Global miRNA microarray profiling of SCA1 transgenic cerebellar Purkinje neurons revealed that miR-150, whose target is the vascular endothelial growth factor (VEGF), was upregulated in SCA1 (Rodriguez-Lebron *et al*. 2013) and overexpression of Vegf ameliorated the SCA1 phenotype (Cvetanovic *et al*. 2011).

1.2.5.3 miRs dysregulated in Machado-Joseph disease/ Spinocerebellar ataxia type 3 (MJD/SCA3)

Bonini and colleagues were first to show the involvement of miRNAs in MJD. miR bantam was identified as a potential modulator of SCA3 pathogenesis by reducing the degeneration induced by the mutant ataxin-3 (Bilen *et al*. 2006). However, in another MJD *D. melanogaster* model, no evidence for miRNA dysregulation was observed (Reinhardt *et al*. 2012). Nevertheless, miRNA microarray profiling revealed a dysregulation for miR-25, miR-125b, miR-29a and miR-34b which were differentially expressed in serum samples obtained from human MJD patients, highlighting their potential application as as biomarkers for SCA3 (Shi *et al*. 2014). The same group investigated the effects of these differentially expressed miRNAs by transfecting cells with mimics of miR-25, miR-125b, miR-29a and miR-34b. Among

the four miRNAs, miR-25 mimic treatment reduced the endogenous ataxin-3, apoptosis, ataxin-3 aggregate formation and increased cell viability. Moreover, through a luciferase assay, the authors demonstrated that miR-25 directly targets ataxin-3 mRNA (Huang *et a*l. 2014).

1.2.5.4 miRs dysregulated in SCA7

In SCA7, a lnc-SCA7 (long non-coding RNA) was identified as a post-transcriptional regulator of ataxin-7, where the interaction is mediated by miR-124. The expression levels of miR-124 were observed to be downregulated in a SCA7 knock-in mouse model (Yoo *et al*. 2003, Chen *et al*. 2012) and in SCA7 patient fibroblasts. This was associated with increased expression of ataxin-7 and lnc-SCA7 in retina and cerebellum. Moreover, they also observed that STAGA is required for the transcription activation of miR-124, which mediates the interaction between the lnc-SCA7 and ataxin-7. Overexpression of miR-124 decreased the expression of lnc-SCA7 and ataxin-7 in N2a cells and in a SCA7 knock-in model (Tan *et al*. 2014).

1.2.5.5 miR dysregulation in Spinal and bulbar muscular atrophy (SBMA)

Regarding SBMA, miR-196a was found to be up-regulated by greater than 2 fold in a SBMA transgenic mouse model (Katsuno *et al*. 2003). This miRNA was found to target CUGBP Elav-like family member 2 (CELF2) a protein which promotes the stabilization of the androgen receptor mRNA. Importantly, upon miR-196a overexpression, the mRNA and the protein levels of the androgen receptor were reduced in transgenic mice, HEK293T cells and human fibroblasts. This was achieved by silencing CELF2 and indirectly promoting the decay of the mutant androgen receptor mRNA (Miyazaki *et al*. 2012).

1.2.6 Role of miR-10b

miR-10b has been associated with Huntington's disease and glioblastoma. The available data regarding the role of this miRNA in these diseases is discussed in the next following sections.

1.2.6.1 miR-10b in Huntington's disease (HD)

Recent findings obtained from postmortem brain tissues of HD patients showed that miR-10b is one of nine miRNAs differentially expressed in the prefrontal cortex. All the differentially expressed miRs were significantly associated with Vonsattel grade, which is used to assess the striatal involvement. Particularly, miR-10b expression levels were associated with striatal involvement (determined by Hadzi-Vonsattel striatal score) after adjustments for CAG length. Besides being associated with the observed striatal changes, miR-10b-5p expression levels were also strongly correlated with the age of onset in HD. Altogether, miR-10b-5p has the potential to be used as a biomarker for HD, being related with the age of onset of the disease and with the level of striatal involvement (Hoss *et al*. 2015).

1.2.6.2 miR-10b in Glioblastoma (GBM)

miR-10b is abundantly overexpressed in tumors and glioma cells but absent in the normal human brain (Sasayama *et al*. 2009). Interestingly, inhibition of miR-10b resulted in a reduction of cell growth and in cell cycle arrest in glioma cells, while also leading to a reduction of tumor growth in a human glioma mouse model. The authors demonstrated that these effects observed upon miR-10b inhibition were mediated by an induction of apoptosis and autophagy. Target identification showed that the inhibition of this miRNA leads to increased expression of BCL2L1, TFAP2C, p21, and p16 which normally protect cells from uncontrolled growth. Accordingly, the survival rate for glioblastoma patients with elevated levels of miR-10 is significantly reduced when compared to patients with low expression levels of miR-10b. These findings suggest an important role for miR-10b in glioma pathogenesis and simultaneously established mir-10b inhibition as novel candidate therapeutic approach for the treatment of GBM (Gabriely *et al*. 2011).

Following the previous findings, the profiling of miR-10b levels in a GBM stem cell line demonstrated that miR-10b levels were also found to be up-regulated in these cells. Importantly, miR-10b inhibition resulted in a reduction of cell invasion and migration in glioblastoma stem cells, as well as in a reduced growth of stem cell-derived orthotopic GBM xenografts *in-vivo* (Guessous *et al*. 2013).

Even though the targets of miR-10b were previously identified, the mechanism contributing to the miR-10b sustained viability of glioma-initiating stem-like cells (GSC) was still unknown (Gabriely *et al*. 2011, Guessous *et al*. 2013). More recently, Teplyuk and colleagues identified miR-10b as a regulator of cell cycle and alternative splicing, through non-canonical targeting of the 5' UTR of MBNL1-3, SART3, and RSRC1 in heterogeneous GSCs. Treatment with either intracranial injection, systemic intravenous injections and continuous osmotic delivery of miR-10b antisense oligonucleotides resulted in the targets derepression and in reduced growth and progression of the established intracranial GBM (Teplyuk *et al*. 2016).

1.2.7 Profiling of microRNAs

Currently, three methods are available for profiling miRNA expression: Quantitative reverse transcription PCR (qRT-PCR), miRNA microarray and RNA seq.

These methods characteristics, advantages and disadvantages are summarized below in Table 1.2.

Table 1.2. List of methods available for miRNA profiling

miRNA profiling method	Advantages	Disadvantages
Quantitative reverse transcription PCR (qRT-PCR) **-Sybr green based (Varkonyi-Gasic *et al*. 2007).** **-Taqman based (Chen *et al*. 2005).**	Sensitive, specific, well established method and can be used for absolute quantification	Cannot identify novel miRNAs. Only limited number of samples or miRNAs can be analysed per day
miRNA microarray **miRNAs samples are fluorescently labelled and then hybridized to array of DNA-based capture probes, followed by washing and scanning of array (Liu *et al*. 2008, Marioni *et al*. 2008, Mortazavi *et al*. 2008, Sultan *et al*. 2008)**	Well established method, low-cost and high-throughput	Lower specificity than qRT-PCR or RNA sequencing. Difficult to use for absolute quantification. Cannot identify novel miRNAs
RNA seq: high-throughput and smaller scale next-generation sequencing **The procedure begins with the preparation of microRNA to cDNA library. Adaptor ligation allows the cDNA library to be fixed onto a solid (Chiang *et* al. 2010)**	High accuracy in distinguishing miRNAs that are very similar in sequence, as well as isomiRs. Can detect novel miRNAs	Substantial computational support needed for data analysis. Cannot be used for absolute quantification

1.2.8 miRNA-Target prediction

One of the main obstacles in miRNA research is to identify the specific sequence on target genes to which miRNAs will have partial or full complementarity. In order for precise identification of their target genes, several algorithms have been developed. Currently available target prediction tools are based on diverse algorithms, which can be improved depending on the required research approach and needs (Lewis *et al*. 2003). Seed match, binding site conservation, free energy, and site accessibility are the most commonly used features by miRNA target prediction tools (Lewis *et al*. 2003, Yue *et al*. 2009).

When compared to animals, miRNA target prediction in plants is easier and more accurate as the plant miRNA binding sites are located within the open reading

frames (ORFs) of the target mRNAs and have perfect or near perfect complementarity with its correspondent miRNAs (Voinnet 2009). However, in animals, perfect complementarity between the miRNA and the target mRNA is very rare (Yekta *et al*. 2004). Importantly miRNA binding sites are predominantly located in the 3' untranslated regions (3' UTRs) of the target genes and rarely located in the ORFs or in the 5' UTR (Lytle *et al*. 2007).

The following table summarizes some databases available to predict targets of miRNAs.

Table 1.3 MicroRNA target prediction tools

Databases	Features	Website links	References
PicTar	Predicts 5' dominant target sites. Analysis based on evolutionary site conservation.	http://pictar.mdc-berlin.de	(Krek *et al*. 2005)
Target Scan / Target ScanS	Predicts 5' dominant target sites. Strict complementarity in the seed region is required Identifies non-conserved sites.	http://www.targetscan.org	(Lewis *et al*. 2003)
Diana-MicroT	Requires seed complementarity Presence of compensatory binding in the 3' regions of miRNA (allows some mismatches in the seed sequence)	http://www.microrna.gr/microT-CDS	(Kiriakidou *et al*. 2004)
MicroRNA.org	Predicts miRNA targets using the miRanda algorithm (based on sequence complementarity between the mature miRNA and the target site, and binding energy of the miRNA/mRNA duplex)	http://microrna.org	(John *et al*. 2004, Betel *et al*. 2010)

1.2.9 Experimental validation of predicted target sites of the miRNA

Taking into account the possibility of obtaining false positive results upon bioinformatic prediction of miRNA binding sites using the previously described algorithms, microRNA targets need to be experimentally validated. This can be achieved by transfecting cells lines with miRNA inhibitors or mimics and by quantifying the levels of the target mRNA or protein.

Moreover, the direct interaction between a miRNA and its target transcripts needs to be experimentally validated. The most commonly used technique to identify the direct interaction between a miRNA and its target is the luciferase gene reporter assay. Luciferase gene encodes a 61- kDa enzyme that oxidizes D-luciferin in the presence of oxygen, ATP and Mg^{++} resulting in light emission. Cells are co-transfected with both the luciferase construct cloned with the 3' UTR of the target gene and with the miRNA mimic or with a miRNA inhibitor such as sponges or tough decoy RNA. Luciferase activity is then quantified using a luminometer (Smale 2010). An expected increase in light emission should be observed upon co-transfection of cells with miRNA inhibitors and luciferase bound 3' UTR, while a decrease in the light emission should be observed when the cells are co-transfected with mimics and the luciferase bound 3' UTR. This results are indicative of a direct and specific interaction between the target and the miRNA (Lee *et al*. 2008).

In the case of MJD, a recent study took advantage of a luciferase gene reporter assay to validate miR-25 as a direct target of ataxin-3. In order to perform this validation, the 3'UTR of ataxin-3 or a mutated control 3'UTR were inserted to the 3'end of a luciferase gene. As expected, the co-transfection of a miR-25 mimic and 3'UTR of ataxin-3 significantly reduced the luciferase activity while the co-transfection of miR-25 mimic and a mutated 3'UTR sequence had no effect on the luciferase activity (Huang *et al*. 2014) showing that miR-25 is in fact a direct target of ataxin-3.

1.2.10 Therapeutic modulation of miRNAs

Due to the potential therapeutic significance of miRNAs, substantial efforts have been made to build tools in order to better understand and control the function of miRNAs. In order to take advantage of the function of miRNAs involved in disease conditions, the identification of molecules that can effectively inhibit or mimic mature miRNAs is needed in order to achieve a loss or gain of miRNA function. Table 1.4 summarizes the main strategies for miR inhibition or overexpression.

Table 1.4. miR inhibition and overexpression strategies

Inhibition strategies	Advantages	Disadvantages
Modified antisense oligonucleotides	Easy design, gene specific effects and no off-target effects	Delivery into cells and animals difficult, limited scope (one target)
miRNA sponges	Suitable to silence more than one miRNA meaning that blockage of the members of the same family is possible	Delivery into cells and animals difficult, off-target effects
Small molecule inhibitors	Easy delivery, systemic distribution, reversible effects, to control miRNA function on multiple levels of the miRNA pathway	Difficult to identify, structure-activity relationship required for optimization, specificity not predictable
Over-expression strategies	**Advantages**	**Disadvantages**
Synthetic double stranded miRNA	Protect against exonucleases making it to be more stable and doesn't interfere with RISC loading	Potential off-target effects because of the uptake of the miRNA by tissues that do not normally express the miRNA of interest
Viral vector	Drive the expression in particular regions such as the brain using AAV vectors Reduce the off target effects	Packaging capacity

1.2.10.1 miRNA inhibition strategies

miRNA inhibition strategies include antisense oligonucleotides, miRNA sponges and small-molecule inhibitors as discussed below:

1.2.10.1.1 Antisense oligonucleotides

Boutla and colleagues were the first to demonstrate the potential of unmodified antisense DNA oligonucleotides to inhibit the miRNA expression in *D. melanogaster* (Boutla *et al*. 2003). However, unmodified antisense DNA oligonucleotides were sensitive to degradation by serum nucleases suggesting the need for the development of the chemical modifications that could improve the stability and efficiency of the oligonucleotides for *in vitro* and *in vivo* applications (Boutla *et al*. 2003). One year later, miRNA function was blocked in vitro and in cultured human cells using 2'-O-Methyl modified oligonucleotides (Hutvagner *et al*. 2004). Even though 2'-O-Methyl modified oligonucleotides were more efficient compared with the original antisense oligonucleotides, they were still prone to degradation by serum exonucleases, making them non suitable for *in vivo* use. Since exonucleases cleave the phosphate bonds between nucleotides, modifying this reaction was crucial to protect 2'-O-Methyl from degradation. Phosphodiester bonds were substituted with phosphorothioate bonds to attain the most favorable condition in order to increase nuclease resistance as well as to retain the ability to bind the target miRNAs (Krutzfeldt *et al*. 2005).

The addition of methoxyethyl (2'-MOE) or fluorine groups (2'-F with phosphorothioate linkage) further enhanced binding affinity and nuclear resistance compared with the 2'-OMe modifications (Davis *et al*. 2006). However, the strongest affinity for the target miRNA was achieved with locked nucleic acid modifications, which contain a methylene linker bridging the 2’-O-oxygen to the 4’-position conferring increased thermodynamic stability (Chan *et al*. 2005).

1.2.10.1.2 miRNA sponges

Extending the concept of complementary miRNA binding sites, miRNA sponges have been developed and reported to be very effective at blocking miRNA expression for long term *in-vitro* and *in-vivo* (Care *et al*. 2007, Ebert *et al*. 2007). miRNA sponges contain multiple binding sites complementary to a miRNA of the interest. These binding sites were designed with a bulge at positions 9-12 to protect against endonucleolytic cleavage by Argonaute 2 and degradation of the sponge

RNA (Ebert *et al*. 2007). Since the interaction between miRNAs and their targets depends on imperfect base pairing in the seed region, miRNA sponges allow for an interaction and inhibition of different members of miRNA families rather than interacting with a single miRNA like antisense oligonucleotides. Mammalian cells transfected with miRNA sponges performed at least as well as modified LNAs, not just for one miRNA, but also for members of the same miRNA family (Ebert *et al*. 2007).

1.2.10.1.3 Small-molecule inhibitors

The expression levels of miRNAs can be modulated using drugs by targeting signaling pathways that result in the activation of transcription factors responsible for the regulation of miRNA expression. Key elements in the miRNA pathway that contribute to miRNA maturation and degradation processes can also be modulated. For example, a method to screen for small molecule miRNA inhibitors was developed for miR-21, which was selected due to its role as an anti-apoptic factor in cancer cells, being frequently over-expressed in cancer (Chan *et al*. 2005). Complementary sequences for miR-21 were cloned into a luciferase reporter gene, which was then used as a sensor to detect the presence of mature miRNA molecules. HeLa cells were transfected with the construct expressing high miR-21 levels, which induces low luciferase activity. Following this, more than 1000 small molecule compounds were evaluated and the diazobenzene 1 compound resulted in a 250% increase in the intensity of the luciferase signal compared to the untreated cells. Further characterization revealed that diazobenzene 1 compound affects the transcription of miR-21. This approach can be applied to screen several small molecule inhibitors for many miRNAs that were previously shown to be deregulated in various diseases (Gumireddy *et al*. 2008).

1.2.10.2 miR over-expression strategies

miRNAs can be overexpressed by using two approaches. (1) Synthetic double-stranded miRNAs and (2) Viral vector based approach, as discussed in the following sections.

1.2.10.2.1 Synthetic double-stranded miRNA

Synthetic double-stranded RNAs were designed to mimic endogenous miRNAs of interest with chemical modifications to improve their stability and cellular uptake (Thorsen *et al*. 2012). The guide strand is identical to the miRNA of interest, while the passenger strand is less stable and modified by a linkage to a molecule such as cholesterol to enhance the cellular uptake. In addition to the cholesterol molecules linked to the passenger strand, this strand may also contain chemical modifications to prevent RISC loading (Chen *et al*. 2008). The chemical modifications to the guide strand are limited as it should function as a miRNA and be readily recognized by the cell (Chiu and Rana 2003). Although this method restores the miRNA levels that may be lost during the disease progression, it may also result in potential off-target effects because of the uptake of the miRNA by tissues that do not normally express the miRNA of interest. This suggests the need for approaches to selectively drive the miRNA expression in an appropriate cell type or tissue.

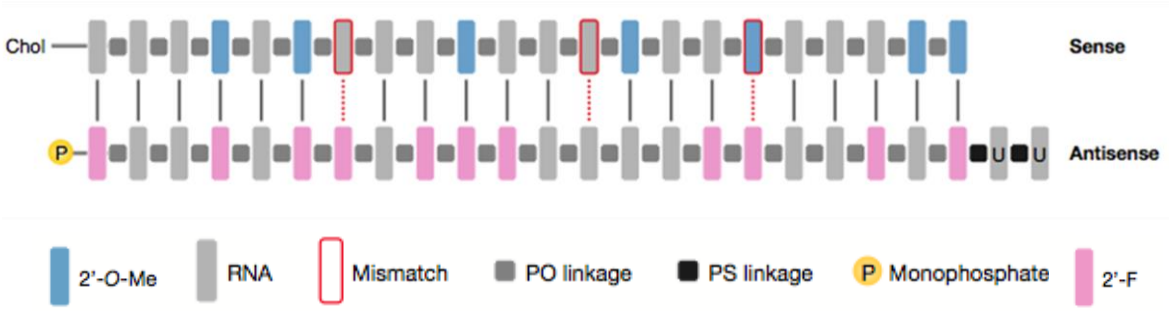

Figure 1.3. Design of a synthetic double stranded miRNA. Adapted from (van Rooij and Kauppinen 2014).

1.2.10.2.2 Viral vector based overexpression

Another method to increase miRNA expression levels is by taking advantage of viral vectors including lentivirus, adenovirus or adeno associated viruses. To eliminate the possible off target effects, adeno or adeno-associated viruses were used in order to drive the miRNA expression in specific cell types or tissues. One advantage of viral

vectors is the sustained expression of the miRNAs of interest. Tissue specific promoters allow further specificity by driving miRNA expression in selected tissues (Miyazaki *et al*. 2012). In addition to the use of a tissue specific promoter, different AAV serotypes also allow for tissue specificity due to their natural tropism toward different organs based on each individual AAV serotype (Kota *et al*. 2009).

1.3 Transthyretin (TTR)

Transthyretin is a tetrameric protein mainly synthesized in the liver and choroid plexus. This was initially termed as prealbumin since this protein from human plasma and cerebrospinal fluid samples was migrating ahead of albumin in the electrophoresis (Kabat *et al*. 1942, Seibert and Nelson 1942). The main functions of transthyretin are related to its binding properties to thyroid hormones (Ingbar 1958) and retinol binding protein (Raz and Goodman 1969). After the discovery of its function, it was renamed as transthyretin abbreviated as TTR (Transporter of Thyroxine and Retinol).

Transthyretin was initially described in familial amyloidotic polyneuropathy (FAP) where a single point mutation in the TTR gene leading to a mutant form of TTR (TTR Val30Met) was associated with the disease (Andrade 1952). Since then, around 100 different mutations have been reported in the TTR gene (Sekijima *et al*. 1993). TTR is associated with a group of diseases, which are related to protein aggregation linked with amyloid fibril deposition. Recently, aggregate and amyloid fibril deposition was also observed in preeclampsia placenta tissue carrying a normal TTR gene (Kalkunte *et al*. 2013). However, the mechanism behind TTR aggregation is largely unknown.

1.3.1 Transthyretin expression in the nervous system

A study conducted with TTR null mice revealed reduced signs of depressions like behavior and increased locomotor activities compared to the wild type mice. Increase in the expression levels of noradrenaline in the limbic forebrain could be a possible explanation for a significant change in the behavior compared to the wild type mice (Sousa *et al*. 2004). Similarly neuropeptide Y expression levels were also increased in the TTR null mice (Nunes *et al*. 2006). TTR null mice displayed memory impairment (Sousa *et al*. 2007) and the treatment with retinoic acid reversed the memory deficits both in the TTR null mice and aged rats showing the importance of TTR in the maintenance of normal cognitive processes (Brouillette and Quirion 2008). TTR null mice also revealed the impairment in the neurite outgrowth and nerve regeneration (Fleming *et al*. 2007). Further to these findings, the same authors delivered TTR in the crushed sciatic nerves of the TTR null mice and rescued the regeneration phenotype of TTR null mice. A decrease in the megalin expression levels was observed, which lead to the decreased nerve regeneration showing that megalin's action is TTR dependent (Fleming *et al*. 2009).

1.3.2 Transthyretin in diseases of the nervous system

TTR expression levels are differentially expressed in many neurological disorders. TTR expression levels in plasma and cerebrospinal fluid (CSF) have been shown to be upregulated in Guillain-Barre syndrome (GBS), frontotemporal dementia (FDT), and Parkinson's disease (PD) when compared to the controls (Ruetschi *et al*. 2005, Arguelles *et al*. 2010, Zhang *et al*. 2012). TTR expression was also upregulated in CSF samples from the rapid progression form of ALS compared to the slow progression form of ALS, highlighting the importance of TTR as a candidate biomarker to evaluate the disease progression in ALS (Brettschneider *et al*. 2010).

Other studies have linked TTR to a neuroprotective role. Santos and colleagues induced brain ischemia by permanently blocking the middle cerebral artery and found no significant difference in cortical infarction 24 hours post brain ischemia in TTR null mice compared with the control $TTR^{+/+}$ littermates. However, TTR null mice

with the compromised heat shock transcription factor 1 response ($TTR^{-/-}HSF1^{+/-}$) showed significant increase in cortical infarction, inflammation and edema formation suggesting the importance of transthyretin as a neuroprotector (Santos *et al*. 2010).

Several groups suggest the neuroprotective role of TTR in Alzheimer's disease (AD). The decreased expression level of TTR was observed in CSF of AD patients in 1986 (Elovaara *et al*. 1986). Recently, using a highly sensitive quantitative assay, a two-fold decrease in the levels of TTR in the CSF of AD patients was observed. Furthermore a significant decrease in the TTR expression levels was observed in plasma samples from AD patients and mild cognitive impairment patients compared to the controls suggesting TTR could be an early biomarker for AD. Moreover, it was previously shown that TTR is able to sequester the beta amyloid protein, preventing the formation of amyloid fibrils (Schwarzman *et al*. 1994), while also decreasing the rate of aggregation by the peptide (Liu and Murphy 2006). After the discovery of the interaction between TTR and Aβ peptides, one study took advantage of TTR overexpression as a therapeutic approach. Wild-type human transthyretin was overexpressed in APP23 transgenic mouse model of AD and found to significantly reduce the amount of Aβ peptides and to protect the AD mice from the behavior deficits when compared to the controls (Buxbaum *et al*. 2008).

On the other hand, it was also demonstrated that silencing the endogenous TTR gene promoted both an increased Aβ deposition and also a neuropathological phenotype (Buxbaum *et al*. 2008), supporting the previously published data from other group showing that young animals lacking TTR gene present a defect in spatial learning even in the absence of genes associated with human AD (Sousa *et al*. 2007).

Other groups have shown that TTR is harmful in AD. Surprisingly, a significant reduction in the Aβ deposition was found in the hippocampus of 4-month old double transgenic AD mice (TgCRND8) with deleted $TTR^{+/-}$ and a slight reduction in the double transgenic AD mice with $TgCRND8/TTR^{-/-}$, as compared to age-matched $TgCRND8/TTR^{+/+}$ (Doggui *et al*. 2010). These findings are in line with the previous study showing a significant decrease in the total and vascular Aβ deposition in $Tg2576/TTR^{-/-}$ mice (Wati *et al*. 2009). Administration of iododiflunisal, a TTR

tetrameric stabilizer, in AD/TTR$^{+/-}$ mice resulted in a reduction in the brain Aβ expression levels, Aβ deposition and also improved cognitive function (Ribeiro *et al*. 2014). The beneficial effects that were observed with the treatment of iododiflunisal open a new door to the design of novel drugs to the treatment of AD and other disorders where TTR may be involved.

1.4 Objectives

The main goal of this PhD project was to identify the differentially expressed microRNAs in MJD and to re-establish their normal levels in a striatal lentiviral mouse model of MJD and *D. melanogaster* model of MJD.

The specific objectives of this thesis were the following:

- To identify the differentially expressed miRNAs in a striatal lentiviral MJD mouse model (Chapter 2)
- To characterize the expression levels of this miRNAs in other MJD models such as in MJD transgenic mice, in a lentiviral cerebellar mouse model, and in engineered MJD cell lines (Chapter 2)
- To re-establish the normal levels of miR-10b in the MJD *D. melanogaster* model (Chapter 2)
- To re-establish the normal levels of miR-10b in a striatal lentiviral MJD mouse model and to investigate whether this could reduce intranuclear inclusions and striatal neurodegeneration (Chapter 3)
- To identify and validate a potential target gene of miR-10b and to clone it in a lentiviral backbone construct (Chapter 3)

CHAPTER 2

MicroRNA dysregulation in MJD - Applications in a *D. melanogaster* MJD model

2.1 Abstract

Machado-Joseph disease (MJD) / Spinocerebellar ataxia type 3 (SCA3) is an autosomal dominant neurodegenerative disorder caused by the abnormal CAG expansion in the coding region of *ATXN3* gene. Until now, there is no therapy to prevent or delay the disease progression in MJD. Over the last decade, microRNAs, which are non-coding RNA molecules, have been reported to be dysregulated in many diseases including neurodegenerative disorders.

Therefore, the aim of this study was to screen the differentially expressed microRNAs in a striatal lentiviral MJD mouse model and to take advantage of microRNA regulation as a therapy towards MJD. For this, we took advantage of the previously developed lentiviral striatal MJD mouse model developed by our group to perform a screening of miRs expression.

Here we report the complete profile of the microRNA expression in the striatal lentiviral MJD mouse model using miRNA microarray analysis. miRNA microarray revealed numerous differentially expressed miRNAs, which were further validated using qRT-PCR. Let-7b, Let-7i, miR-27b, miR-181a and miR-30e were significantly downregulated in MJD whereas miR-10b was robustly up-regulated in MJD. Concomitantly, miR-10b expression levels were also evaluated in other MJD models and found to be significantly up-regulated in a MJD transgenic mouse model while also showing a trend towards upregulation in human post-mortem brain tissue. To investigate whether manipulation of miR-10b could alleviate MJD, miR-10 was repressed in a MJD *D. melanogaster* model, which resulted in the extension of MJD flies life span.

These results suggest that microRNAs are dysregulated in the striatal lentiviral MJD potentially contributing to the pathogenesis of MJD. Re-establishment of the normal levels of miR-10 in MJD flies improved their life span suggesting an important role for miR-10 in the pathogenic process.

2.2 Introduction

Machado-Joseph disease (MJD), also known as spinocerebellar ataxia type 3 (SCA3), is a rare dominantly-inherited neurodegenerative disorder caused by an abnormal CAG expansion in the coding region of the *ATXN3/MJD1* gene (Kawaguchi *et al*. 1994). Mutation in the *ATXN3* gene confers a toxic gain-of-function to the ataxin-3 protein leading to neurodegeneration and severe motor impairments (Rubinsztein *et al*. 1999, Zoghbi 2000, Duenas *et al*. 2006). Dysfunction and neurodegeneration occur in selective brain regions such as cerebellar dentate nucleus, striatum, brain stem, substantia nigra and thalamus, but the exact mechanisms contributing to the selective neurodegeneration remain largely unknown (Yamada *et al*. 2008, Reetz *et al*. 2013). Currently, there is no treatment to prevent or delay the disease progression.

MicroRNAs are small non-coding RNA molecules composed of 19-22 nucleotides in length that play a regulatory role in gene expression at the post-transcriptional level resulting in mRNA degradation or translational repression (Ambros 2004, Bartel 2004). Over the last decade, microRNAs have been implicated in a variety of neurodegenerative disorders including Machado-joseph disease (MJD) and also found to be potential therapeutic targets for many diseases including neurodegenerative disorders such as Huntington's disease and Spinocerebellar ataxias type 1 and 3 (Packer *et al*. 2008, Miyazaki *et al*. 2012, Cheng *et al*. 2013, Rodriguez-Lebron *et al*. 2013).

Bonini and colleagues were first to show the involvement of microRNAs in a MJD *D. melanogaster* model by mutating the dicer-1 enzyme, an important player for the biogenesis of microRNAs. Simultaneously, taking advantage of a genetic screening, the authors observed that the overexpression of the miR Bantam could alleviate neurodegeneration induced by the toxic ataxin-3 protein (Bilen *et al*. 2006). Another recent study evaluated the expression levels of microRNAs in serum samples from MJD patients observing that miR-25, miR-125b, miR-29a and miR-34b were

differentially expressed and therefore could be used as biomarkers for SCA3 (Shi *et al*. 2014).

Our study was designed to screen and identify differentially expressed miRNAs in a striatal lentiviral MJD mouse model (Alves *et al*. 2008, Simoes *et al*. 2012). The identified dysregulated miRNAs were also investigated in other MJD models and their potential as a target for therapy was evaluated in a *D. melanogaster* MJD model. This model is characterized by severe loss of pigmentation in the eye and also decreased life span upon induction of human mutant ataxin-3 expression.

In this chapter, we present the complete miRNA expression profile of the mouse striatal tissue upon expression of mutant as compared to wild-type ataxin-3. Several miRNAs were found to be significantly dysregulated. Interestingly miR-10b (mmu-miR-10b-5p) was strongly up-regulated in this and in another transgenic MJD mouse model (Torashima *et al* 2008). To investigate whether inhibition of miR-10 could be beneficial in MJD, flies expressing a miR-10 inhibitor were crossed with MJD flies generating a MJD fly model where miR-10 expression is repressed. MJD flies with miR-10 inhibitor resulted in an increased life span compared to the MJD flies with a control miR inhibitor clearly suggesting that miR-10 inhibition may be associated with the protective mechanism.

2.3 Materials and Methods

2.3.1 Animals

Four-week-old C57BL/6J mice were obtained from Charles River. The animals were housed in a temperature-controlled room maintained on a 12 h light/12 h dark cycle. Food and water were provided ad libitum. The experiments were carried out in accordance with the European Community directive (2010/63/EU) for the care and use of laboratory animals. The researchers received adequate training (FELASA certified course) and certification to perform the experiments from the Portuguese authorities (Direcção Geral de Veterinária).

2.3.2 Lentiviral vector production

Lentiviral vectors encoding for mutant ataxin-3 with 72 CAG repeats and wild type ataxin-3 with 27 CAG repeats (Alves *et al*. 2008), miR-10b tough decoy RNA inhibitor, miR-negative tough decoy RNA inhibitor were produced in human embryonic kidney 293T cells with a four plasmid system as previously described (de Almeida *et al*. 2002). The lentiviral particles were resuspended in 1% bovine serum albumin in sterile PBS. The viral particle content of batches was determined by assessing HIV-1 p24 antigen levels (Retro Tek, Gentaur). Viral stocks were stored at −80°C.

2.3.3 Stereotaxic injection into the striatum

Five-week-old C57BL/6J mice were anaesthetized with avertin (14 µl g^{-1} and 250 mg kg^{-1} intraperitoneally). One thousand and fifty nanograms of p24 antigen of lentiviral vectors in a final volume of 3 µl encoding for human wild type ataxin-3 or mutant ataxin-3 were stereotaxically injected into the striatum in the following coordinates: anteroposterior: +0.6 mm, lateral: ±1.8 mm, ventral:−3.3 mm and tooth bar: 0 for the development of the striatal lentiviral MJD mouse model (Alves, Regulier et al. 2008, Simoes, Goncalves et al. 2012).

Five-week-old mice were anaesthetized with avertin (14 µl g^{-1} and 250 mg kg^{-1} intraperitoneally). Three hundred and fifty nanograms of p24 antigen of lentiviral vectors in a final volume of 4 µl encoding for human mutant ataxin-3 and miR-10b TuD inhibitor were stereotaxically co-injected into one side of the hemisphere and human mutant ataxin-3 and miR-neg TuD inhibitor into other side of the hemisphere of the mouse striatum in the following coordinates: anteroposterior: +0.6 mm, lateral: ±1.8 mm, ventral:−3.3 mm and tooth bar: 0.

2.3.4 Stereotaxic injection into the cerebellum

LV were injected into the cerebellar vermis of C57BL/6J wild-type mice. One group was injected with LV encoding human mutant ataxin-3 with 72 CAG repeats (Atx3MUT), while a control group was injected with vectors encoding human wild-type ataxin-3 (Atx3WT). The animals received a single 6-µl injection of LV (250,000 ng of p24/ml) at a rate of 0.25 µl/min by means of an automatic injector (Stoelting Co., Wood Dale, IL, USA), at the following coordinates of −1.6 mm rostral to lambda, 0 mm midline, and 1 mm ventral to the skull surface, with the mouth bar set at −3.3 mm. After injection, the syringe needle was left in place for an additional 5 min to allow for the diffusion of vectors and minimize backflow.

2.3.5 Total RNA extraction from mouse tissue, cells and flies

Total RNA was extracted using miRCURY™ RNA Isolation Kits (Exiqon). For the extraction of total RNA from the mouse tissue, mice were sacrificed by cervical dislocation and striatal punches or total cerebellum were stored at -80°C. For the extraction of total RNA from the flies, the whole *D. melanogaster* was stored at -20°C and then the head of the fly was cut from the body using a surgical blade by viewing the flies through a microscope. All samples were treated with DNAse digestion (Qiagen) during extraction. The quantity of total RNA was measured by optical density (OD) using a Nanodrop 2000 spectrophotometer (Thermo Scientific) and total RNA was stored at -80°C.

2.3.6 miRNA microarray

miRNA microarray was performed by LC Sciences based on their proprietary µParaflo®Microfluidic Biochip technology which is updated with miRBase. Each sequence is repeated twice on the chip to ensure consistency. miRNA microarray procedure includes sample labeling, array hybridization, image data processing and in-depth data analysis. No reference miRNA was used for these arrays as the control groups were compared with the disease groups for statistical analysis.

2.3.7 Real Time qRT-PCR for miRNA

cDNAs were synthesized from total RNA using a TaqMan MicroRNA Reverse Transcription Kit combined with specific TaqMan MicroRNA Assays (Applied Biosystems) for each miRNA (miR-10b-5p ID002218; let-7b ID002619; let-7i ID002221; miR-181a ID000480; miR-27b ID000409; miSnoRNA202 ID001232) according to manufacturer's instructions. Real-time PCR was performed using TaqMan®Universal PCR Master Mix II with UNG and specific TaqMan® probes described previously. Small nucleolar RNA 202 (SNOR202) used as a reference to quantify the miRNA expression levels for all the miRNAs described previously. All reactions were performed in duplicate at a final volume of 10 µl per well. Relative miRNA quantification was performed using the ΔCt method for genes with the same amplification efficiency.

2.3.8 SH-SY5Y cell line culture and transduction

SH-SY5Y cells were maintained in DMEM/F12 (Gibco) medium supplemented with 10% fetal bovine serum (Life Technologies) and 1% Penicillin/Streptomycin (Gibco).
For the transduction of SH-SY5Y cells, 24 hours after plating, the culture medium was replaced with fresh medium containing lentivirus encoding for wtATXN3 or mutATXN3 (400ng of P24 per 200 000 cells). Twelve hours later the medium was replaced with regular complete medium and cells were cultured and expanded in standard conditions.

2.3.9 *D. melanogaster* strains and husbandry

The following lines were used for MJD/ SCA3 models: elavGS> UAS-Atxn3-70Q and elavGS> UAS-Atxn3-19Q (Reinhardt, Feuillette et al. 2012). Flies with miR-10 inhibitor RNAi construct were obtained from Bloomington (Perkins *et al*. 2015). Atxn3 lines were crossed with miR-10 inhibitor flies and the *D. melanogaster* strains were raised on standard cornmeal-yeast agar medium with or without RU486 (Mifepristone, Betapharma-Shanghai Co., Ltd., China) at a final concentration of 1% ethanol and 200 µg/ml RU486. Fly cultures and crosses were carried out at 25°C. For longevity, once in two days, the flies were transferred to new tubes containing fresh media with or without RNU486 and these procedures was repeated until all the flies die. For miRNA and mRNA expression analysis, once in two days, the flies were transferred to new tubes containing fresh media with or without RNU486 for seven days and then they were stored at -80°C.

2.3.10 Statistical analysis

Statistical analysis was performed with paired or unpaired Student's t-test and one-way or two-way analysis of variance. Results are expressed as mean±s.e.m. Significant thresholds were set at $P<0.05$, $P<0.01$ and $P<0.001$, as defined in the text

2.4 Results

2.4.1 Differentially expressed miRNAs in a striatal lentiviral MJD mouse model

To characterize transcriptional abnormalities and to identify microRNAs whose levels are dysregulated in MJD, we took advantage of a previously developed striatal lentiviral MJD mouse model (Alves *et al*. 2008, Simoes *et al*. 2012). This was performed by using lentiviral vectors encoding mutant ataxin-3 with 72 CAG repeats to transduce one striatum hemisphere (right) and wild type ataxin-3 with 27 CAG repeats to transduce the other hemisphere as internal control (left) (Fig 1A and 1B). Two weeks post-injection, mice were sacrificed and total RNA was extracted from the ataxin-3 expressing region (right and left striatum) and miRNA microarray was performed.

miRNA microarray profiling revealed a large set of miRNAs that are differentially expressed between the hemispheres expressing mutant ataxin-3 and wild type ataxin-3 with $P<0.05$ and are presented in Fig 1C, whereas miRs with $P>0.05$ were not shown in the Heatmap. Of interest, 8 miRNAs were selected based on central nervous system expression and taking into account those conserved between different species, particularly regarding human miRNAs. Furthermore, miRs with $P>0.05$ were selected for further validation using qRT-PCR. QPCR analysis demonstrated a significant downregulation for let-7b, let-7i, miR-30e, miR-181a and miR-27b (Fig 1D). Moreover, microarray data indicated that miR-10b was significantly up-regulated upon mutant ataxin-3 overexpression, a result which was validated upon qRT-PCR analysis (Fig 1E).

Among the dysregulated miRNAs, miR-10b presented the most robustly increased expression levels upon mutant ataxin-3 overexpression, indicating that it could be a potential candidate for a miRNA based therapy towards MJD.

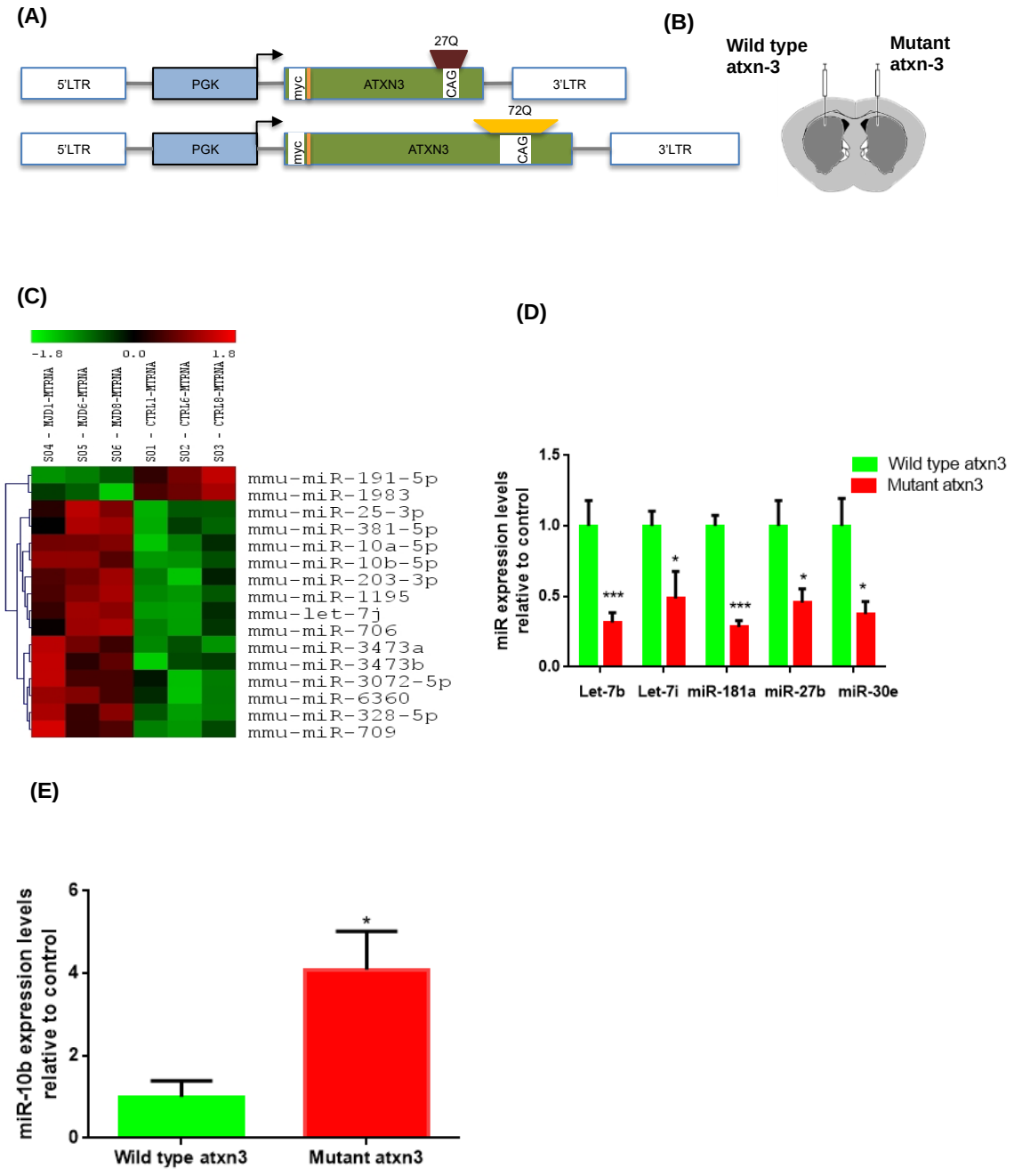

Figure 2.1. Deregulated miRNAs in the striatal lentiviral MJD mouse model. (A) Schematic representation of lentiviral constructs encoding for human wild type ataxin-3 or mutant ataxin-3 (Alves *et al*. 2008). **(B)** Schematic representation of stereotaxic procedure for mice. Lentiviral vectors encoding wild type and mutant ataxin-3 were injected bilaterally in the striatum of 5 weeks old C57/BL6 mice (Alves *et al*. 2008, Simoes *et al*. 2012). **(C)** Heat map of miRNA profiles showing differential expression in the mice injected with the lentiviral vectors encoding mutant ataxin-3 in one hemisphere compared with wild type ataxin-3 injected in the other hemisphere of the striatum. Colours represent relative signal intensities. Red and green colours denote high and low expression of miRNAs respectively (n=3). (D, E) Validation of miRNA microarray results by qRT-PCR. **(D)** 5 miRNAs were down-regulated upon mutant ataxin-3

overexpression (n=8). **(E)** miR-10b was robustly up-regulated in the samples injected with human mutant ataxin-3 by qRT-PCR showing the similar pattern that was seen in the miRNA microarray (n=8). Statistical analysis was performed using unpaired Student's *t*-test (C and D) or paired Student's *t*-test (E) (*$P < 0.05$; **$P < 0.01$; ***$P < 0.001$). Data are expressed as mean ± SEM; SEM = standard error of the mean.

2.4.2 miR-10b expression levels in other MJD models

Next, we evaluated the levels of mir-10b in other MJD models from cells to human post-mortem brain tissue. For this purpose, we started by using qRT-PCR to check miR-10b expression in human post-mortem brain tissue. Although no statistically significant changes were observed, there was a trend towards upregulation (Fig. 2.2A). To further investigate miR-10b up-regulation in another MJD model, we quantified miR-10b expression levels in cerebellum samples of a transgenic mouse model of MJD at 8 weeks of age. We found that miR-10b levels were upregulated in accordance with the striatal lentiviral MJD mouse model (Fig. 2.2B). Similarly, SH-SY5Y cell line infected with mutant ataxin-3 shows a trend towards up-regulation compared to the wild type ataxin-3 (Fig. 2.2D). Furthermore, we also quantified miR-10b expression in cerebellum samples from a lentiviral based MJD model and found no differences between MJD and the control group (Fig. 2.2C). Even though, miR-10b is significantly up-regulated in some but not in all the discussed MJD models, overall our results suggest a trend towards upregulation. However, increasing the sample size would give a better understanding of the miR-10b expression levels.

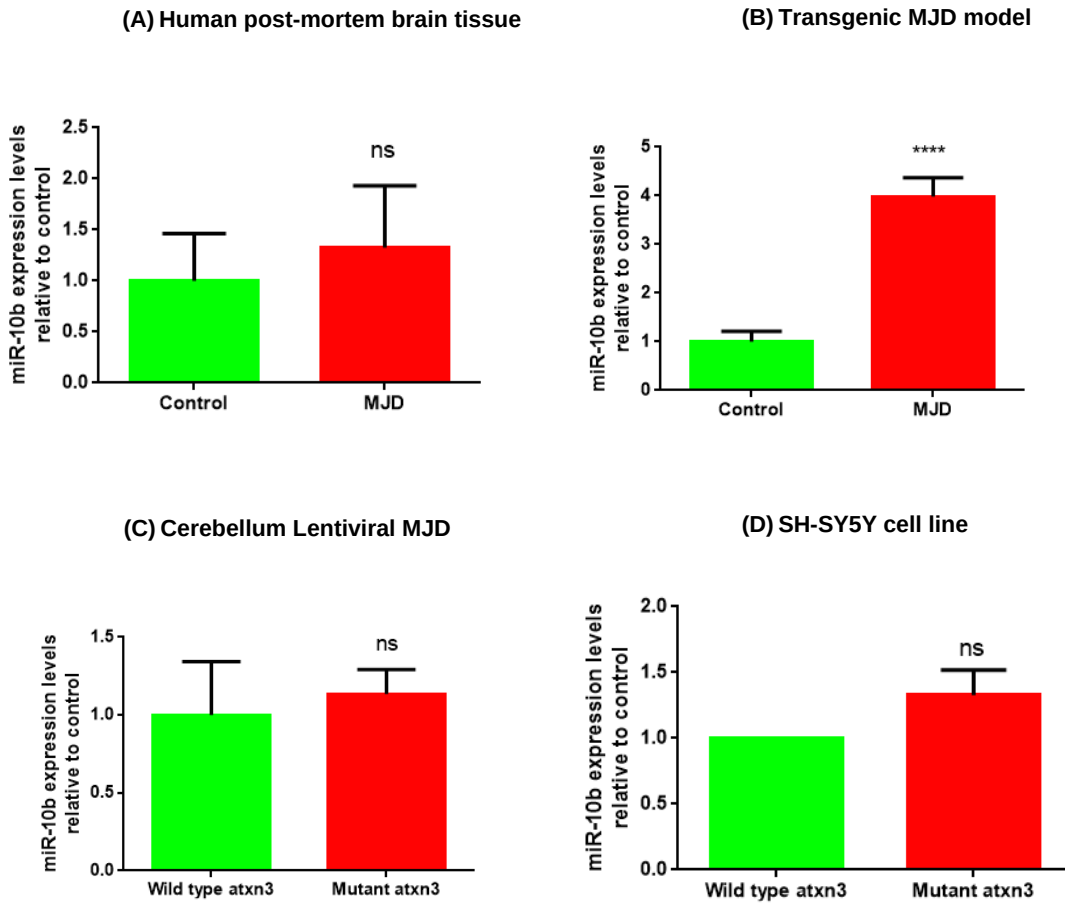

Figure 2.2. miR-10b expressions in other MJD model. (A) miR-10b expression in the human post-mortem brain tissue showed a tendency for up-regulation compared with the controls (N=6/6). **(B)** miR-10b expression levels were significantly upregulated in the cerebellum samples of the MJD transgenic mice (Torashima *et al*. 2008) at 8 weeks of age compared to the control (N=16/8). **(C)** There are no differences in miR-10b expression levels in the lentiviral-based cerebellum MJD model (N=9/9). **(D)** miR-10b expression levels were also quantified in SH-SY5Y cell line infected with wild type and mutant ataxin-3 and despite a tendency towards miR-10b upregulation in the SH-SY5Y cell line infected with mutant ataxin-3 compared to the wild type ataxin-3, no significant differences were observed (N=6/6). Statistical analysis was performed using unpaired Student's *t*-test (B, C and D) or paired Student's *t*-test (D) (**P* < 0.05; ***P* < 0.01; ****P* < 0.001). Data are expressed as mean ± SEM; SEM = standard error of the mean.

2.4.3 miR-10b expression in the MJD *D. melanogaster* model

Next we investigated the levels of miR-10b in a fruit fly *D. melanogaster* model of MJD. For that we took advantage of a RU486 inducible MJD *D. melanogaster* model previously developed (Reinhardt *et al*. 2012). Two sets of control samples were used. Firstly, miR-10b expression levels in the flies where the ataxin-3 is expressed in neurons after RU486 feeding (elavGS> UAS-Atxn3-Q70 (abbreviated as EAT3 in the following) -RU100), were compared with the flies where ataxin-3 is not expressed in the absence of inducer (EAT3-RU0). Secondly, miR-10b expression levels in the flies where the ataxin-3 is expressed in neurons (EAT3-RU100) were compared with the flies where ElavGS driver is present but not the UAS-Atxn3-Q70 transgene, preventing ataxin-3 expression. No significant differences were observed between the MJD flies (EAT3-RU100) and the controls (EAT3-RU0 and Elavgs-RU100) (Fig. 2.3A and B). These results suggest that in this *D. melanogaster* model mutant ataxin-3 expression does not induce a transcriptional dysregulation of miR10b.

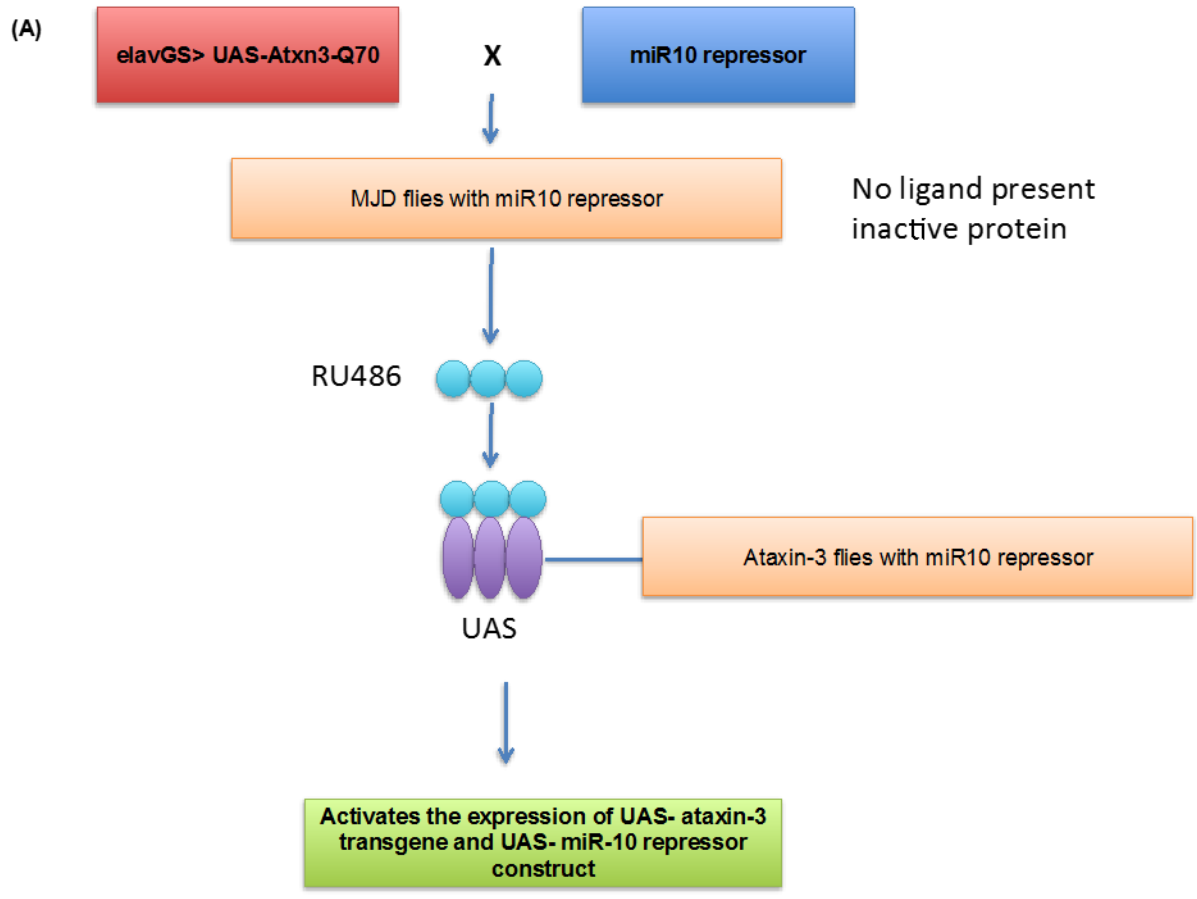

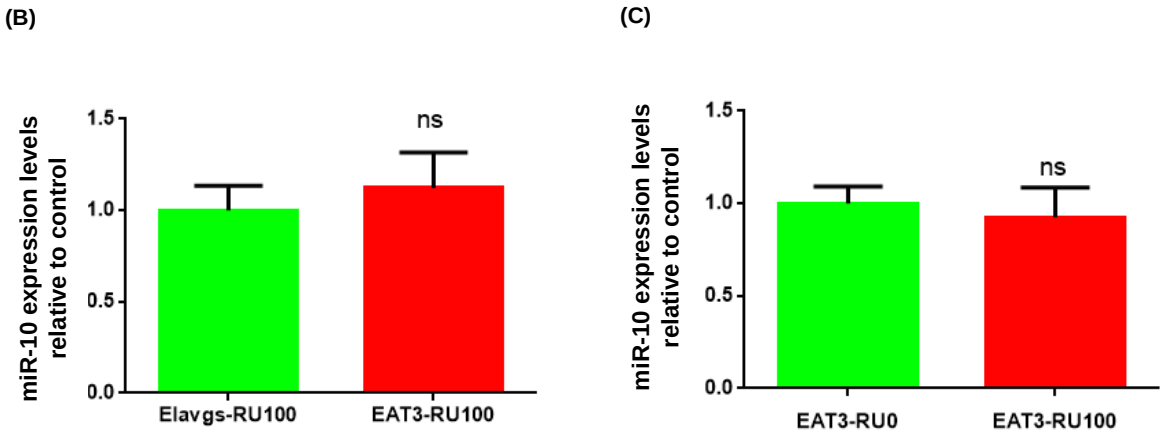

Figure 2.3. miR-10 expressions in MJD *D. melanogaster* model. (A) Schematic representation of the MJD transgenic *D. melanogaster* model with miR-10 repressor using GeneSwitch/UAS expression system. Using the elav promoter, the expression of the ataxin-3 and miR-10 repressor was driven in neuronal cells. In the absence of an activator RU486, crossed ataxin-3 flies with miR-10 repressor flies are expressed in neurons but remains transcriptionally inactive. Therefore ataxin-3 carrying 70Q and miR-10 repressor is not expressed. Delivery of RU486 in the food, makes ataxin-3 protein and miR-10 repressor becomes active and mediates the transcription of Ataxin-3 and miR-10 repressor construct in neurons. In addition, in all stages, the level of inactivation can be controlled with the concentration of RU486. **(B)** miR-10 expression in the flies reared in the presence of inducer (RU100 condition) where ataxin-3 is expressed compared with the flies where ataxin-3 construct is not present revealed no significant differences. **(C)** miR-10 expression in the flies where ataxin-3 is expressed (RU100 condition) was compared with the control flies where no ataxin-3 is expressed (RU0 condition). No significant difference in expression was observed.

2.4.4 Inhibition of miR-10 could not rescue the eye phenotype induced by the mutant ataxin-3 expression

Expression of a truncated expanded form of human Atxn3 (MJDQ78, Warrick and Bonini) in the developing fly eye with the GMR-GAL4 driver, causes retinal degeneration associated with eye depigmentation.

Although no differences in miR-10 expression were observed in the MJD flies, we crossed GMR-GAL4> MJDQ78 flies, with a miR-10 repressor line that expressed dsRNA directed against mir-10 (Perkins *et al*. 2015) or a RNAi control line (TRIP-HMS01569). We developed this MJD model with miR-10 inhibitor assuming that the

process controlled by miR-10 can be conserved in fly but not its regulation. However, miR-10 repression in MJD flies was not able to revert the pigmentation loss induced by eye expression of mutant ataxin-3 in both male (Fig. 2.4E) and female flies (Fig. 2.4G) compared to the control inhibitor flies (Fig. 2.4D and 2.4F).

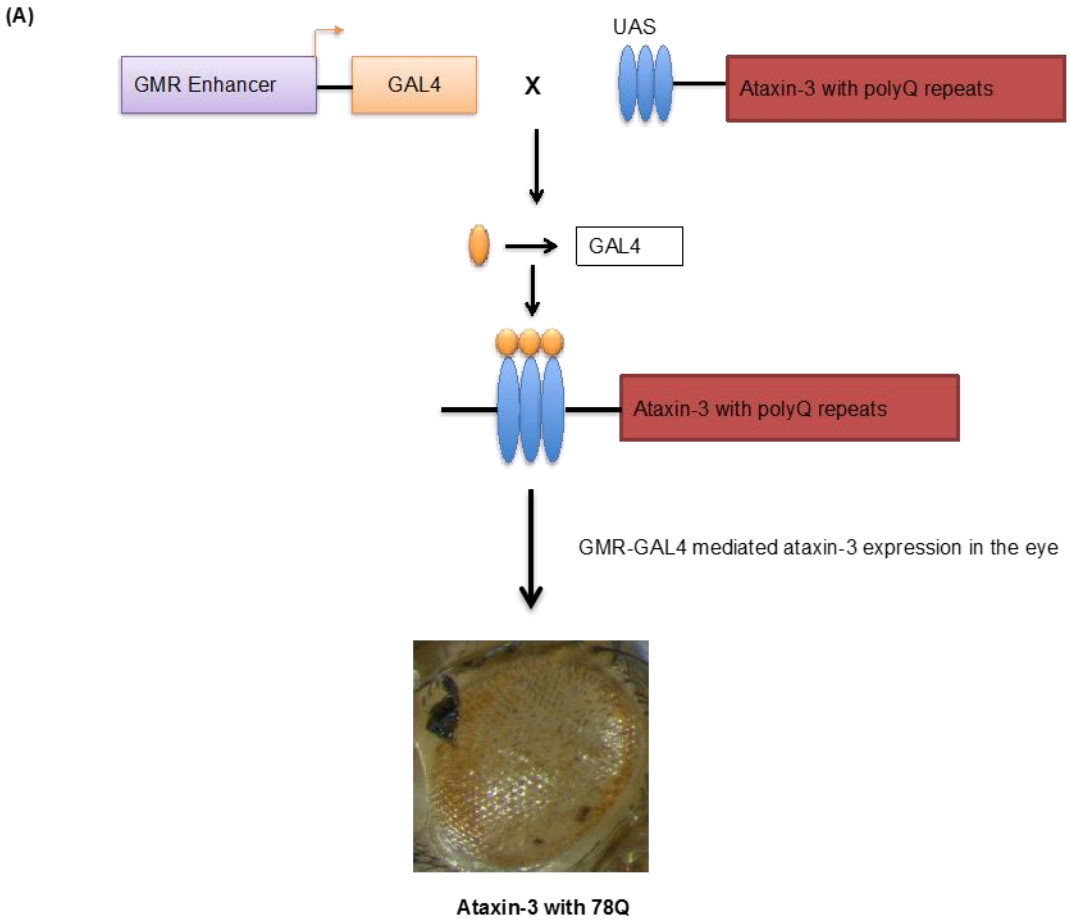

(B) GMR-GAL4/+ flies (male)

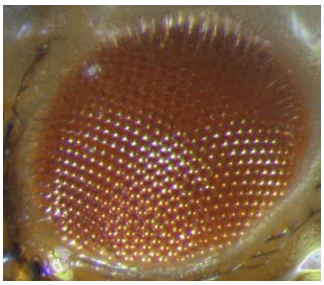

(C) GMR-GAL4/+ flies (female)

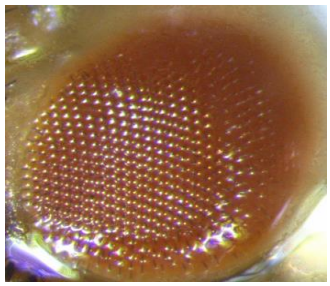

(D) miR-control inhibitor male

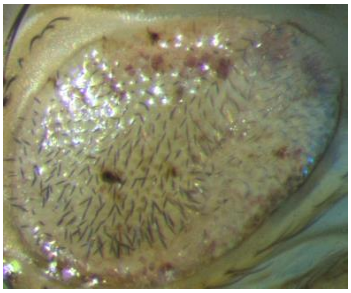

(E) miR-10 inhibitor male

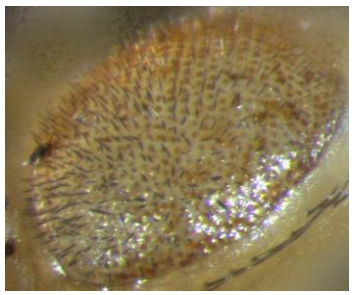

(F) miR-control inhibitor female

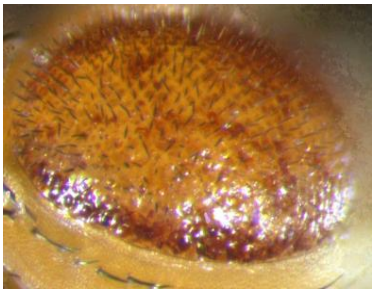

(G) miR-10 inhibitor female

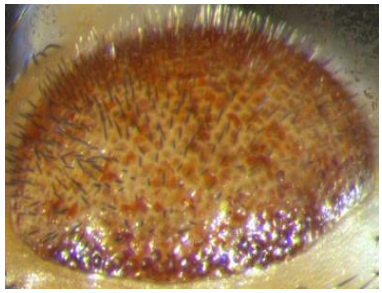

Figure 2.4. miR-10 inhibition did not rescue the eye phenotype induced by the mutant ataxin-3. Representative microscopic images of the eyes of *D. melanogaster* lines (2.4B-F). **2.4A)** Schematic representation of the *D. melanogaster* carrying GMR-GAL4/+ and 78Q in the eye **2.4B** and **2.4C** represent the wild type male and female flies used as a control. There is no difference in the eye phenotype between GMR-GAL4> MJDQ78 flies co-expressing the miR-10 inhibitor **(2.4E and 2.4G)** control construct **(2.4D and 2.4F)** for both male and female flies.

2.4.5 miR-10 inhibition extends the life span of MJD *D. melanogaster* model

Next, we decided to investigate whether miR-10 inhibition could extend the life span of MJD flies. For that, we crossed the elavGS> UAS-Atxn3-Q70 flies which have human mutant ataxin-3 expression in neurons in presence of RU, with the miR-10 inhibitor flies obtained from Bloomington (Perkins *et al*. 2015) in order to generate MJD flies with no or low expression of miR-10 levels. After performing a longevity assay we observed that miR-10 inhibition resulted in extended lifespan compared to MJD flies with a control line (TRIP-HMS01569) (Fig. 2.5A). However, the elongated life span was very short in female flies compared to the male flies (Fig. 2.5B). Furthermore, we checked the levels of CG9701, the klotho ortholog in *D. melanogaster*,in the MJD/miR-10 inhibitor flies as klotho has been previously shown to be involved with anti-ageing processes and since we also observed klotho has a trend towards up-regulation with miR-10b inhibitor treatment and could be a target of miR-10 in mice, as will be discussed in detail in the next chapter. We found that CG9701 has a trend towards up-regulation in the MJD flies crossed with miR-10 inhibitor compared to the miR-control inhibitor (Fig. 2.5C). These results suggest that miR-10 inhibition may play an important role in the protection against pathological Atxn3 during aging, possibly by modulating different genes involved in anti-ageing process such as klotho, which should be further evaluated in this model.

(A)

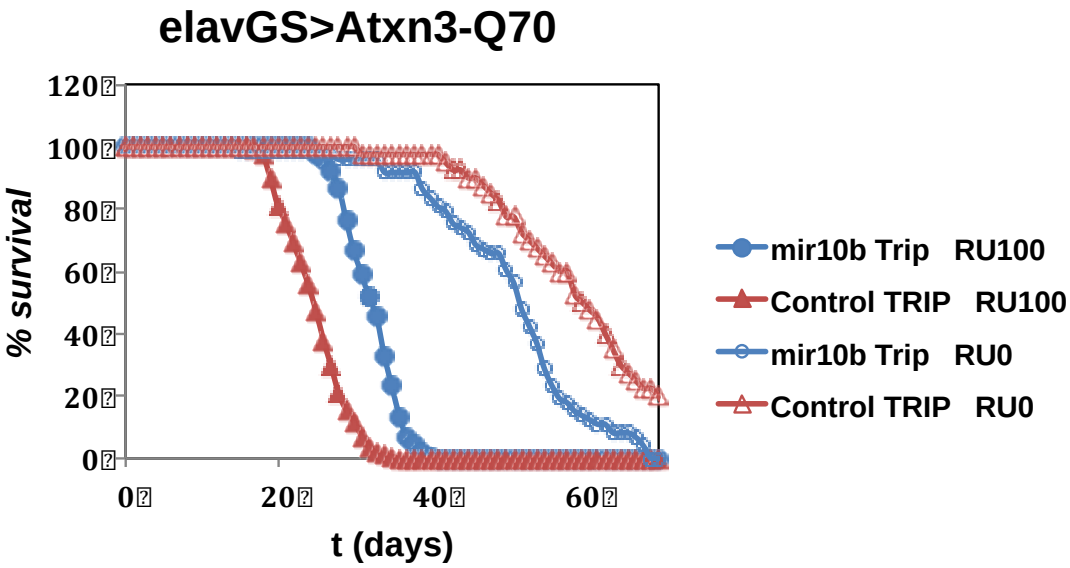
elavGS>Atxn3-Q70
120
100
80
60
40
20
0
% survival
0
20
40
60
t (days)
mir10b Trip RU100
Control TRIP RU100
mir10b Trip RU0
Control TRIP RU0

(B)

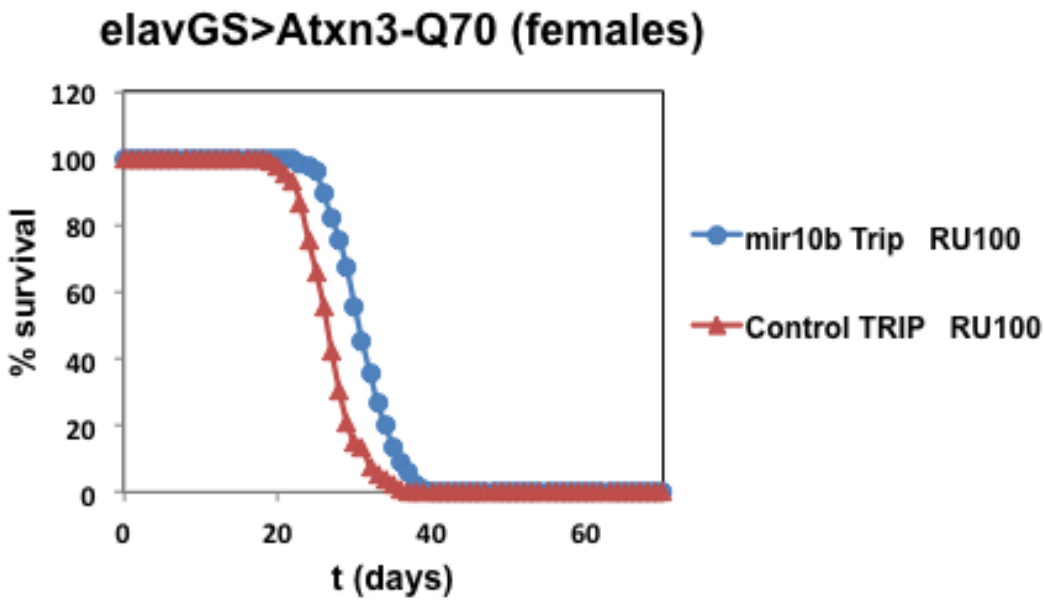
elavGS>Atxn3-Q70 (females)
120
100
80
60
40
20
0
% survival
0
20
40
60
t (days)
mir10b Trip RU100
Control TRIP RU100

(C)

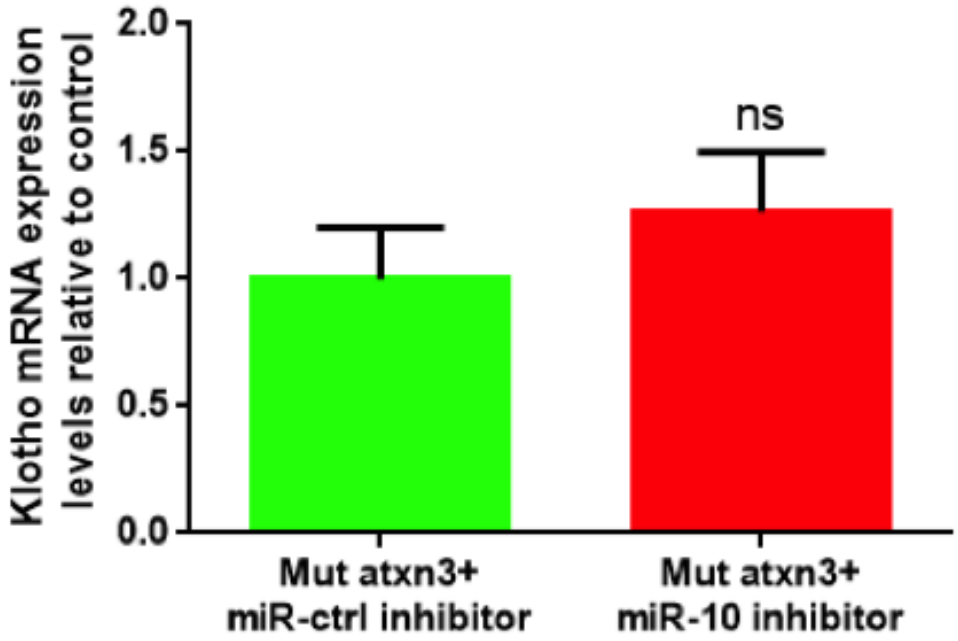

Figure 2.5. miR-10 inhibition extends the lifespan of MJD *D. melanogaster* model. (A) Life span shortened by the overexpression of human mutant ataxin-3 in the neurons was rescued by miR-10 inhibition in both male and female flies. **(B)** Life span expansion was not very high in the MJD *D. melanogaster* using only the female flies with miR-10 inhibition compared to the male flies. elavGS>Atxn3-Q70 express Atxn3-Q70 expression in neurons when RU486 is present (RU100 condition) but not in its absence (RU0 condition). miR10b inhibitor and control inhibitor corresponds to flies where miR-10b expression is inhibited and the control inhibitor respectively. **(C)** Klotho mRNA expression levels were quantified in MJD/miR10 inhibitor flies and has a trend towards up-regulation in MJD/miR10 inhibitor flies compared with MJD/miR control inhibitor flies.

2.5 Discussion

In the present study, we provide evidence of microRNA dysregulation in genetic animal models of MJD and show that inhibition of miR-10b extended the life span of MJD flies.

We investigated transcriptional deregulation in MJD focusing on miRNAs, first using a striatal lentiviral MJD mouse model previous developed by our group (Alves *et al*. 2008, Simoes *et al*. 2012). This model allows precise quantitative analysis of aggregation, neuronal dysfunction and degeneration in a region physiologically relevant to the disease when taking into account both our previous data (Alves et al. 2008, Simoes *et al*. 2012) and recently reported data showing that changes in striatal volume were the most significant and sensitive magnetic resonance imaging (MRI) markers of progression of MJD/SCA3 disease in patients (Reetz *et al*. 2013).

MicroRNAs are non-coding RNA molecules that have been shown to play an important role in many neurodegenerative diseases, and possibly MJD (Bilen *et al*. 2006, Miyazaki *et al*. 2012, Cheng *et al*. 2013, Rodriguez-Lebron *et al*. 2013, Huang *et al*. 2014, Shi *et al*. 2014). Therefore, we investigated microRNA deregulation in MJD. For this, we screened the miRNA profile in a striatal lentiviral MJD mouse model and found that many miRNAs were differentially expressed upon mutant ataxin-3 overexpression. Let-7b, let-7i, miR-181a, miR-27b and miR-30e in particular were downregulated, while miR-10b was robustly upregulated upon mutant ataxin-3 over expression.

We focused on miR-10b for further analysis. This upregulation of miR-10b in the striatal MJD model is in line with the previous findings showing very high expression of miR-10b in postmortem brain tissue from patients of another polyglutamine disease, Huntington's disease (Hoss *et al*. 2015). Moreover, miR-10b upregulation is also associated with the neuropathological involvement and striatum was the region subjected to change. A significant relationship was observed between miR-10b upregulation and CAG length-adjusted age of onset in Huntigton's disease (Hoss *et*

al. 2015). miR-10b is also abundantly expressed in tumors, glioma cells and also in the glioblastoma stem cell lines but absent in normal brain cells. Inhibition of miR-10b has been reported to promote reduction of glioma cell growth (Sasayama *et al*. 2009, Gabriely *et al*. 2011, Guessous *et al*. 2013). Furthermore, our data also show that miR-10b is robustly and significantly upregulated in a transgenic MJD mouse model further reinforcing what was observed in the striatal lentiviral model (Torashima *et al*. 2008). Moreover, miR-10b expression levels were also checked in human post-mortem brain tissue and in a SH-SY5Y cell line infected with mutant ataxin-3 and wild type ataxin-3 where a trend towards up-regulation was observed. These evidence clearly suggest that miR-10b is upregulated not only in MJD but also in other central nervous system diseases, having the potential to be used as a biomarker of neurodegeneration.

In the second part of the study, miR-10 expression was inhibited in the MJD *D. melanogaster* model. Even though, miR-10 inhibition did not rescue the eye phenotype induced by the mutant ataxin-3, miR-10 inhibition was able to extend the life span of the MJD flies. miR-10 could be targeting genes involved in the ageing process. Previous findings from Morimoto's group showed that elongation of life span delays the onset of polyQ associated aggregation and toxicity (Morley *et al*. 2002). Therefore our findings may be relevant not only on the extension of the life span but also regarding the reduction of the toxicity induced by the toxic polyQ-expanded ataxin-3 protein. Furthermore, small heat-shock proteins, which are involved in promoting longevity, were also shown to delay the onset of aggregation induced by the expanded polyglutamine protein (Hsu *et al*. 2003). Further investigation will help us to clarify whether the genes involved in the elongation of the life span of the MJD flies, also modify the toxicity and aggregation properties of mutant ataxin-3, which should be checked upon the treatment with miR-10 inhibitor. Altogether, these results suggest an important role for miR-10 in the ageing and MJD pathogenic processes.

CHAPTER 3

Re-establishing the normal levels of miR-10b reduces mutATXN3 inclusions and associated neuropathology in a striatal lentiviral MJD mouse model

3.1 Abstract

Machado-Joseph disease is a fatal neurodegenerative disorder, which belongs to the family of polyglutamine diseases. Currently, there is no effective therapy to delay or modify disease progression. In this context, the delivery of microRNAs that were previously shown to be downregulated in the disease condition or the delivery of miRNA inhibitors that were found to be up-regulated in the disease condition represents a promising approach to treat MJD. Based on this hypothesis, we cloned a miR-10b inhibitor using a tough decoy RNA strategy into a lentiviral backbone in order to achieve long term expression of the microRNA inhibitor *in vivo*. Lentiviral vectors encoding for miR-10b TuD inhibitor were injected in the striatum of the mouse brain. The treatment with the miR-10b inhibitor significantly reduced the number of mutant ataxin-3 inclusions and associated neuronal dysfunction *in vivo*. In addition, we identified transthyretin as a target of miR-10b, a promising candidate for further studies evaluating its role in the pathogenesis of MJD. In conclusion, our results identified a novel miR-based therapeutic strategy towards the treatment of MJD.

3.2 Introduction

Machado-Joseph disease (MJD), also known as spinocerebellar ataxia type 3 (SCA3), is an autosomal dominant neurodegenerative disorder caused by an expanded polyglutamine repeat in the coding region of the ATXN3/MJD1 gene (Kawaguchi *et al*. 1994) that confers a toxic gain of function to the ataxin-3 protein (Rubinsztein *et al*. 1999, Zoghbi 2000, Duenas *et al*. 2006). Ataxia and rigidity, dystonia and peripheral neuropathy, bulging, staring eyes and parkinsonism are the most common symptoms that are developed in MJD patients from early to mid-age (Paulson 2007). Neuronal intranuclear inclusions are a pathological hallmark of MJD (Paulson *et al*. 1997) resulting in neuronal dysfunction and degeneration in selective brain regions such as the thalamus, substantia nigra, striatum, cerebellum and brain stem (Yamada *et al*. 2008, Reetz *et al*. 2013). Despite extensive research has been carried out in MJD, current pharmacological only to improve specific symptoms but not to modify or delay the course of disease.

Recent evidence suggests that transcriptional dysregulation may play a crucial role in the pathogenesis of polyQ diseases. Previous studies have reported that the transcription factor (TATA-binding protein) and transcription co-factor (CREB binding protein) are incorporated into nuclear inclusions caused by mutant ataxin-3 (Steffan *et al*. 2000, Li *et al*. 2002). Alterations in the numerous mRNA transcripts such as PLC β4 or synaptotagmin, CaMKK- α, MKP-1, myosin Va or NeuroD1 have been reported in a MJD/SCA3 transgenic mouse model (Chou *et al*. 2008). Restoring the levels of specific mRNA transcripts in transgenic mice using T1-11, JMF1907 and HDAC inhibitor sodium butyrate (Chou *et al*. 2011, Chou *et al*. 2015) or in a *D. melanogaster* model using the HDAC inhibitor vaproic acid (Yi *et al*. 2013) was able to mitigate the neurodegeneration induced by mutant ataxin-3 (Yi *et al*. 2013, Chou *et al*. 2015).

MicroRNAs belong to the family of small non-coding RNAs and function as a regulator of gene expression (Ambros 2004, Bartel 2004). MicroRNAs have been

reported to play a significant role in many diseases including Machado-joseph disease (MJD) being used as a therapeutic approach to treat different diseases such as Huntington's disease, Spinocerebellar ataxia type 1 and 3 and SBMA (Packer *et al*. 2008, Miyazaki *et al*. 2012, Cheng *et al*. 2013, Rodriguez-Lebron *et al*. 2013). The importance of microRNAs was first shown in the MJD *D. melanogaster* model (Bilen, *et al*. 2006). More recently, miR-25 was reported to directly target ATXN3 while overexpression of miR-25 resulted in alleviation of pathology in a cellular model of MJD (Huang *et al*. 2014).

Our study was designed in order to re-establish the levels of miR-10b in a striatal lentiviral MJD mouse model in order to evaluate its potential as a target for therapy in MJD (Alves *et al*. 2008, Simoes *et al*. 2012). To investigate whether reinstating normal miR-10b levels would alleviate MJD neuropathology we used lentiviral vectors to inhibit miR10b expression in the striatum of the MJD model and found a significant reduction in neuronal dysfunction and neurodegeneration. In addition, we explored the targets of miR-10b and identified transthyretin as a direct target for miR-10b. Furthermore, we also cloned the human transthyretin into the lentiviral construct and validated the transthyretin expression in the HEK293T cells using qRT-PCR and western blot upon overexpression of human transthyretin. Our findings clearly indicate that miR-10b and possibly transthyretin could be potential targets for MJD therapy.

3.3 Materials and Methods

3.3.1 Construction of miR-10b Tough decoy RNA inhibitor (TuD)

We designed two complementary oligonucleotides containing a miR-10b TuD cassette which after annealing where ligated into the pRNA-U6-TUD shuttle vector (Haraguchi *et al*. 2009). This plasmid was digested with EcoRI and HindIII for the cloning of the U6-miR-10b TUD cassette into pENTR/pSUPER+ (Addgene #17338). This vector was lately gateway recombined into LTR-SIN-PGK-GFP-WPRE-attR1-ccdb-attR2-LTR in order to generate final lentiviral TuD vector: LTR-SIN-PGK-GFP-WPRE-U6-10bTuD-LTR.

3.3.2 Cloning of transthyretin into a lentiviral backbone

A plasmid with human TTR (a kind gift from professor Maria Joao Saraiva, Instituto de Ciências Biomédicas Abel Salazar, University of Porto, Porto, Portugal). Both the TTR plasmid and the lentiviral backbone construct were digested with BamHI and the human transthyretin sequences were ligated into the lentiviral construct with the PGK promoter (Alves *et al*. 2008)

3.3.3 Cell lines, culturing conditions and transfection

HEK293T cells were obtained from the American Type Culture Collection. HEK293T cells were maintained in Dulbecco's modified Eagle's medium (Sigma- Aldrich). Medium was supplemented with 10% heat-inactivated FBS (Gibco) and 1% Penicillin-Streptomycin (Gibco) and cultured at 37 °C under a humidified atmosphere containing 5% CO2. For the transfection of HEK293T cell line, cells were initially plated on tissue treated plates. After 24 hours, medium was changed and cells were transfected with a mixture of DNA/polethyleneimine complexes (MW40000, PolySciences) diluted in complete DMEM. Cell collection was performed 48 hours post-transfection.

3.3.4 Animals

Four-week-old C57BL/6J mice were obtained from Charles River. The animals were housed in a temperature-controlled room maintained on a 12 h light/12 h dark cycle. Food and water were provided ad libitum. The experiments were carried out in accordance with the European Community directive (2010/63/EU) for the care and use of laboratory animals. The researchers received adequate training (FELASA certified course) and certification to perform the experiments from the Portuguese authorities (Direcção Geral de Veterinária).

3.3.5 Lentiviral vector production

Lentiviral vectors encoding for mutant ataxin-3 with 72 CAG repeats and wild type ataxin-3 with 27 CAG repeats (Alves *et al*. 2008), miR-10b tough decoy RNA inhibitor, miR-negative tough decoy RNA inhibitor were produced in human embryonic kidney 293T cells with a four plasmid system as previously described (de Almeida *et al*. 2002). The lentiviral particles were resuspended in 1% bovine serum albumin in sterile PBS. The viral particle content of batches was determined by assessing HIV-1 p24 antigen levels (Retro Tek, Gentaur). Viral stocks were stored at −80°C.

3.3.6 Stereotaxic injection into the striatum

Five-week-old C57BL/6J mice were anaesthetized with avertin (14 µl g^{-1} and 250 mg kg^{-1} intraperitoneally). One thousand and fifty nanograms of p24 antigen of lentiviral vectors in a final volume of 3 µl encoding for human wild type ataxin-3 or mutant ataxin-3 were stereotaxically injected into the striatum in the following coordinates: anteroposterior: +0.6 mm, lateral: ±1.8 mm, ventral:−3.3 mm and tooth bar: 0 for the development of the striatal lentiviral MJD mouse model (Alves *et al*. 2008, Simoes *et al*. 2012).

Five-week-old C57BL/6J mice were anaesthetized with avertin (14 µl g^{-1} and 250 mg kg^{-1} intraperitoneally). Three hundred and fifty nanograms of p24 antigen of

lentiviral vectors in a final volume of 4 µl encoding for human mutant ataxin-3 and miR-10b TuD inhibitor were stereotaxically co-injected into one side of the hemisphere and human mutant ataxin-3 and miR-neg TuD inhibitor into other side of the hemisphere of the mouse striatum in the following coordinates: anteroposterior: +0.6 mm, lateral: ±1.8 mm, ventral:−3.3 mm and tooth bar: 0.

3.3.7 Total RNA extraction from mouse tissue and cells

Total RNA was extracted using miRCURY™ RNA Isolation Kits (Exiqon). For the extraction of total RNA from the mouse tissue, mice were sacrificed by cervical dislocation and the punches were stored at -80°C. All samples were treated with DNAse digestion (Qiagen) during extraction. The quantity of total RNA was measured by optical density (OD) using a Nanodrop 2000 spectrophotometer (Thermo Scientific) and total RNA was stored at -80°C.

3.3.8 mRNA microarray

mRNA microarray was performed by Comprehensive Biomarker Center based on Agilent's mRNA microarray platform. Sensitive and selective oligonucleotide probes allowed distinguishing between closely related mRNAs.

3.3.9 Real Time qRT-PCR for miRNA

cDNAs were synthesized from totalRNA using a TaqMan MicroRNA Reverse Transcription Kit combined with specific TaqMan MicroRNA Assays (Applied Biosystems) for each miRNA (miR-10b-5p ID002218; miSnoRNA202 ID001232) according to manufacturer's instructions. Real-time PCR was performed using TaqMan®Universal PCR Master Mix II with UNG and specific TaqMan® probes described previously. Small nucleolar RNA 202 (SNOR202) used as a reference to quantify the miRNA expression levels for all the miRNAs described previously. All reactions were performed in duplicate at a final volume of 10 µl per well. All data

were normalized to SNOR202 levels. Relative mRNA quantification was performed using the ΔCt method for genes with the same amplification efficiency.

3.3.10 Real time qRT-PCR for mRNA

mRNA microarray results were validated using qRT-PCR. Prior to the reverse transcription, 500ng of total RNA samples were treated with DNase to remove residual genomic DNA contamination and reverse transcribed to cDNA using iScript™ cDNA Synthesis Kit (Bio-Rad). qPCR was performed in the Step one plus Real-Time PCR system (Applied Biosystems). Primers for mouse hypoxanthinephophoribosyltransferase (HPRT), human mutant ataxin-3, mouse transthyretin and human transthyretin were pre-designed and validated by QIAGEN (QuantiTect primers, QIAGEN). Appropriate negative controls were prepared. The above transcripts were amplified from the cDNA using the specific primers and SsoAdvanced Universal SYBR Green Supermix (Bio-Rad). All data were normalized to mice hprt levels. All reactions were performed in duplicate at a final volume of 10 µl per well. The reactions were performed according to the manufacturer's recommendations: 95°C for 30 sec. followed by 45 cycles at 95°C for 5 sec, 55°C for 15 sec. All data were normalized to hprt levels. Relative mRNA quantification was performed using the ΔCt method for genes with the same amplification efficiency.

3.3.11 Immunohistochemistry

Five weeks post injection, mice were anesthetized using xylazine and ketamine mix (1:4) respectively and transcardially perfused with phosphate-buffered saline solution (PBS) for 5 mins followed by 4% Paraformaldehyde (PFA) for 20 mins for the fixation. Brains were placed in the 4% PFA solution for 24 hours for the post-fixation and incubated in 30% sucrose for 48 hours to cryoprotect the tissues. Brains were frozen at -80°C. Brains were cut coronally with the thickness of 25 µm using cryostat followed by the collection of the brain sections in a 48-multi well plates containing PBS with 0.05 µM sodium azide and stored at 4°C.

Brain sections were incubated with phenylhydrazine diluted in PBS (1:1000) for 30 mins at 37°C followed by washing the sections with PBS, blocking the brain sections for 1 hour to prevent the non-specific binding of the primary antibodies and then incubated with following primary antibodies mouse monoclonal anti-ataxin-3 (1H9; 1:5000), rabbit polyclonal anti-DARP-32 (1:1000), rabbit polyclonal anti-ubiquitin (1:1000) overnight at 4°C followed by the incubation of the brain sections with the biotinylated secondary antibodies (1:200). Finally brain sections were incubated both with the avidin-biotin-peroxidase for 30 mins at room temperature to form the complex (Vectastain ABC Elite kit, Vector Laboratories) and the substrate-diaminobenzidine tetrahydrochloride solution until the brown precipitate develops in the brain sections.

Images were captured using Zeiss Axioskop 2 plus microscope. Ubiquitin and ataxin-3 positive inclusion were quantified by scanning 8-11 coronal sections per animal in and around the striatum using 20x objective. Inclusions were counted manually using an image analysis tool (image J).

DARP-32 lesion was quantified by scanning 8-11 coronal sections per animal using 5x objective. The area of the striatum showing a loss of DARP-32 (neuronal marker) was estimated as previously described (Alves *et al*., 2008a) using an image analysis tool (image J). The volume was then calculated with the following formula: volume = $d(a_1+a_2+a_3 \ldots)$, where d is distance between serial sections (500 µm), and a_1, a_2, a_3 are DARPP-32-depleted region for individual serial sections.

3.3.12 Protein extraction and western blot

To extract the protein, brain samples were lysed in a mix containing radioimmunoprecipitation assay buffer solution (RIPA) and protease inhibitor followed by sonicating the samples for 5 sec pulses twice. Total protein lysates were stored at -20°C. The concentration of the protein was quantified using Bradford assay (Bio-Rad). 60 µg of protein was loaded in a sodium dodecyl sulphate-polyacrylamide gels (12% resolving gel and 4% stacking gel). The proteins were then transferred from the gel to a polyvinylidene difluoride (PVDF) membranes (GE

Healthcare) followed by blocking and incubating both with primary antibodies monoclonal anti-ataxin 3 antibody (1H9; 1:5000; Merck Millipore), mouse anti-β-actin antibody (AC74; 1:10000; Sigma Aldrich) overnight at 4°C and alkaline phosphatase-linked respective secondary antibody (1:10000; Thermo Scientific Pierce) for 2 hours at room temperature. The membranes were revealed using enhanced chemiflourescence substrate (GE Healthcare) and the bands were captured using chemiflourescence imaging (VersaDoc, Bio-Rad). Semi-quantitative analysis was carried out based on the optical density of scanned membranes (Quantity One® 1-D image analysis software version 4.5.2). The specific optical density was then normalized with respect to the amount of -β-actin loaded in the corresponding lane of the same gel.

3.3.13 Dual luciferase reporter assay

A dual luciferase reporter construct with 3'UTR region of transthyretin was acquired from GeneCopoeia. To evaluate the direct interaction of miR-10b to 3'UTR region of TTR, 2,75X10^4 HEK293T cells were seeded per well in 12-well plates (Fisher Scientific). 24 hours after plating, cells were transfected with 375ng of the luciferase reporter with 3'UTR of TTR and 375ng of miR-10b TuD inhibitor constructs per well (in triplicates) using polyethyleneimine as transfection reagent. Forty-eight hours post-transfection, cells were washed with 1x PBS and frozen at -80°C. Collected cells were lysed with FLAR-T buffer containing 20mM tricine, 100 μM EDTA, 25 μM $MgCl_2$, 2,67 mM $MgSO_4$, 17 mM DTT and 0,1% Triton in milli-Q grade water pH 7.8. For the lumninescent reaction, 30 μl of cell lysate were loaded on a 96 well plate and the firefly luminescence activity was measured on a luminometer after automatic injection of FLAR buffer containing 20mM tricine, 100 μM EDTA, 25 μM $MgCl_2$, 2,67 mM $MgSO_4$, 17 mM DTT, 250 μM ATP and 250 μM D-luciferin (Synchem). Renilla luminescence activity was measured after automatic injection of RAB buffer containing 1.1 M NaCl, 2.2 mM Na_2 EDTA, 0.22 M K_xPO_4, 0.44 mg/ml BSA, 1.3 mM NaN_3 and 1.43 mM coelenterazine (Life Technologies) in milli-Q grade

water pH 5.0 to use as a normalization control. Unless stated, all reagents were purchased from Sigma-Aldrich.

3.3.14 Statistical analysis

Statistical analysis was performed with paired or unpaired Student's t-test and one-way or two-way analysis of variance. Results are expressed as mean±s.e.m. Significant thresholds were set at $P<0.05$, $P<0.01$ and $P<0.001$, as defined in the text.

3.4 Results

3.4.1 Re-establishing the normal levels of miR-10b in the striatal lentiviral MJD mouse model

As miR-10b is strongly overexpressed in the MJD mouse model and the inhibition of miR-10b showed beneficial effects in the MJD *D. melanogaster* model. Next, we decided to re-establish the normal levels of the miR-10b in the striatal lentiviral MJD mouse model. For that, we cloned a miR-10b and miR-neg inhibitor using Tough decoy RNA Strategy (TuD) (Haraguchi *et al*. 2009) in a lentiviral vector system co-expressing eGFP under the control of a PGK promoter (Alves *et al*. 2008) (Fig. 3.1A). Lentiviral particles encoding for miR-10b or control inhibitors were bilaterally injected in to the mouse striatum along with lentivral particles encoding for human mutant ataxin-3 (Fig. 3.1B).

At 5 weeks post-injection, mice were sacrificed and the brain was extracted. The transduction efficiency of the virus encoding the tough decoy RNA was checked by fluorescence microscopy of the GFP reporter (Fig. 3.1C) showing that expression of the constructs was robust and spread over a large portion of the striatum. miR-10b expression levels were quantified by qRT-PCR in the mice treated with the miR-10b TuD inhibitor and miR-neg TuD inhibitor. Importantly, we found that miR-10b expression levels were reduced by 85% in the mice co-injected with mutant ataxin-3 and miR-10b TuD inhibitor compared with mutant ataxin-3 and miR-neg TuD inhibitor (Fig. 3.1D).

We next investigated the targets of miR-10b in the brain samples co-injected with mutant ataxin-3 and miR-10b TuD inhibitor in one hemisphere and mutant ataxin-3 and miR-neg TuD inhibitor in the other hemisphere. To identify the targets of miR-10b, a mRNA microarray was performed with the previous mouse striatum samples by Comprehensive Biomarker Center where they used agilent microarray platform. The quality of the RNA samples was checked using Agilent 2100 Bioanalyzer.

The mRNA microarray data revealed a large set of genes that were differentially expressed upon miR-10b inhibition (Fig. 3.1E). Several genes from the mRNA microarray were selected for further analysis based on their upregulation upon miR-10b TuD inhibition, based on their microarray result (P-value <0.05) and based on previously published data showing their beneficial effects against disease conditions. Among them, we found transthyretin to be significantly upregulated upon miR-10b TuD inhibition (Fig. 3.1F), a gene which was also found to be downregulated in the striatal lentiviral MJD mouse model analyzed in the previous chapter (Fig. 3G).

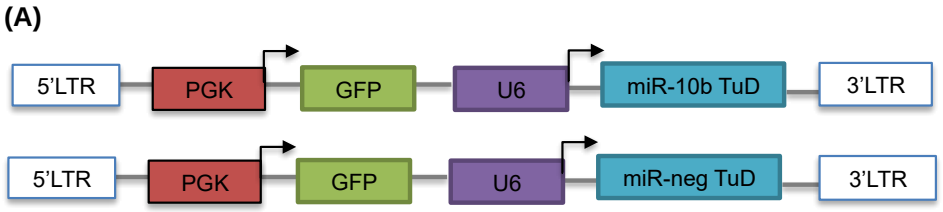
(A)
5'LTR
PGK
GFP
U6
miR-10b TuD
3'LTR
5'LTR
PGK
GFP
U6
miR-neg TuD
3'LTR

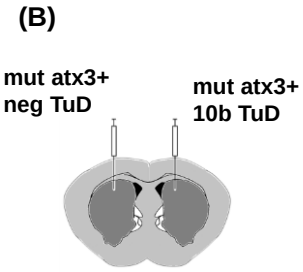
(B)
mut atx3+ neg TuD
mut atx3+ 10b TuD

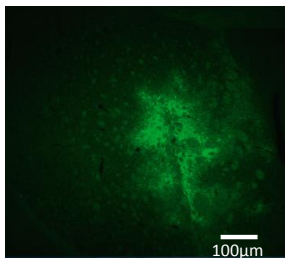
(C)
100µm

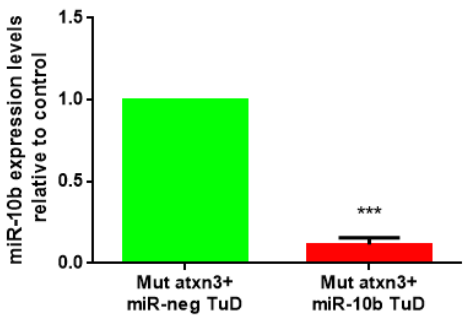
(D)
miR-10b expression levels relative to control
1.5
1.0
0.5
0.0
***
Mut atxn3+ miR-neg TuD
Mut atxn3+ miR-10b TuD

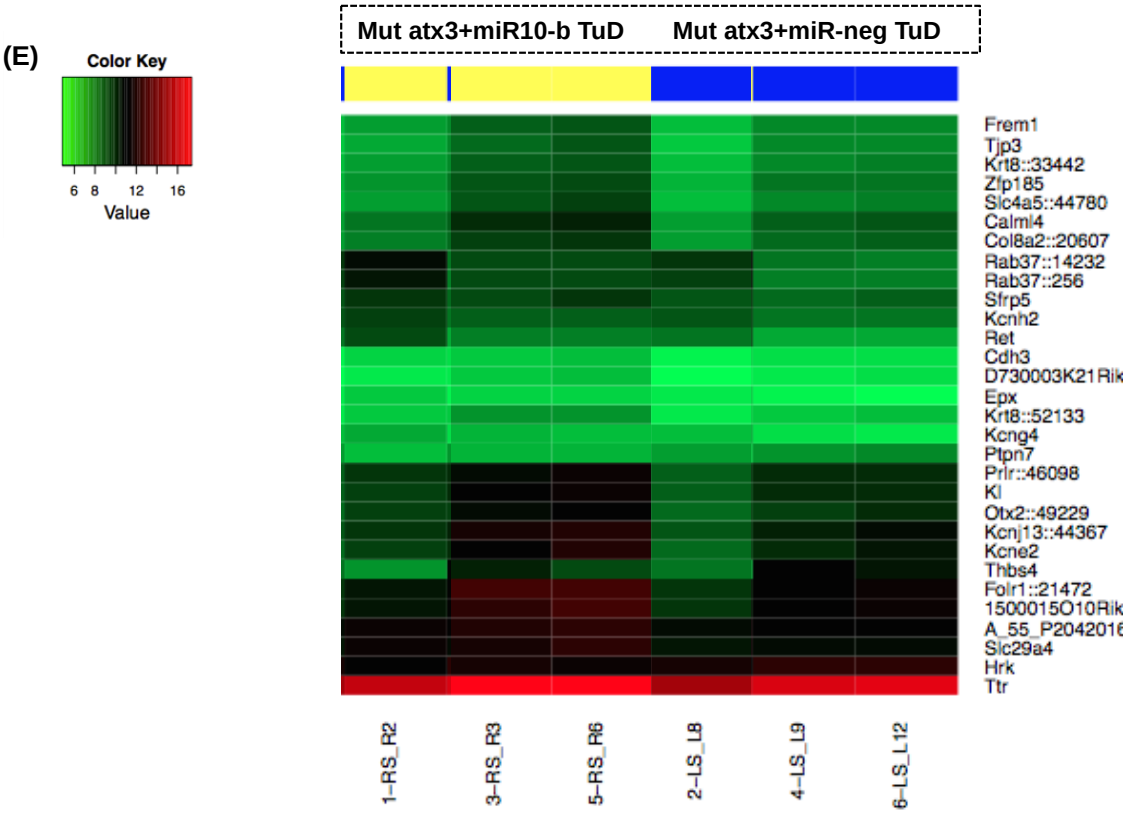
(E)
Color Key
6 8 12 16
Value
Mut atx3+miR10-b TuD
Mut atx3+miR-neg TuD
Frem1
Tjp3
Krt8::33442
Zfp185
Slc4a5::44780
Calml4
Col8a2::20607
Rab37::14232
Rab37::256
Sfrp5
Kcnh2
Ret
Cdh3
D730003K21Rik
Epx
Krt8::52133
Kcng4
Ptpn7
Prlr::46098
Kl
Otx2::49229
Kcnj13::44367
Kcne2
Thbs4
Folr1::21472
1500015O10Rik
A_55_P2042016
Slc29a4
Hrk
Ttr
1-RS_R2
3-RS_R3
5-RS_R6
2-LS_L8
4-LS_L9
6-LS_L12

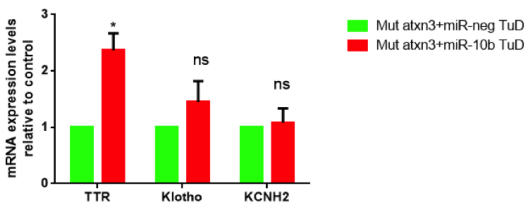
(F)
mRNA expression levels relative to control
3
2
1
0
*
ns
ns
TTR
Klotho
KCNH2
Mut atxn3+miR-neg TuD
Mut atxn3+miR-10b TuD

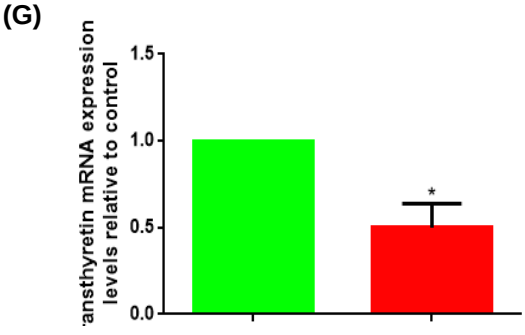
(G)
ansthyretin mRNA expression levels relative to control
1.5
1.0
0.5
0.0
*

Figure 3.1 Re-establishing the normal levels of miR-10b in the striatal lentiviral MJD mouse model. (A) Schematic representation of lentiviral vector encoding RNA Pol III-transcribed Tough Decoy (TuD) for miR-10b. **(B)** Schematic representation of stereotaxic procedure for mice. Lentiviral vectors encoding for mutant ataxin-3 and the miR-10b TuD inhibitor were co-injected in to the mouse striatum in one hemisphere and mutant ataxin-3 and the miR-Neg TuD inhibitor in the other hemisphere (internal control). **(C)** Transduction efficiency of the lentivirus encoding miR-10b tough decoy (TuD) inhibitor into the mouse striatum was seen using the GFP reporter expression. **(D)** 5 weeks post-injection, miR-10b expression level was quantified by qRT-PCR using TaqMan miRNA assays. **(E)** Heat map of mRNA profiles. Many genes were differentially expressed upon the co-injection of mutant ataxin-3 and the miR-10b TuD inhibitor when compared with the co-injection of mutant ataxin-3 and the miR-neg TuD inhibitor (n=3). **(F)** Few genes from the mRNA microarray were further validated by qRT-PCR and found only transthyretin was significantly up-regulated upon the co-injection of vectors encoding mutant ataxin-3 and miR-10b TuD (n=4). **(G)** Transthyretin mRNA expression levels were also quantified in the striatal lentiviral MJD mouse model and found to be down-regulated upon mutant ataxin-3 overexpression when compared with the wild type ataxin-3 overexpression (n=6). Statistical analysis was performed using paired Student's *t*-test (*$P < 0.05$; **$P < 0.01$; ***$P < 0.001$). Data are expressed as mean ± SEM; SEM = standard error of the mean.

3.4.2 Transthyretin (TTR) is a direct target of miR-10b

To investigate whether miR-10b directly regulates transthyretin levels by interacting with its 3'UTR, we cloned the transthyretin 3'UTR downstream of a dual luciferase cDNA construct (dual luciferase construct from genecopoeia). Firefly and Renilla luciferases were used as co-reporters for normalizing the assay (McNabb *et al*. 2005). HEK293T cells were co-transfected with the transthyretin-3'UTR luciferase construct and miR-10b TuD inhibitor and firefly/renilla luminescence ratio was quantified. We found that when co-transfected with the 3'UTR of transthyretin luciferase construct the miR-10b TuD inhibitor mediated a significant increase in the luciferase activity.

These results support the previous observations suggesting that miR10b inhibition leads to an overexpression of the transthyretin and suggests that the interaction between the miR10b and transthyretin is direct (Fig. 3.2B).

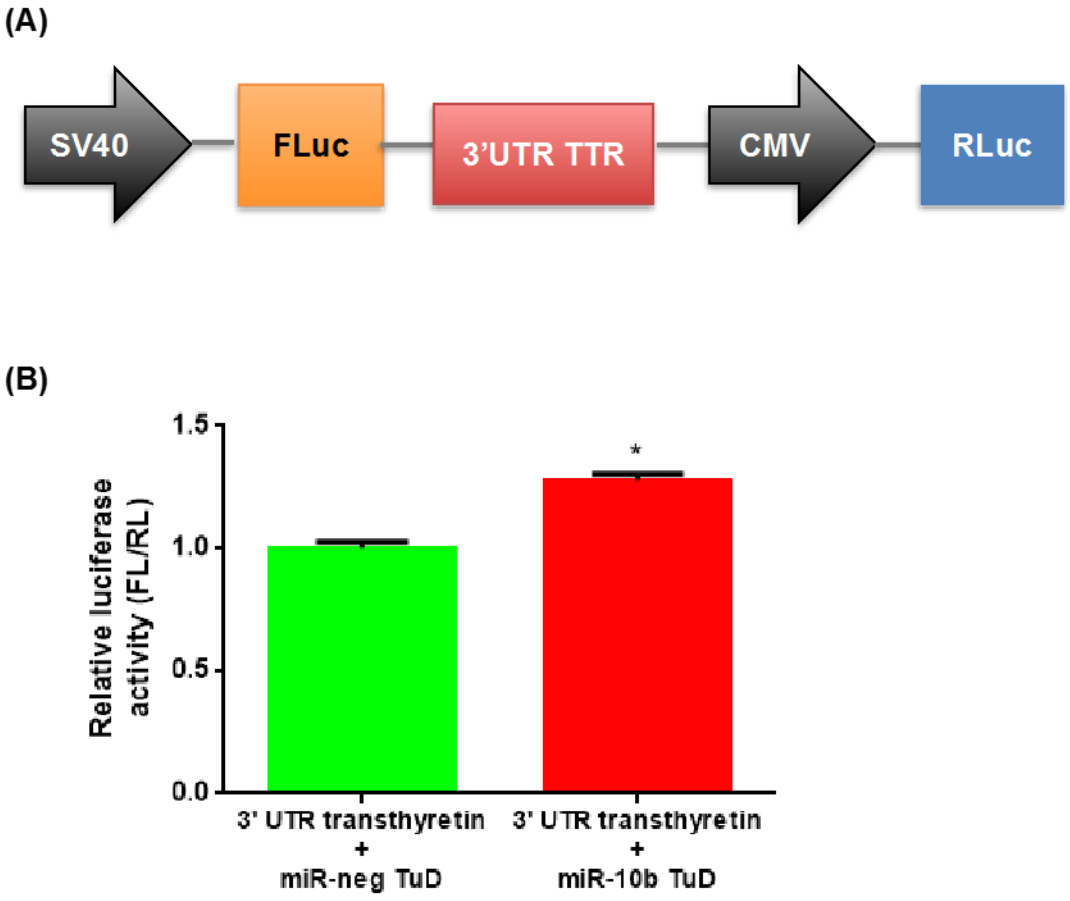

Figure 3.2 Transthyretin is the direct target of miR-10b in MJD mouse model. Direct interaction between miR-10b and the 3' UTR of transthyretin was validated using a dual luciferase reporter assay. **(A)** Schematic representation of the luciferase reporter constructs. FLuc and RLuc represents Firefly luciferase and Renilla luciferase respectively. **(B)** HEK293T cells were co-transfected with the luciferase reporter construct containing 3' UTR of transthyretin and miR-10b TuD inhibitor. 48 hours post-transfection, luminescence signal was measured using luminometer. Data are represented as a ratio of Firefly/Renilla luciferase normalized to the negative TuD (n=4). miR-10b TuD inhibitor significantly increased the luciferase activity of 3' UTR of transthyretin compared to the miR-neg TuD inhibitor. Statistical analysis was performed using paired Student's *t*-test (*$P < 0.05$; **$P < 0.01$; ***$P < 0.001$). Data are expressed as mean ± SEM; SEM = standard error of the mean.

3.4.3 miR-10b inhibition reduces intranuclear inclusions in the striatal lentiviral MJD mouse model

We then investigated whether we would reduce the number of mutant ataxin-3 inclusions upon miR-10b inhibition. For that, brain sections labelled with anti-ubiquitin and anti-ataxin-3 antibodies revealed a significant reduction in the number of ubiquitin and ataxin-3 positive inclusions in the brain sections of the animals treated with miR-10b TuD inhibitor (Fig. 3.3A, C, F, D and G) as compared to the miR-neg TuD inhibitor (Fig. 3.3A, B, E, D and G). We further evaluated the aggregate levels by western blot and found a significant reduction in high molecular weight species in mouse samples injected with miR-10b TuD inhibitor as compared to miR-neg TuD inhibitor (Fig. 3.3H and I). Altogether these results suggest that inhibition of miR-10b in the striatum of the mouse brain reduces aggregation and the number of mutant ataxin-3 inclusions.

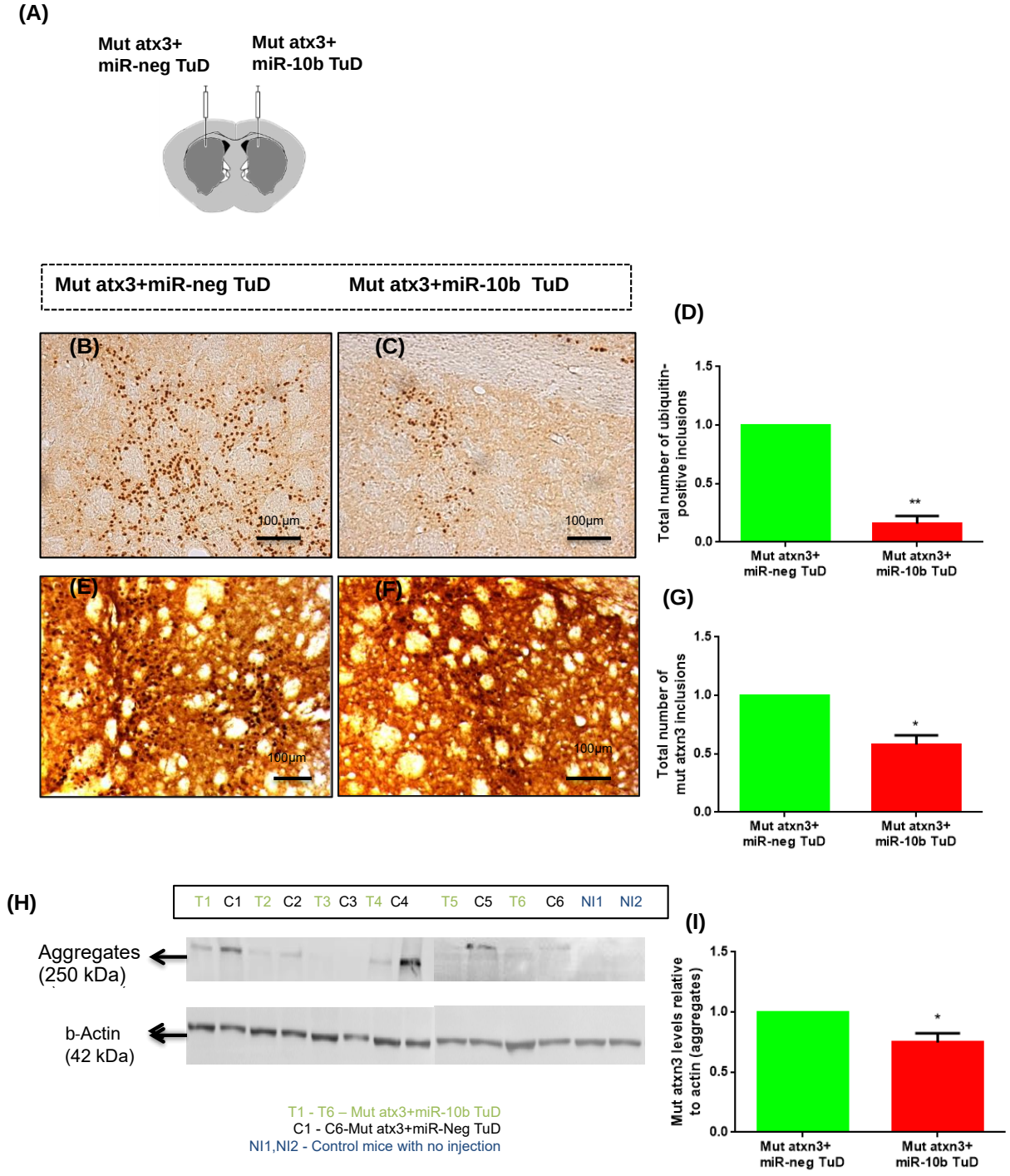

Figure 3.3 miR-10b inhibition reduces intranuclear inclusions in the striatal lentiviral MJD mouse model. (A) Schematic representation of stereotaxic procedure in mice. Lentiviral vectors encoding mutant ataxin-3 and the miR-10b TuD inhibitor were co-injected in to the mouse striatum in one hemisphere and mutant ataxin-3 and the miR-neg TuD inhibitor in the other hemisphere (internal control). **(B-G)** Immunohistochemistry analysis of striatal sections injected with mutant ataxin-3 and miR-10b TuD inhibitor in one hemisphere and miR-neg TuD in the other hemisphere (n=4). At 5 weeks post-injection, brain sections were stained with ubiquitin

positive inclusions **(B, C). (D)** Quantification of the ubiquitin positive inclusions at 5 weeks post-injection. Brain sections were stained with ataxin-3 positive inclusions **(E, F). (G)** Quantification of the ataxin-3 positive inclusions at 5 weeks post-injection **(H)** Western blot analysis of mouse striatal samples. Representative western blot loaded with the samples injected with mutant ataxin-3 and miR-10b TuD inhibitor in one lane and mutant ataxin-3 and miR-Neg TuD inhibitor in the next lane respectively (n=6). The membranes were labelled with anti-ataxin-3 and anti-β-actin antibodies. **(I)** Quantification of aggregates was performed by normalizing each ataxin-3 lane with actin (ataxin-3 aggregates / actin). One side of the hemisphere is normalized with the other side of hemisphere. Statistical analysis was performed using paired Student's *t*-test (**P* < 0.05; ***P* < 0.01; ****P* < 0.001). Data are expressed as mean ± SEM; SEM = standard error of the mean.

3.4.4 miR-10b inhibition drastically reduces neuronal dysfunction in the striatal lentiviral MJD mouse model

We then investigated whether miR-10b inhibition would modify neuronal dysfunction caused by mutant ataxin-3 overexpression. We previously showed that lentiviral expression of mutant ataxin-3 produces loss of the DARPP-32 neuronal marker, which can be precisely quantitated (Alves *et al*. 2008). Therefore, immunohistochemical analysis for DARPP-32 (Fig. 3.4A and B) was performed in the samples obtained from the previous experiment.

We found that miR-10b inhibition significantly reduced the volume of the region depleted of darpp-32 staining by 90% (Fig. 3.4B and C) compared to the negative inhibitor (Fig. 3.4A and C) at 5 weeks post injection (n=4).

These results suggest that inhibition of miR-10b reduces neuronal dysfunction induced by mutant ataxin-3 expression.

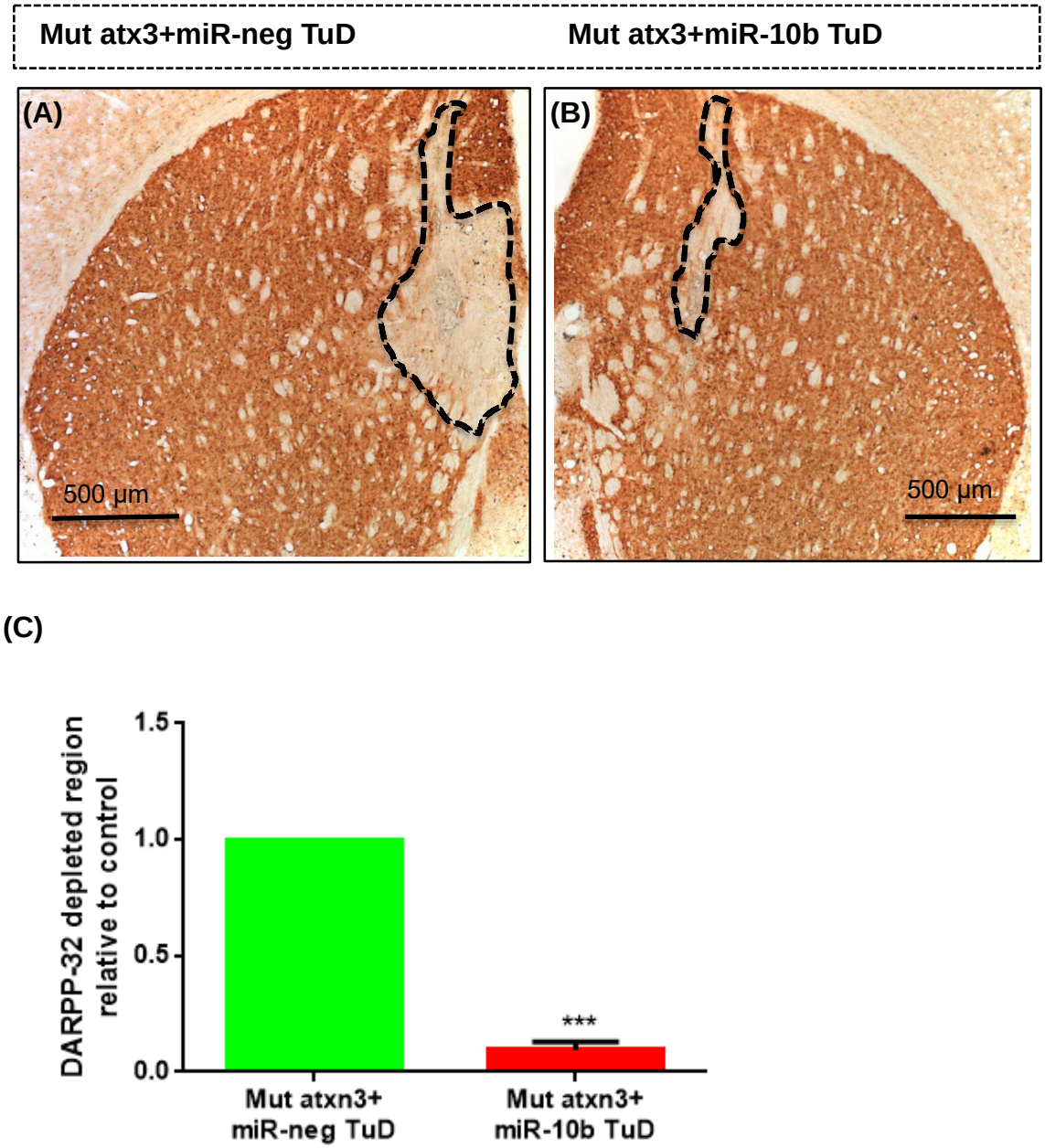

Figure 3.4. miR-10b inhibition resulted in the reduction of neuronal dysfunction. Immunohistochemistry analysis of mouse striatal sections with mutant ataxin-3 and miR-10b TuD inhibitor in one hemisphere and mutant ataxin-3 and miR-Neg TuD (n=4) in the other hemisphere. **(A, B)** At 5 weeks post-injection, brain sections were stained with anti-DARP-32 antibody (neuronal marker DARPP-32, *upper*, scale bar = 500 µm) **(C)** Quantification analysis of the DARPP-32 depleted region in the mouse brains. The lesion volume is much smaller in the sections injected with miR-10b TuD inhibitor than the miR-Neg TuD inhibitor (control) suggesting a neuroprotective role against mutant ataxin-3 overexpression upon miR-10b TuD inhibition. One side of the hemisphere is normalized with the other side of hemisphere. Statistical analysis was

performed using paired Student's *t*-test (*$P < 0.05$; **$P < 0.01$; ***$P < 0.001$). Data are expressed as mean ± SEM; SEM = standard error of the mean.

3.4.5 Overexpression of human transthyretin in HEK293T cells

Having identified transthyretin as a direct target of miR-10b, our aim was to clone the human transthyretin and to confirm the presence of transthyretin in HEK293T cells upon overexpression of human transthyretin. HEK293T cells were transfected with the human transthyretin and its mRNA and protein levels were evaluated using qRT-PCR and western bot respectively. Either by qPCR or by western blot, we observed successful overexpression of the human transthyretin (Fig. 3.5B and C). These results validate the cloning of transthyretin in a lentiviral construct which will, in the future, allow the production of lentiviral particles which will be injected together with the mutant ataxin-3 in the mouse brain in order to evaluate its role in MJD.

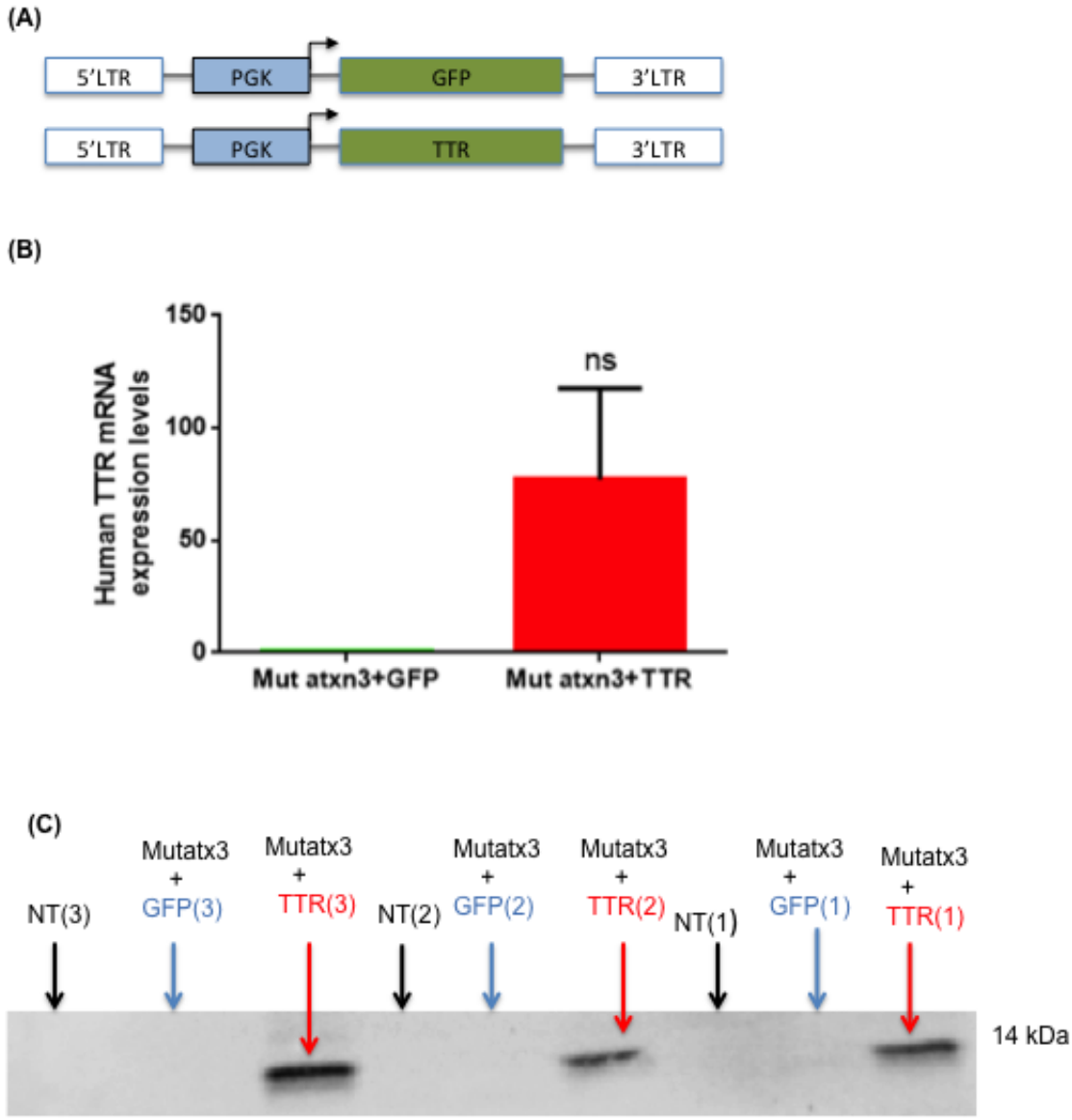

Figure 3.5 over expression of human transthyretin in HEK293T cells. (A) Schematic representation of lentiviral vector encoding human transthyretin. **(B)** Human transthyretin mRNA expression levels in HEK293T cells transfected with the TTR plasmid compared with HEK293T cells transfected with the GFP plasmid. TTR expression was highly up regulated compared with the plasmids transfected with GFP upon TTR over expression **(C)** Human transthyretin protein expression levels in HEK293T cells transfected with the TTR plasmid, GFP plasmid and also in the non-transfected cells.

3.5 Discussion

In this study, we applied a tough decoy RNA Strategy associated to lentiviral vectors in order to reduce miR-10b levels to their normal state in the context of MJD and to evaluate the beneficial effects miR-10b inhibition in a striatal lentiviral MJD mouse model.

Importantly, miR-10b inhibition was highly efficient, robustly reducing miR10b levels. Next, we explored the targets of miR-10b after the treatment with the described inhibitor. mRNA microarray profile revealed that a large set of genes were differentially expressed and in particular, we found transthyretin (TTR) to be significantly up-regulated upon treatment with miR-10b TuD inhibitor. In parallel, transthyretin expression levels were also quantified in the striatal lentiviral model and found to be significantly downregulated in MJD. Furthermore, we show that the interaction between miR-10b and the 3' UTR transthyretin is direct. Importantly, these data show that transthyretin expression, which was initially downregulated in the lentiviral MJD model, was brought to the normal levels upon miR-10b TuD inhibitor treatment.

The relevance of TTR in other neurodegenerative disorders has been previously investigated. In fact, decreased in TTR levels in cerebrospinal fluid (CSF) of Alzheimer's disease (AD) patients was initially reported in 1986 (Elovaara *et al*. 1986). Moreover, it has been previously reported that overexpression of wild type human transthyretin in APP23 transgenic mouse model of AD protects AD mice from behavior defects and also resulted in significantly reduced Aβ peptide levels compared to the control APP23 transgenic model of AD (Buxbaum *et al*. 2008). On the other hand, silencing the endogenous TTR gene promoted both the increase in Aβ deposition and also the neuropathological phenotype (Buxbaum *et al*. 2008) supporting the previously published data from other groups showing that young animals lacking TTR gene develop a defect in spatial learning even in the absence of genes associated with human AD (Sousa *et al*. 2007). These findings in AD clearly show the importance of transthyretin expression in the brain.

While transthyretin may be a pathway through which miR-10b is modifying MJD pathogenesis we cannot exclude the contribution of many other mRNAs that are

predicted to be targeted by miR-10b. Importantly, restoration of miR-10b levels significantly reduces the number of mutant ataxin-3 inclusions and neuronal dysfunction. Overall, these results indicate that miR-10b inhibition mediates neuroprotection in the striatal lentiviral MJD mouse model.

In the future, it would be important to overexpress transthyretin in the striatal lentiviral MJD mouse model in order to investigate whether the same beneficial effects observed using miR-10b TuD inhibitor are replicated with transthyretin. This would help clarifying the mechanisms behind the beneficial effects that we observed. However, we should not forget that one third of the human genes are regulated by microRNAs and each microRNA can target many transcripts (Lewis *et al*. 2005, Baek *et al*. 2008). So, not only transthyretin but also many other genes may also be involved in contributing to the alleviation of neuropathology induced by mutant ataxin-3.

In conclusion, our study identified a novel target gene for miR-10b, transthyretin, a gene previously implicated in other neurodegenerative diseases. Importantly, lentiviral-mediated inhibition of miR-10b was not only capable of restoring its endogenous levels but also resulted in robust neuroprotection in a MJD mouse model. Altogether, we believe our study identified a novel disease pathway in MJD and, at the same time, opens a new door for the development of a miR-based therapeutic strategy towards MJD.

CHAPTER 4

Final conclusions and future perspectives

4.1 Final Conclusions and Future Perspectives

This thesis focused on developing a microRNA based therapeutic strategy for Machado-Joseph disease using striatal lentiviral MJD mouse model and *D. melanogaster* MJD model.

In the first part of our study, we identified the dysregulated microRNAs in the striatal lentiviral MJD mouse model by performing the complete miRNA profile using miRNA microarray. miRNA microarray revealed numerous miRNAs that were differentially expressed which was further validated using qRT-PCR and found miR-10b, miR-181a, miR-27b, Let-7b, Let-7i and miR-30e were significantly differentially expressed in the striatal lentiviral MJD mouse model. Among the differentially expressed miRNAs, miR-10b expression levels were robustly up-regulated and decided to focus on this microRNA for further analysis. miR-10b expression levels were also checked in other MJD model from cells to human post-mortem brain tissue. miR-10b expression in the transgenic MJD mouse model is in line with the striatal lentiviral MJD mouse model (Torashima, Koyama et al. 2008). miR-10b expression was not significantly upregulated in all the different MJD models. However, miR-10b expression shows a trend towards upregulation in post-mortem brain tissue from MJD patients, SH-SY5Y cell line infected with mutant ataxin-3 and cerebellum lentiviral MJD mouse model.

In the second part of the work, miR-10b expression levels were quantified in the MJD *D. melanogaster* model and found to be the same between MJD flies and control flies. Despite, no differences were observed in the miR-10 expression in MJD *D. melanogaster* model, MJD flies with miR-10 repressor was developed assuming that the process controlled by miR-10 can be conserved in fly but not its regulation. Next, we want to know whether we could alleviate the eye phenotype induced by the mutant ataxin-3 overexpression. For that we crossed the MJD flies with miR-10 repressor with GMR line, which drives the expression in the eye and found that we could not rescue the eye phenotype upon miR-10 inhibitor treatment. Next, we evaluated whether miR-10 inhibitor treatment could extend the life span of the MJD *D. melanogaster* flies. We found that MJD flies with miR-10 inhibitor were able to

elongate the life span compared to the MJD flies with miR-control inhibitor. These clearly suggest the miR-10 involvement in anti-ageing process.

In the last part of our work, we investigated the miR-10b inhibition in the striatal lentiviral MJD mouse model. For that we cloned the miR-10b inhibitor and the miR-negative inhibitor using tough decoy RNA (TuD) strategy into the lentiviral backbone construct. The efficiency of the miR-10b inhibitor and the control inhibitor was confirmed with the GFP expression. This TuD inhibitor strategy resulted in more than 80% reduction in the miR-10b expression levels. mRNA microarray revealed many genes were differentially expressed in the striatal lentiviral MJD mouse model upon miR-10b inhibitor treatment. Few of the interesting genes were validated using qRT-PCR and found transthyretin to be significantly upregulated in the MJD mouse model. Next we investigated whether the interaction between the miR-10b and the TTR is direct. Using dual luciferase assay , we found that there is a significant increase in the luciferase activity upon miR-10b TuD treatment concluding that the interaction is direct. As intranuclear inclusions are hallmark of MJD (Paulson, Perez et al. 1997), we quantified the ubiquitin-positive inclusions and ataxin-3 positive inclusions in the mouse striatum. miR-10b inhibition promoted a significant reduction in the ubiquitin-positive inclusions and ataxin-3 positive inclusions. Furthermore, miR-10b inhibition also reduced the neuronal dysfunction and degeneration induced by mutant ataxin-3 overexpression in the striatal lentiviral MJD mouse model.

Overall, our results demonstrate that delivery of miR-10b inhibitor significantly reduced the number of aggregates and neuronal dysfunction in the striatal lentiviral MJD mouse model (Fig 3.3 and 3.4). Furthermore, administration of miR-10 also extended the life span of the MJD flies reinforcing the role of mir-10b and the potential of its inhibition as a therapeutic approach for MJD (Fig 2.5A)

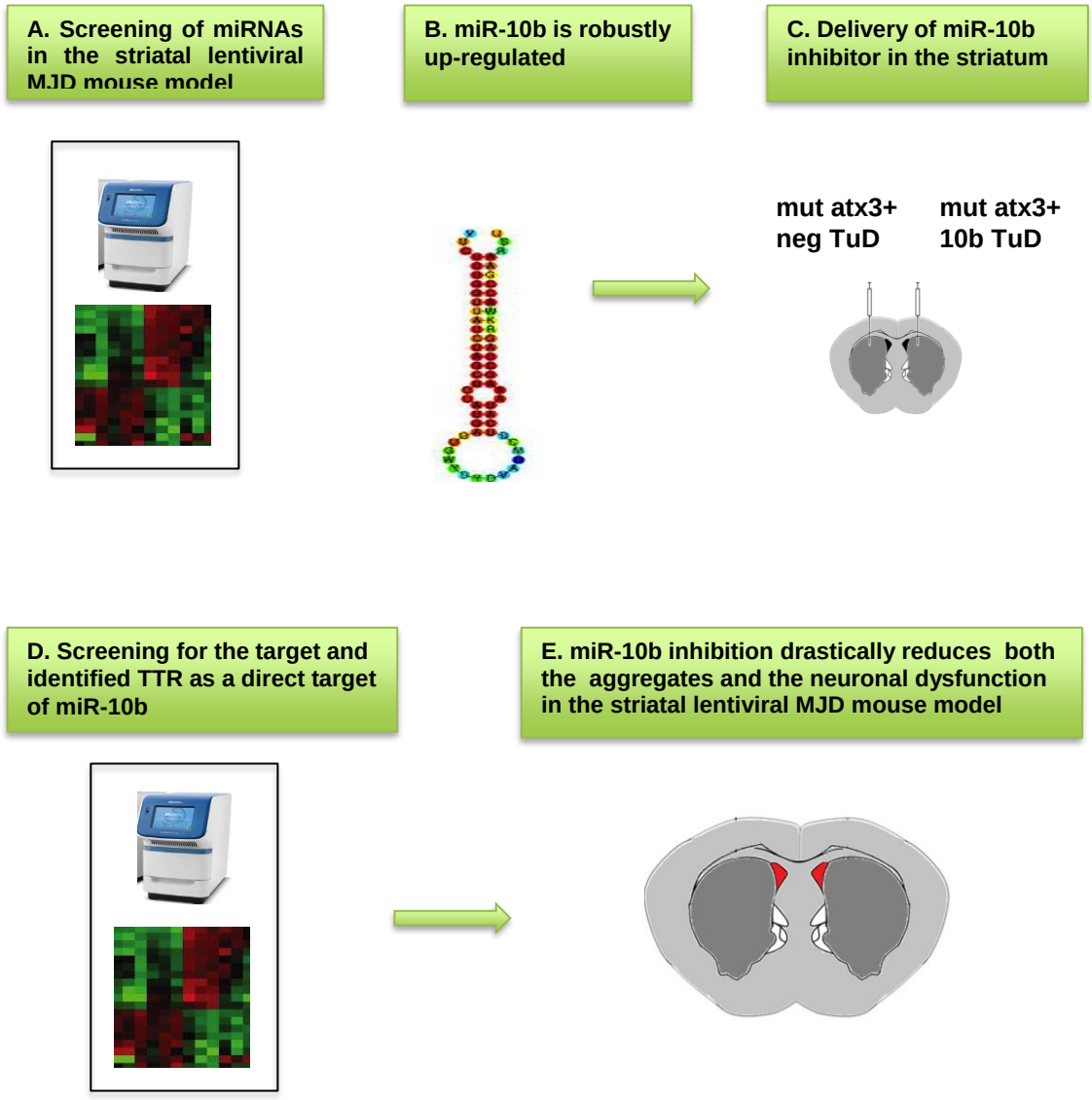

Figure 4.1. Schematic representation of our findings. (A) Heat map profile of the dysregulated microRNAs in the striatal lentiviral MJD mouse model using miRNA microarray and validated using qRT-PCR **(B)** Structure of the microRNA to show that one of the miRs, miR-10b was robustly up-regulated compared to the othere miRNAs that were differentially expressed. **(C)** miR-10b was cloned using tough decoy RNA strategy and injected along with mutant ataxin-3 in the striatum in one hemisphere and miR-neg TuD inhibitor and the mutant ataxin-3 in the other hemisphere. **(D)** Targets were screened in the mice injected with the miR-10b TuD inhibitor using mRNA microarray and identified transthyretin as a target. **(E)** miR-10b inhibition drastically reduces both the aggregates and the neuronal dysfunction in the striatal lentiviral MJD model constituting a promising therapy for Machado-Joseph disease.

Despite promising, additional studies are needed to clarify the mechanisms behind TTR. Namely, it is important to overexpress transthyretin in the striatal lentiviral MJD mouse model to investigate whether the same beneficial effects observed using miR-10b TuD inhibitor are replicated with transthyretin. This would help clarifying the mechanisms behind the beneficial effects that we observed in the striatal lentiviral MJD mouse model. It is also important to identify the pathway or genes involved in extending the life span of the MJD flies.

Finally, some aspects of our strategy could be refined to enhance therapeutic benefits for MJD, namely: 1) delivering multiple microRNA 2) testing other genes that could alleviate the neuropathological deficits 3) using non-invasive approach to deliver the microRNAs.

In conclusion, our study provides compelling evidence for a dysregulation of microRNAs in MJD, showing, for the first time, that miR-10b is upregulated in MJD. Moreover, we have validated a novel target gene for miR-10b, transthyretin, a gene previously implicated in other neurodegenerative diseases. Importantly, lentiviral-mediated inhibition of miR-10b was not only capable of restoring its endogenous levels but also resulted in robust neuroprotection in a MJD mouse model. Furthermore, miR-10 inhibition extends the lifespan of MJD flies. Altogether, we believe our study identifies a novel disease pathway in MJD and, at the same time, opens a new door for the development of a miR-based therapeutic strategy towards MJD.

References

References

Ajayi, A., X. Yu, S. Lindberg, U. Langel and A. L. Strom (2012). "Expanded ataxin-7 cause toxicity by inducing ROS production from NADPH oxidase complexes in a stable inducible Spinocerebellar ataxia type 7 (SCA7) model." BMC Neurosci **13**: 86.

Ao-Lin Hsu, Coleen T. Murphy, Cynthia Kenyon (2003). "Regulation of Aging and Age-Related Disease by DAF-16 and Heat-Shock. " Science. 300.

Al-Ramahi, I., Y. C. Lam, H. K. Chen, B. de Gouyon, M. Zhang, A. M. Perez, J. Branco, M. de Haro, C. Patterson, H. Y. Zoghbi and J. Botas (2006). "CHIP protects from the neurotoxicity of expanded and wild-type ataxin-1 and promotes their ubiquitination and degradation." J Biol Chem **281**(36): 26714-26724.

Alves, S., I. Nascimento-Ferreira, G. Auregan, R. Hassig, N. Dufour, E. Brouillet, M. C. Pedroso de Lima, P. Hantraye, L. Pereira de Almeida and N. Deglon (2008). "Allele-specific RNA silencing of mutant ataxin-3 mediates neuroprotection in a rat model of Machado-Joseph disease." PloS one **3**: e3341.

Alves, S., E. Regulier, I. Nascimento-Ferreira, R. Hassig, N. Dufour, A. Koeppen, A. L. Carvalho, S. Simoes, M. C. P. de Lima, E. Brouillet, V. C. Gould, N. Deglon and L. P. de Almeida (2008). "Striatal and nigral pathology in a lentiviral rat model of Machado-Joseph disease." Human molecular genetics **17**: 2071-2083.

Ambros, V. (2004). "The functions of animal microRNAs." Nature **431**: 350-355.

Andrade, C. (1952). "A peculiar form of peripheral neuropathy; familiar atypical generalized amyloidosis with special involvement of the peripheral nerves." Brain **75**(3): 408-427.

Arguelles, S., J. L. Venero, S. Garcia-Rodriguez, M. Tomas-Camardiel, A. Ayala, J. Cano and A. Machado (2010). "Use of haptoglobin and transthyretin as potential biomarkers for the preclinical diagnosis of Parkinson's disease." Neurochem Int **57**(3): 227-234.

Baek, D., J. Villen, C. Shin, F. D. Camargo, S. P. Gygi and D. P. Bartel (2008). "The impact of microRNAs on protein output." Nature **455**: 64-71.

Bartel, D. P. (2004). "MicroRNAs: Genomics, Biogenesis, Mechanism, and Function." Cell **116**: 281-297.

Bartel, D. P. (2009). "MicroRNAs: target recognition and regulatory functions." Cell **136**(2): 215-233.

Becher, M. W. and C. A. Ross (1998). "Intranuclear neuronal inclusions in DRPLA." Mov Disord **13**(5): 852-853.

Bernstein, E., A. A. Caudy, S. M. Hammond and G. J. Hannon (2001). "Role for a bidentate ribonuclease in the initiation step of RNA interference." Nature **409**(6818): 363-366.

Betel, D., A. Koppal, P. Agius, C. Sander and C. Leslie (2010). "Comprehensive modeling of microRNA targets predicts functional non-conserved and non-canonical sites." Genome Biol **11**(8): R90.

Bilen, J., N. Liu, B. G. Burnett, R. N. Pittman and N. M. Bonini (2006). "MicroRNA Pathways Modulate Polyglutamine-Induced Neurodegeneration." Molecular Cell **24**: 157-163.

Bird, T. D. (1993). Hereditary Ataxia Overview. GeneReviews(R). R. A. Pagon, M. P. Adam, H. H. Ardinger et al. Seattle (WA).

Bohnsack, M. T., K. Czaplinski and D. Gorlich (2004). "Exportin 5 is a RanGTP-dependent dsRNA-binding protein that mediates nuclear export of pre-miRNAs." Rna **10**(2): 185-191.

Boutla, A., C. Delidakis and M. Tabler (2003). "Developmental defects by antisense-mediated inactivation of micro-RNAs 2 and 13 in *D. melanogaster* and the identification of putative target genes." Nucleic Acids Res **31**(17): 4973-4980.

Brennecke, J., A. Stark, R. B. Russell and S. M. Cohen (2005). "Principles of microRNA-target recognition." PLoS Biol **3**(3): e85.

Brettschneider, J., V. Lehmensiek, H. Mogel, M. Pfeifle, J. Dorst, C. Hendrich, A. C. Ludolph and H. Tumani (2010). "Proteome analysis reveals candidate markers of disease progression in amyotrophic lateral sclerosis (ALS)." Neurosci Lett **468**(1): 23-27.

Brouillette, J. and R. Quirion (2008). "Transthyretin: a key gene involved in the maintenance of memory capacities during aging." Neurobiol Aging **29**(11): 1721-1732.

Buxbaum, J. N., Z. Ye, N. Reixach, L. Friske, C. Levy, P. Das, T. Golde, E. Masliah, A. R. Roberts and T. Bartfai (2008). "Transthyretin protects Alzheimer's mice from the behavioral and biochemical effects of Abeta toxicity." Proceedings of the National Academy of Sciences of the United States of America **105**: 2681-2686.

Cai, X., C. H. Hagedorn and B. R. Cullen (2004). "Human microRNAs are processed from capped, polyadenylated transcripts that can also function as mRNAs." RNA **10**(12): 1957-1966.

Care, A., D. Catalucci, F. Felicetti, D. Bonci, A. Addario, P. Gallo, M. L. Bang, P. Segnalini, Y. Gu, N. D. Dalton, L. Elia, M. V. Latronico, M. Hoydal, C. Autore, M. A. Russo, G. W. Dorn, 2nd, O. Ellingsen, P. Ruiz-Lozano, K. L. Peterson, C. M. Croce, C. Peschle and G. Condorelli (2007). "MicroRNA-133 controls cardiac hypertrophy." Nat Med **13**(5): 613-618.

Chai, Y., S. L. Koppenhafer, N. M. Bonini and H. L. Paulson (1999). "Analysis of the role of heat shock protein (Hsp) molecular chaperones in polyglutamine disease." J Neurosci **19**(23): 10338-10347.

Chai, Y., S. L. Koppenhafer, S. J. Shoesmith, M. K. Perez and H. L. Paulson (1999). "Evidence for proteasome involvement in polyglutamine disease: localization to nuclear inclusions in SCA3/MJD and suppression of polyglutamine aggregation in vitro." Hum Mol Genet **8**(4): 673-682.

Chai, Y., L. Wu, J. D. Griffin and H. L. Paulson (2001). "The role of protein composition in specifying nuclear inclusion formation in polyglutamine disease." J Biol Chem **276**(48): 44889-44897.

Chan, J. A., A. M. Krichevsky and K. S. Kosik (2005). "MicroRNA-21 is an antiapoptotic factor in human glioblastoma cells." Cancer Res **65**(14): 6029-6033.

Chen, C., D. A. Ridzon, A. J. Broomer, Z. Zhou, D. H. Lee, J. T. Nguyen, M. Barbisin, N. L. Xu, V. R. Mahuvakar, M. R. Andersen, K. Q. Lao, K. J. Livak and K. J. Guegler (2005). "Real-time quantification of microRNAs by stem-loop RT-PCR." Nucleic Acids Res **33**(20): e179.

Chen, P. Y., L. Weinmann, D. Gaidatzis, Y. Pei, M. Zavolan, T. Tuschl and G. Meister (2008). "Strand-specific 5'-O-methylation of siRNA duplexes controls guide strand selection and targeting specificity." Rna **14**(2): 263-274.

Chen, Y. C., J. R. Gatchel, R. W. Lewis, C. A. Mao, P. A. Grant, H. Y. Zoghbi and S. Y. Dent (2012). "Gcn5 loss-of-function accelerates cerebellar and retinal degeneration in a SCA7 mouse model." Hum Mol Genet **21**(2): 394-405.

Chendrimada, T. P., R. I. Gregory, E. Kumaraswamy, J. Norman, N. Cooch, K. Nishikura and R. Shiekhattar (2005). "TRBP recruits the Dicer complex to Ago2 for microRNA processing and gene silencing." Nature **436**(7051): 740-744.

Cheng, P. H., C. L. Li, Y. F. Chang, S. J. Tsai, Y. Y. Lai, A. W. S. Chan, C. M. Chen and S. H. Yang (2013). "MiR-196a ameliorates phenotypes of huntington disease in cell, transgenic mouse, and induced pluripotent stem cell models." American Journal of Human Genetics **93**: 306-312.

Chiang, H. R., L. W. Schoenfeld, J. G. Ruby, V. C. Auyeung, N. Spies, D. Baek, W. K. Johnston, C. Russ, S. Luo, J. E. Babiarz, R. Blelloch, G. P. Schroth, C. Nusbaum and D. P. Bartel (2010). "Mammalian microRNAs: experimental evaluation of novel and previously annotated genes." Genes Dev **24**(10): 992-1009.

Chiu, Y. L. and T. M. Rana (2003). "siRNA function in RNAi: a chemical modification analysis." Rna **9**(9): 1034-1048.

Chou, A. H., S. Y. Chen, T. H. Yeh, Y. H. Weng and H. L. Wang (2011). "HDAC inhibitor sodium butyrate reverses transcriptional downregulation and ameliorates ataxic symptoms in a transgenic mouse model of SCA3." Neurobiol Dis **41**(2): 481-488.

Chou, A. H., Y. L. Chen, C. C. Chiu, S. J. Yuan, Y. H. Weng, T. H. Yeh, Y. L. Lin, J. M. Fang and H. L. Wang (2015). "T1-11 and JMF1907 ameliorate polyglutamine-expanded ataxin-3-induced neurodegeneration, transcriptional dysregulation and ataxic symptom in the SCA3 transgenic mouse." Neuropharmacology **99**: 308-317.

Chou, A. H., T. H. Yeh, P. Ouyang, Y. L. Chen, S. Y. Chen and H. L. Wang (2008). "Polyglutamine-expanded ataxin-3 causes cerebellar dysfunction of SCA3 transgenic mice by inducing transcriptional dysregulation." Neurobiol Dis **31**(1): 89-101.

Coutinho, P. and C. Andrade (1978). "Autosomal dominant system degeneration in Portuguese families of the Azores Islands. A new genetic disorder involving cerebellar, pyramidal, extrapyramidal and spinal cord motor functions." Neurology **28**(7): 703-709.

Cvetanovic, M., J. M. Patel, H. H. Marti, A. R. Kini and P. Opal (2011). "Vascular endothelial growth factor ameliorates the ataxic phenotype in a mouse model of spinocerebellar ataxia type 1." Nat Med **17**(11): 1445-1447.

D'Abreu, A., M. C. Franca, Jr., H. L. Paulson and I. Lopes-Cendes (2010). "Caring for Machado-Joseph disease: current understanding and how to help patients." Parkinsonism Relat Disord **16**(1): 2-7.

Davis, S., B. Lollo, S. Freier and C. Esau (2006). "Improved targeting of miRNA with antisense oligonucleotides." Nucleic Acids Res **34**(8): 2294-2304.

de Almeida, L. P., C. A. Ross, D. Zala, P. Aebischer and N. Deglon (2002). "Lentiviral-mediated delivery of mutant huntingtin in the striatum of rats induces a selective neuropathology modulated by polyglutamine repeat size, huntingtin expression levels,

and protein length." The Journal of neuroscience : the official journal of the Society for Neuroscience **22**: 3473-3483.

Dean, N. M., R. McKay, T. P. Condon and C. F. Bennett (1994). "Inhibition of protein kinase C-alpha expression in human A549 cells by antisense oligonucleotides inhibits induction of intercellular adhesion molecule 1 (ICAM-1) mRNA by phorbol esters." J Biol Chem **269**(23): 16416-16424.

Denli, A. M., B. B. Tops, R. H. Plasterk, R. F. Ketting and G. J. Hannon (2004). "Processing of primary microRNAs by the Microprocessor complex." Nature **432**(7014): 231-235.

Diederichs, S. and D. A. Haber (2007). "Dual role for argonautes in microRNA processing and posttranscriptional regulation of microRNA expression." Cell **131**(6): 1097-1108.

Doggui, S., J. Brouillette, J. G. Chabot, M. Farso and R. Quirion (2010). "Possible involvement of transthyretin in hippocampal beta-amyloid burden and learning behaviors in a mouse model of Alzheimer's disease (TgCRND8)." Neurodegener Dis **7**(1-3): 88-95.

Doss-Pepe, E. W., E. S. Stenroos, W. G. Johnson and K. Madura (2003). "Ataxin-3 interactions with rad23 and valosin-containing protein and its associations with ubiquitin chains and the proteasome are consistent with a role in ubiquitin-mediated proteolysis." Molecular and cellular biology **23**: 6469-6483.

Duenas, A. M., R. Goold and P. Giunti (2006). "Molecular pathogenesis of spinocerebellar ataxias." Brain : a journal of neurology **129**: 1357-1370.

Duursma, A. M., M. Kedde, M. Schrier, C. le Sage and R. Agami (2008). "miR-148 targets human DNMT3b protein coding region." Rna **14**(5): 872-877.

Ebert, M. S., J. R. Neilson and P. A. Sharp (2007). "MicroRNA sponges: competitive inhibitors of small RNAs in mammalian cells." Nat Methods **4**(9): 721-726.

Elovaara, I., C. P. Maury and J. Palo (1986). "Serum amyloid A protein, albumin and prealbumin in Alzheimer's disease and in demented patients with Down's syndrome." Acta Neurol.Scand. **74**: 245-250.

Fleming, C. E., F. M. Mar, F. Franquinho, M. J. Saraiva and M. M. Sousa (2009). "Transthyretin internalization by sensory neurons is megalin mediated and necessary for its neuritogenic activity." J Neurosci **29**(10): 3220-3232.

Fleming, C. E., M. J. Saraiva and M. M. Sousa (2007). "Transthyretin enhances nerve regeneration." J Neurochem **103**(2): 831-839.

Forstemann, K., M. D. Horwich, L. Wee, Y. Tomari and P. D. Zamore (2007). "*D. melanogaster* microRNAs are sorted into functionally distinct argonaute complexes after production by dicer-1." Cell **130**(2): 287-297.

Gabriely, G., M. Yi, R. S. Narayan, J. M. Niers, T. Wurdinger, J. Imitola, K. L. Ligon, S. Kesari, C. Esau, R. M. Stephens, B. A. Tannous and A. M. Krichevsky (2011). "Human glioma growth is controlled by microRNA-10b." Cancer Research **71**: 3563-3572.

Gaughwin, P. M., M. Ciesla, N. Lahiri, S. J. Tabrizi, P. Brundin and M. Björkqvist (2011). "Hsa-miR-34b is a plasma-stable microRNA that is elevated in pre-manifest Huntington's disease." Human Molecular Genetics **20**: 2225-2237.

Ghatak, S. and S. Raha (2015). "Micro RNA-214 contributes to proteasome independent downregulation of beta catenin in Huntington's disease knock-in striatal cell model

STHdhQ111/Q111." Biochemical and biophysical research communications **459**: 509-514.

Ghildiyal, M., J. Xu, H. Seitz, Z. Weng and P. D. Zamore (2010). "Sorting of *D. melanogaster* small silencing RNAs partitions microRNA* strands into the RNA interference pathway." Rna **16**(1): 43-56.

Goswami, A., P. Dikshit, A. Mishra, S. Mulherkar, N. Nukina and N. R. Jana (2006). "Oxidative stress promotes mutant huntingtin aggregation and mutant huntingtin-dependent cell death by mimicking proteasomal malfunction." Biochem Biophys Res Commun **342**(1): 184-190.

Gregory, R. I., K. P. Yan, G. Amuthan, T. Chendrimada, B. Doratotaj, N. Cooch and R. Shiekhattar (2004). "The Microprocessor complex mediates the genesis of microRNAs." Nature **432**(7014): 235-240.

Grimson, A., K. K. Farh, W. K. Johnston, P. Garrett-Engele, L. P. Lim and D. P. Bartel (2007). "MicroRNA targeting specificity in mammals: determinants beyond seed pairing." Mol Cell **27**(1): 91-105.

Grishok, A., A. E. Pasquinelli, D. Conte, N. Li, S. Parrish, I. Ha, D. L. Baillie, A. Fire, G. Ruvkun and C. C. Mello (2001). "Genes and mechanisms related to RNA interference regulate expression of the small temporal RNAs that control C. elegans developmental timing." Cell **106**(1): 23-34.

Guessous, F., M. Alvarado-Velez, L. Marcinkiewicz, Y. Zhang, J. Kim, S. Heister, B. Kefas, J. Godlewski, D. Schiff, B. Purow and R. Abounader (2013). "Oncogenic effects of miR-10b in glioblastoma stem cells." Journal of Neuro-Oncology **112**: 153-163.

Gumireddy, K., D. D. Young, X. Xiong, J. B. Hogenesch, Q. Huang and A. Deiters (2008). "Small-molecule inhibitors of microrna miR-21 function." Angew Chem Int Ed Engl **47**(39): 7482-7484.

Haberhausen, G., M. S. Damian, F. Leweke and U. Muller (1995). "Spinocerebellar ataxia, type 3 (SCA3) is genetically identical to Machado-Joseph disease (MJD)." J Neurol Sci **132**(1): 71-75.

Haacke, A., S. A. Broadley, R. Boteva, N. Tzvetkov, F. U. Hartl and P. Breuer (2006). "Proteolytic cleavage of polyglutamine-expanded ataxin-3 is critical for aggregation and sequestration of non-expanded ataxin-3. " Hum Mol Genet **15**(4): 555-68.

Hammond, S. M., S. Boettcher, A. A. Caudy, R. Kobayashi and G. J. Hannon (2001). "Argonaute2, a link between genetic and biochemical analyses of RNAi." Science **293**(5532): 1146-1150.

Han, J., Y. Lee, K. H. Yeom, Y. K. Kim, H. Jin and V. N. Kim (2004). "The Drosha-DGCR8 complex in primary microRNA processing." Genes Dev **18**(24): 3016-3027.

Haraguchi, T., Y. Ozaki and H. Iba (2009). "Vectors expressing efficient RNA decoys achieve the long-term suppression of specific microRNA activity in mammalian cells." Nucleic Acids Research **37**.

Horman, S. R., M. M. Janas, C. Litterst, B. Wang, I. J. MacRae, M. J. Sever, D. V. Morrissey, P. Graves, B. Luo, S. Umesalma, H. H. Qi, L. J. Miraglia, C. D. Novina and A. P. Orth (2013).

"Akt-mediated phosphorylation of argonaute 2 downregulates cleavage and upregulates translational repression of MicroRNA targets." Mol Cell **50**(3): 356-367.

Hoss, a. G., a. Labadorf, J. C. Latourelle, V. K. Kartha, T. C. Hadzi, J. F. Gusella, M. E. MacDonald, J. F. Chen, S. Akbarian, Z. Weng, J. P. Vonsattel and R. H. Myers (2015). "miR-10b-5p expression in Huntington's disease brain relates to age of onset and the extent of striatal involvement." BMC Med Genomics **8**: 10.

Huang, F., L. Zhang, Z. Long, Z. Chen, X. Hou, C. Wang, H. Peng, J. Wang, J. Li, R. Duan, K. Xia, D. M. Chuang, B. Tang and H. Jiang (2014). "MiR-25 alleviates polyQ-mediated cytotoxicity by silencing ATXN3." FEBS Letters **588**: 4791-4798.

Hubener, J., J. J. Weber, C. Richter, L. Honold, A. Weiss, F. Murad, P. Breur, U Wullner, P. Bellstedt, F. Paquet-Durand, J. Takano, T. C. Saido, O. Riess and H. P. Nguyen (2013). "Calpain-mediated ataxin-3 cleavage in the molecular pathogenesis of spinocerebellar ataxia type 3 (SCA3)." Hum Mol Genet **22**(3): 508-18.

Hutvagner, G., J. McLachlan, A. E. Pasquinelli, E. Balint, T. Tuschl and P. D. Zamore (2001). "A cellular function for the RNA-interference enzyme Dicer in the maturation of the let-7 small temporal RNA." Science **293**(5531): 834-838.

Hutvagner, G., M. J. Simard, C. C. Mello and P. D. Zamore (2004). "Sequence-specific inhibition of small RNA function." PLoS Biol **2**(4): E98.

Ikeda, H., M. Yamaguchi, S. Sugai, Y. Aze, S. Narumiya and A. Kakizuka (1996). "Expanded polyglutamine in the Machado-Joseph disease protein induces cell death in vitro and in vivo." Nature genetics **13**: 196-202.

Ingbar, S. H. (1958). "Pre-albumin: a thyroxinebinding protein of human plasma." Endocrinology **63**(2): 256-259.

Jana, N. R., P. Dikshit, A. Goswami, S. Kotliarova, S. Murata, K. Tanaka and N. Nukina (2005). "Co-chaperone CHIP associates with expanded polyglutamine protein and promotes their degradation by proteasomes." J Biol Chem **280**(12): 11635-11640.

James F. Morley, Heather R. Brignull, Jill J. Weyers, and Richard I. Morimoto (2002). "The threshold for polyglutamine-expansion protein aggregation and cellular toxicity is dynamic and influenced by aging in Caenorhabditis elegans." PNAS 99(16): 10417–10422.

Jannot, G., M. E. Boisvert, I. H. Banville and M. J. Simard (2008). "Two molecular features contribute to the Argonaute specificity for the microRNA and RNAi pathways in C. elegans." Rna **14**(5): 829-835.

Jiang, F., X. Ye, X. Liu, L. Fincher, D. McKearin and Q. Liu (2005). "Dicer-1 and R3D1-L catalyze microRNA maturation in *D. melanogaster*." Genes Dev **19**(14): 1674-1679.

John, B., A. J. Enright, A. Aravin, T. Tuschl, C. Sander and D. S. Marks (2004). "Human MicroRNA targets." PLoS Biol **2**(11): e363.

Kabat, E. A., D. H. Moore and H. Landow (1942). "AN ELECTROPHORETIC STUDY OF THE PROTEIN COMPONENTS IN CEREBROSPINAL FLUID AND THEIR RELATIONSHIP TO THE SERUM PROTEINS." J Clin Invest **21**(5): 571-577.

Kalkunte, S. S., S. Neubeck, W. E. Norris, S. B. Cheng, S. Kostadinov, D. Vu Hoang, A. Ahmed, F. von Eggeling, Z. Shaikh, J. Padbury, G. Berg, A. Olofsson, U. R. Markert and S. Sharma (2013). "Transthyretin is dysregulated in preeclampsia, and its native form prevents the onset of disease in a preclinical mouse model." Am J Pathol **183**(5): 1425-1436.

Katsuno, M., H. Adachi, A. Inukai and G. Sobue (2003). "Transgenic mouse models of spinal and bulbar muscular atrophy (SBMA)." Cytogenet Genome Res **100**(1-4): 243-251.

Kawaguchi, Y., T. Okamoto, M. Taniwaki, M. Aizawa, M. Inoue, S. Katayama, H. Kawakami, S. Nakamura, M. Nishimura, I. Akiguchi, J. Kimura, S. Narumiya and A. Kakizuka (1994). "CAG expansions in a novel gene for Machado-Joseph Disease at chromosome 14q32.1." Nature genetics **8**: 221-228.

Kawamata, T. and Y. Tomari (2010). "Making RISC." Trends Biochem Sci **35**(7): 368-376.

Kazachkova, N., M. Raposo, R. Montiel, T. Cymbron, C. Bettencourt, A. Silva-Fernandes, S. Silva, P. Maciel and M. Lima (2013). "Patterns of mitochondrial DNA damage in blood and brain tissues of a transgenic mouse model of Machado-Joseph disease." Neurodegener Dis **11**(4): 206-214.

Ketting, R. F., S. E. Fischer, E. Bernstein, T. Sijen, G. J. Hannon and R. H. Plasterk (2001). "Dicer functions in RNA interference and in synthesis of small RNA involved in developmental timing in C. elegans." Genes Dev **15**(20): 2654-2659.

Kim, H. J. and S. C. Bae (2011). "Histone deacetylase inhibitors: molecular mechanisms of action and clinical trials as anti-cancer drugs." Am J Transl Res **3**(2): 166-179.

Kim, S. J., T. S. Kim, S. Hong, H. Rhim, I. Y. Kim and S. Kang (2003). "Oxidative stimuli affect polyglutamine aggregation and cell death in human mutant ataxin-1-expressing cells." Neurosci Lett **348**(1): 21-24.

Kiriakidou, M., P. T. Nelson, A. Kouranov, P. Fitziev, C. Bouyioukos, Z. Mourelatos and A. Hatzigeorgiou (2004). "A combined computational-experimental approach predicts human microRNA targets." Genes Dev **18**(10): 1165-1178.

Kocerha, J., Y. Xu, M. S. Prucha, D. Zhao and A. W. S. Chan (2014). "microRNA-128a dysregulation in transgenic Huntington's disease monkeys." Molecular brain **7**: 46.

Koch, P., P. Breuer, M. Peitz, J. Jungverdorben, J. Kesavan, D. Poppe, J. Doerr, J. Ladewig, J. Mertens, T. Tuting, P. Hoffmann, T. Klockgether, B. O. Evert, U. Wullner and O. Brustle (2011). "Excitation-induced ataxin-3 aggregation in neurons from patients with Machado-Joseph disease." Nature **480**(7378): 543-546.

Kota, J., R. R. Chivukula, K. A. O'Donnell, E. A. Wentzel, C. L. Montgomery, H. W. Hwang, T. C. Chang, P. Vivekanandan, M. Torbenson, K. R. Clark, J. R. Mendell and J. T. Mendell (2009). "Therapeutic microRNA delivery suppresses tumorigenesis in a murine liver cancer model." Cell **137**(6): 1005-1017.

Krek, A., D. Grun, M. N. Poy, R. Wolf, L. Rosenberg, E. J. Epstein, P. MacMenamin, I. da Piedade, K. C. Gunsalus, M. Stoffel and N. Rajewsky (2005). "Combinatorial microRNA target predictions." Nat Genet **37**(5): 495-500.

Krutzfeldt, J., N. Rajewsky, R. Braich, K. G. Rajeev, T. Tuschl, M. Manoharan and M. Stoffel (2005). "Silencing of microRNAs in vivo with 'antagomirs'." Nature **438**(7068): 685-689.

Laco, M. N., C. R. Oliveira, H. L. Paulson and A. C. Rego (2012). "Compromised mitochondrial complex II in models of Machado-Joseph disease." Biochim Biophys Acta **1822**(2): 139-149.

Lai, E. C. (2004). "Predicting and validating microRNA targets." Genome Biol **5**(9): 115.

Larrouy, B., C. Blonski, C. Boiziau, M. Stuer, S. Moreau, D. Shire and J. J. Toulme (1992). "RNase H-mediated inhibition of translation by antisense oligodeoxyribonucleotides: use of backbone modification to improve specificity." Gene **121**(2): 189-194.

Latouche, M., C. Lasbleiz, E. Martin, V. Monnier, T. Debeir, A. Mouatt-Prigent, M. P. Muriel, L. Morel, M. Ruberg, A. Brice, G. Stevanin and H. Tricoire (2007). "A conditional pan-neuronal *D. melanogaster* model of spinocerebellar ataxia 7 with a reversible adult phenotype suitable for identifying modifier genes." J Neurosci **27**(10): 2483-2492.

Lee, J. Y., S. Kim, D. W. Hwang, J. M. Jeong, J. K. Chung, M. C. Lee and D. S. Lee (2008). "Development of a dual-luciferase reporter system for in vivo visualization of MicroRNA biogenesis and posttranscriptional regulation." J Nucl Med **49**(2): 285-294.

Lee, R. C., R. L. Feinbaum and V. Ambros (1993). "The C. elegans heterochronic gene lin-4 encodes small RNAs with antisense complementarity to lin-14." Cell **75**(5): 843-854.

Lee, Y., C. Ahn, J. Han, H. Choi, J. Kim, J. Yim, J. Lee, P. Provost, O. Radmark, S. Kim and V. N. Kim (2003). "The nuclear RNase III Drosha initiates microRNA processing." Nature **425**(6956): 415-419.

Lee, Y., K. Jeon, J. T. Lee, S. Kim and V. N. Kim (2002). "MicroRNA maturation: stepwise processing and subcellular localization." Embo j **21**(17): 4663-4670.

Lee, Y., M. Kim, J. Han, K. H. Yeom, S. Lee, S. H. Baek and V. N. Kim (2004). "MicroRNA genes are transcribed by RNA polymerase II." Embo j **23**(20): 4051-4060.

Lee, Y., R. C. Samaco, J. R. Gatchel, C. Thaller, H. T. Orr and H. Y. Zoghbi (2008). "miR-19, miR-101 and miR-130 co-regulate ATXN1 levels to potentially modulate SCA1 pathogenesis." Nature neuroscience **11**: 1137-1139.

Lewis, B. P., C. B. Burge and D. P. Bartel (2005). "Conserved seed pairing, often flanked by adenosines, indicates that thousands of human genes are microRNA targets." Cell **120**(1): 15-20.

Lewis, B. P., I. H. Shih, M. W. Jones-Rhoades, D. P. Bartel and C. B. Burge (2003). "Prediction of mammalian microRNA targets." Cell **115**(7): 787-798.

Li, F., T. Macfarlan, R. N. Pittman and D. Chakravarti (2002). "Ataxin-3 is a histone-binding protein with two independent transcriptional corepressor activities." Journal of Biological Chemistry **277**: 45004-45012.

Lima, L. and P. Coutinho (1980). "Clinical criteria for diagnosis of Machado-Joseph disease: report of a non-Azorena Portuguese family." Neurology **30**(3): 319-322.

Liu, C. G., G. A. Calin, S. Volinia and C. M. Croce (2008). "MicroRNA expression profiling using microarrays." Nat Protoc **3**(4): 563-578.

Liu, L. and R. M. Murphy (2006). "Kinetics of inhibition of beta-amyloid aggregation by transthyretin." Biochemistry **45**(51): 15702-15709.

Liu, T., W. Im, I. Mook-Jung and M. Kim (2015). "MicroRNA-124 slows down the progression of Huntington's disease by promoting neurogenesis in the striatum." Neural regeneration research **10**: 786-791.

Liu, Y., X. Ye, F. Jiang, C. Liang, D. Chen, J. Peng, L. N. Kinch, N. V. Grishin and Q. Liu (2009). "C3PO, an endoribonuclease that promotes RNAi by facilitating RISC activation." Science **325**(5941): 750-753.

Llave, C., Z. Xie, K. D. Kasschau and J. C. Carrington (2002). "Cleavage of Scarecrow-like mRNA targets directed by a class of Arabidopsis miRNA." Science **297**(5589): 2053-2056.

Ludwig, N., P. Leidinger, K. Becker, C. Backes, T. Fehlmann, C. Pallasch, S. Rheinheimer, B. Meder, C. Stahler, E. Meese and A. Keller (2016). "Distribution of miRNA expression across human tissues." Nucleic acids research **44**: 3865-3877.

Lund, E., S. Guttinger, A. Calado, J. E. Dahlberg and U. Kutay (2004). "Nuclear export of microRNA precursors." Science **303**(5654): 95-98.

Lytle, J. R., T. A. Yario and J. A. Steitz (2007). "Target mRNAs are repressed as efficiently by microRNA-binding sites in the 5' UTR as in the 3' UTR." Proc Natl Acad Sci U S A **104**(23): 9667-9672.

Maciel, P., M. C. Costa, A. Ferro, M. Rousseau, C. S. Santos, C. Gaspar, J. Barros, G. A. Rouleau, P. Coutinho and J. Sequeiros (2001). "Improvement in the molecular diagnosis of Machado-Joseph disease." Arch Neurol **58**(11): 1821-1827.

Mangiarini, L., K. Sathasivam, M. Seller, B. Cozens, A. Harper, C. Hetherington, M. Lawton, Y. Trottier, H. Lehrach, S. W. Davies and G. P. Bates (1996). "Exon 1 of the HD gene with an expanded CAG repeat is sufficient to cause a progressive neurological phenotype in transgenic mice." Cell **87**: 493-506.

Marioni, J. C., C. E. Mason, S. M. Mane, M. Stephens and Y. Gilad (2008). "RNA-seq: an assessment of technical reproducibility and comparison with gene expression arrays." Genome Res **18**(9): 1509-1517.

Marsh, J. L., T. Lukacsovich and L. M. Thompson (2009). "Animal models of polyglutamine diseases and therapeutic approaches." J Biol Chem **284**(12): 7431-7435.

McNabb, D. S., R. Reed and R. A. Marciniak (2005). "Dual luciferase assay system for rapid assessment of gene expression in Saccharomyces cerevisiae." Eukaryot Cell **4**(9): 1539-1549.

Meister, G., M. Landthaler, Y. Dorsett and T. Tuschl (2004). "Sequence-specific inhibition of microRNA- and siRNA-induced RNA silencing." Rna **10**(3): 544-550.

Miller, V. M., R. F. Nelson, C. M. Gouvion, A. Williams, E. Rodriguez-Lebron, S. Q. Harper, B. L. Davidson, M. R. Rebagliati and H. L. Paulson (2005). "CHIP suppresses polyglutamine aggregation and toxicity in vitro and in vivo." J Neurosci **25**(40): 9152-9161.

Miyata, R., M. Hayashi, N. Tanuma, K. Shioda, R. Fukatsu and S. Mizutani (2008). "Oxidative stress in neurodegeneration in dentatorubral-pallidoluysian atrophy." J Neurol Sci **264**(1-2): 133-139.

Miyazaki, Y., H. Adachi, M. Katsuno, M. Minamiyama, Y.-M. Jiang, Z. Huang, H. Doi, S. Matsumoto, N. Kondo, M. Iida, G. Tohnai, F. Tanaka, S.-i. Muramatsu and G. Sobue (2012). "Viral delivery of miR-196a ameliorates the SBMA phenotype via the silencing of CELF2." Nature medicine **18**: 1136-1141.

Morley J. F., H. R. Brignull, J. J. Weyers and R. I. Morimoto (2002). "The threshold for polyglutamine-expansion protein aggregation and cellular toxicity is dynamic and influenced by aging in Caenorhabditis elegans." Proc Natl Acad Sci U S A **99**(16): 10417-22.

Mortazavi, A., B. A. Williams, K. McCue, L. Schaeffer and B. Wold (2008). "Mapping and quantifying mammalian transcriptomes by RNA-Seq." Nat Methods **5**(7): 621-628.

Muljo, S. A., K. M. Ansel, C. Kanellopoulou, D. M. Livingston, A. Rao and K. Rajewsky (2005). "Aberrant T cell differentiation in the absence of Dicer." J Exp Med **202**(2): 261-269.

Nakano, K. K., D. M. Dawson and A. Spence (1972). "Machado disease. A hereditary ataxia in Portuguese emigrants to Massachusetts." Neurology **22**(1): 49-55.

Nascimento-Ferreira, I., C. Nobrega, A. Vasconcelos-Ferreira, I. Onofre, D. Albuquerque, C. Aveleira, H. Hirai, N. Deglon and L. Pereira de Almeida (2013). "Beclin 1 mitigates motor and neuropathological deficits in genetic mouse models of Machado-Joseph disease." Brain **136**(Pt 7): 2173-2188.

Nascimento-Ferreira, I., T. Santos-Ferreira, L. Sousa-Ferreira, G. Auregan, I. Onofre, S. Alves, N. Dufour, V. F. Colomer Gould, A. Koeppen, N. Deglon and L. Pereira de Almeida (2011). "Overexpression of the autophagic beclin-1 protein clears mutant ataxin-3 and alleviates Machado-Joseph disease." Brain **134**(Pt 5): 1400-1415.

Nunes, A. F., M. J. Saraiva and M. M. Sousa (2006). "Transthyretin knockouts are a new mouse model for increased neuropeptide Y." Faseb j **20**(1): 166-168.

Okamura, K., N. Liu and E. C. Lai (2009). "Distinct mechanisms for microRNA strand selection by *D. melanogaster* Argonautes." Mol Cell **36**(3): 431-444.

Packer, A. N., Y. Xing, S. Q. Harper, L. Jones and B. L. Davidson (2008). "The bifunctional microRNA miR-9/miR-9* regulates REST and CoREST and is downregulated in Huntington's disease." The Journal of neuroscience : the official journal of the Society for Neuroscience **28**: 14341-14346.

Parizotto, E. A., P. Dunoyer, N. Rahm, C. Himber and O. Voinnet (2004). "In vivo investigation of the transcription, processing, endonucleolytic activity, and functional relevance of the spatial distribution of a plant miRNA." Genes Dev **18**(18): 2237-2242.

Paulson, H. L. (2007). Dominantly inherited ataxias: Lessons learned from Machado-Joseph disease/spinocerebellar ataxia type 3. Seminars in Neurology. **27:** 133-142.

Paulson, H. L., M. K. Perez, Y. Trottier, J. Q. Trojanowski, S. H. Subramony, S. S. Das, P. Vig, J. L. Mandel, K. H. Fischbeck and R. N. Pittman (1997). "Intranuclear inclusions of expanded polyglutamine protein in spinocerebellar ataxia type 3." Neuron **19**(2): 333-344.

Perkins, L. A., L. Holderbaum, R. Tao, Y. Hu, R. Sopko, K. McCall, D. Yang-Zhou, I. Flockhart, R. Binari, H. S. Shim, A. Miller, A. Housden, M. Foos, S. Randkelv, C. Kelley, P. Namgyal, C. Villalta, L. P. Liu, X. Jiang, Q. Huan-Huan, X. Wang, A. Fujiyama, A. Toyoda, K. Ayers, A. Blum, B. Czech, R. Neumuller, D. Yan, A. Cavallaro, K. Hibbard, D. Hall, L. Cooley, G. J. Hannon, R. Lehmann, A. Parks, S. E. Mohr, R. Ueda, S. Kondo, J. Q. Ni and N. Perrimon (2015). "The Transgenic RNAi Project at Harvard Medical School: Resources and Validation." Genetics **201**(3): 843-852.

Persengiev, S., I. Kondova, N. Otting, A. H. Koeppen and R. E. Bontrop (2011). "Genome-wide analysis of miRNA expression reveals a potential role for miR-144 in brain aging and spinocerebellar ataxia pathogenesis." Neurobiol Aging **32**(12): 2316.e2317-2327.

Perutz, M. F. (1996). "Glutamine repeats and inherited neurodegenerative diseases: molecular aspects." Curr Opin Struct Biol **6**(6): 848-858.

Qi, H. H., P. P. Ongusaha, J. Myllyharju, D. Cheng, O. Pakkanen, Y. Shi, S. W. Lee, J. Peng and Y. Shi (2008). "Prolyl 4-hydroxylation regulates Argonaute 2 stability." Nature **455**(7211): 421-424.

Ranum, L. P., J. K. Lundgren, L. J. Schut, M. J. Ahrens, S. Perlman, J. Aita, T. D. Bird, C. Gomez and H. T. Orr (1995). "Spinocerebellar ataxia type 1 and Machado-Joseph disease: incidence of CAG expansions among adult-onset ataxia patients from 311 families with dominant, recessive, or sporadic ataxia." Am J Hum Genet **57**(3): 603-608.

Raz, A. and D. S. Goodman (1969). "The interaction of thyroxine with human plasma prealbumin and with the prealbumin-retinol-binding protein complex." J Biol Chem **244**(12): 3230-3237.

Reetz, K., A. S. Costa, S. Mirzazade, A. Lehmann, A. Juzek, M. Rakowicz, R. Boguslawska, L. Schols, C. Linnemann, C. Mariotti, M. Grisoli, A. Durr, B. P. van de Warrenburg, D. Timmann, M. Pandolfo, P. Bauer, H. Jacobi, T.-K. Hauser, T. Klockgether and J. B. Schulz (2013). "Genotype-specific patterns of atrophy progression are more sensitive than clinical decline in SCA1, SCA3 and SCA6." Brain : a journal of neurology **136**: 905-917.

Reinhardt, A., S. Feuillette, M. Cassar, C. Callens, H. Thomassin, S. Birman, M. Lecourtois, C. Antoniewski and H. Tricoire (2012). "Lack of miRNA misregulation at early pathological stages in *D. melanogaster* neurodegenerative disease models." Frontiers in Genetics **3**.

Reinhart, B. J., F. J. Slack, M. Basson, A. E. Pasquinelli, J. C. Bettinger, A. E. Rougvie, H. R. Horvitz and G. Ruvkun (2000). "The 21-nucleotide let-7 RNA regulates developmental timing in Caenorhabditis elegans." Nature **403**(6772): 901-906.

Rhoades, M. W., B. J. Reinhart, L. P. Lim, C. B. Burge, B. Bartel and D. P. Bartel (2002). "Prediction of plant microRNA targets." Cell **110**(4): 513-520.

Ribeiro, C. A., S. M. Oliveira, L. F. Guido, A. Magalhaes, G. Valencia, G. Arsequell, M. J. Saraiva and I. Cardoso (2014). "Transthyretin stabilization by iododiflunisal promotes amyloid-beta peptide clearance, decreases its deposition, and ameliorates cognitive deficits in an Alzheimer's disease mouse model." J Alzheimers Dis **39**(2): 357-370.

Rodriguez-Lebron, E., M. d. C. Costa, K. Luna-Cancalon, T. M. Peron, S. Fischer, R. L. Boudreau, B. L. Davidson and H. L. Paulson (2013). "Silencing mutant ATXN3 expression resolves molecular phenotypes in SCA3 transgenic mice." Molecular therapy : the journal of the American Society of Gene Therapy **21**: 1909-1918.

Rodriguez-Lebron, E., G. Liu, M. Keiser, M. A. Behlke and B. L. Davidson (2013). "Altered Purkinje cell miRNA expression and SCA1 pathogenesis." Neurobiol Dis **54**: 456-463.

Rodriguez-Lebron, E., G. Liu, M. Keiser, M. A. Behlke and B. L. Davidson (2013). "Altered Purkinje cell miRNA expression and SCA1 pathogenesis." Neurobiology of Disease **54**: 456-463.

Rosenberg, R. N., W. L. Nyhan, C. Bay and P. Shore (1976). "Autosomal dominant striatonigral degeneration. A clinical, pathologic, and biochemical study of a new genetic disorder." Neurology **26**(8): 703-714.

Ruano, L., C. Melo, M.C. Silva and P. Coutinho (2014). "The global epidemiology of hereditary ataxia and spastic paraplegia: a systematic review of prevalence studies." Neuroepidemiology **42**: 174-83.

Rubinsztein, D. C., A. Wyttenbach and J. Rankin (1999). "Intracellular inclusions, pathological markers in diseases caused by expanded polyglutamine tracts?" Journal of medical genetics **36**: 265-270.

Ruetschi, U., H. Zetterberg, V. N. Podust, J. Gottfries, S. Li, A. Hviid Simonsen, J. McGuire, M. Karlsson, L. Rymo, H. Davies, L. Minthon and K. Blennow (2005). "Identification of CSF biomarkers for frontotemporal dementia using SELDI-TOF." Exp Neurol **196**(2): 273-281.

Saito, K., A. Ishizuka, H. Siomi and M. C. Siomi (2005). "Processing of pre-microRNAs by the Dicer-1-Loquacious complex in *D. melanogaster* cells." PLoS Biol **3**(7): e235.

Santos, S. D., K. L. Lambertsen, B. H. Clausen, A. Akinc, R. Alvarez, B. Finsen and M. J. Saraiva (2010). "CSF transthyretin neuroprotection in a mouse model of brain ischemia." J Neurochem **115**(6): 1434-1444.

Sasayama, T., M. Nishihara, T. Kondoh, K. Hosoda and E. Kohmura (2009). "MicroRNA-10b is overexpressed in malignant glioma and associated with tumor invasive factors, uPAR and RhoC." International journal of cancer **125**: 1407-1413.

Scherzinger, E., R. Lurz, M. Turmaine, L. Mangiarini, B. Hollenbach, R. Hasenbank, G. P. Bates, S. W. Davies, H. Lehrach and E. E. Wanker (1997). "Huntingtin-encoded polyglutamine expansions form amyloid-like protein aggregates in vitro and in vivo." Cell **90**(3): 549-558.

Schmidt, T., G. B. Landwehrmeyer, I. Schmitt, Y. Trottier, G. Auburger, F. Laccone, T. Klockgether, M. Volpel, J. T. Epplen, L. Schols and O. Riess (1998). "An isoform of ataxin-3 accumulates in the nucleus of neuronal cells in affected brain regions of SCA3 patients." Brain Pathol **8**(4): 669-679.

Schmidt, T., K. S. Lindenberg, A. Krebs, L. Schols, F. Laccone, J. Herms, M. Rechsteiner, O. Riess and G. B. Landwehrmeyer (2002). "Protein surveillance machinery in brains with spinocerebellar ataxia type 3: redistribution and differential recruitment of 26S proteasome subunits and chaperones to neuronal intranuclear inclusions." Ann Neurol **51**(3): 302-310.

Schwarzman, A. L., L. Gregori, M. P. Vitek, S. Lyubski, W. J. Strittmatter, J. J. Enghilde, R. Bhasin, J. Silverman, K. H. Weisgraber, P. K. Coyle and et al. (1994). "Transthyretin sequesters amyloid beta protein and prevents amyloid formation." Proc Natl Acad Sci U S A **91**(18): 8368-8372.

Seibert, F. B. and J. W. Nelson (1942). "ELECTROPHORETIC STUDY OF THE BLOOD PROTEIN RESPONSE IN TUBERCULOSIS." Journal of Biological Chemistry **143**(1): 29-38.

Sekijima, Y., K. Yoshida, T. Tokuda and S. Ikeda (1993). Familial Transthyretin Amyloidosis. GeneReviews(R). R. A. Pagon, M. P. Adam, H. H. Ardinger et al. Seattle (WA).

Shen, J., W. Xia, Y. B. Khotskaya, L. Huo, K. Nakanishi, S. O. Lim, Y. Du, Y. Wang, W. C. Chang, C. H. Chen, J. L. Hsu, Y. Wu, Y. C. Lam, B. P. James, X. Liu, C. G. Liu, D. J. Patel and M. C. Hung (2013). "EGFR modulates microRNA maturation in response to hypoxia through phosphorylation of AGO2." Nature **497**(7449): 383-387.

Shi, Y., F. Huang, B. Tang, J. Li, J. Wang, L. Shen, K. Xia and H. Jiang (2014). "MicroRNA profiling in the serums of SCA3/MJD patients." The International journal of neuroscience **124**: 97-101.

Silveira, I., I. Lopes-Cendes, S. Kish, P. Maciel, C. Gaspar, P. Coutinho, M. I. Botez, H. Teive, W. Arruda, C. E. Steiner, W. Pinto-Junior, J. A. Maciel, S. Jerin, G. Sack, E. Andermann, L. Sudarsky, R. Rosenberg, P. MacLeod, D. Chitayat, R. Babul, J. Sequeiros and G. A. Rouleau (1996). "Frequency of spinocerebellar ataxia type 1, dentatorubropallidoluysian atrophy, and Machado-Joseph disease mutations in a large group of spinocerebellar ataxia patients." Neurology **46**(1): 214-218.

Simoes, A. T., N. Goncalves, A. Koeppen, N. Deglon, S. Kugler, C. B. Duarte and L. Pereira de Almeida (2012). "Calpastatin-mediated inhibition of calpains in the mouse brain prevents mutant ataxin 3 proteolysis, nuclear localization and aggregation, relieving Machado-Joseph disease." Brain : a journal of neurology **135**: 2428-2439.

Simoes, A. T., N. Goncalves, R. J. Nobre, C. B. Duarte and L. Pereira de Almeida (2014). "Calpain inhibition reduces ataxin-3 cleavage alleviating neuropathology and motor impairments in mouse models of Machado-Joseph disease." Hum Mol Genet **23**(18): 4932-4944.

Skinner, P. J., B. T. Koshy, C. J. Cummings, I. A. Klement, K. Helin, A. Servadio, H. Y. Zoghbi and H. T. Orr (1997). "Ataxin-1 with an expanded glutamine tract alters nuclear matrix-associated structures." Nature **389**(6654): 971-974.

Smale, S. T. (2010). "Luciferase Assay." Cold Spring Harbor Protocols **2010**(5): pdb.prot5421.

Sousa, J. C., C. Grandela, J. Fernandez-Ruiz, R. de Miguel, L. de Sousa, A. I. Magalhaes, M. J. Saraiva, N. Sousa and J. A. Palha (2004). "Transthyretin is involved in depression-like behaviour and exploratory activity." J Neurochem **88**(5): 1052-1058.

Sousa, J. C., F. Marques, E. Dias-Ferreira, J. J. Cerqueira, N. Sousa and J. A. Palha (2007). "Transthyretin influences spatial reference memory." Neurobiol Learn Mem **88**(3): 381-385.

Sousa, J. o. C., F. Marques, E. Dias-Ferreira, J. o. J. Cerqueira, N. Sousa and J. A. Palha (2007). "Transthyretin influences spatial reference memory." Neurobiology of Learning and Memory **88**: 381-385.

Steffan, J. S., A. Kazantsev, O. Spasic-Boskovic, M. Greenwald, Y. Z. Zhu, H. Gohler, E. E. Wanker, G. P. Bates, D. E. Housman and L. M. Thompson (2000). "The Huntington's disease protein interacts with p53 and CREB-binding protein and represses

transcription." Proceedings of the National Academy of Sciences of the United States of America **97**: 6763-6768.

Sultan, M., M. H. Schulz, H. Richard, A. Magen, A. Klingenhoff, M. Scherf, M. Seifert, T. Borodina, A. Soldatov, D. Parkhomchuk, D. Schmidt, S. O'Keeffe, S. Haas, M. Vingron, H. Lehrach and M. L. Yaspo (2008). "A global view of gene activity and alternative splicing by deep sequencing of the human transcriptome." Science **321**(5891): 956-960.

Takiyama, Y., M. Nishizawa, H. Tanaka, S. Kawashima, H. Sakamoto, Y. Karube, H. Shimazaki, M. Soutome, K. Endo, S. Ohta and et al. (1993). "The gene for Machado-Joseph disease maps to human chromosome 14q." Nat Genet **4**(3): 300-304.

Tan, J. Y., K. W. Vance, M. A. Varela, T. Sirey, L. M. Watson, H. J. Curtis, M. Marinello, S. Alves, B. R. Steinkraus, S. Cooper, T. Nesterova, N. Brockdorff, T. A. Fulga, A. Brice, A. Sittler, P. L. Oliver, M. J. Wood, C. P. Ponting and A. C. Marques (2014). "Cross-talking noncoding RNAs contribute to cell-specific neurodegeneration in SCA7." Nature structural & molecular biology **21**: 955-961.

Tang, G., B. J. Reinhart, D. P. Bartel and P. D. Zamore (2003). "A biochemical framework for RNA silencing in plants." Genes Dev **17**(1): 49-63.

Teplyuk, N. M., E. J. Uhlmann, G. Gabriely, N. Volfovsky, Y. Wang, J. Teng, P. Karmali, E. Marcusson, M. Peter, A. Mohan, Y. Kraytsberg, R. Cialic, E. A. Chiocca, J. Godlewski, B. Tannous and A. M. Krichevsky (2016). "Therapeutic potential of targeting microRNA-10b in established intracranial glioblastoma: first steps toward the clinic." EMBO Mol Med **8**(3): 268-287.

Thorsen, S. B., S. Obad, N. F. Jensen, J. Stenvang and S. Kauppinen (2012). "The therapeutic potential of microRNAs in cancer." Cancer J **18**(3): 275-284.

Torashima, T., C. Koyama, A. Iizuka, K. Mitsumura, K. Takayama, S. Yanagi, M. Oue, H. Yamaguchi and H. Hirai (2008). "Lentivector-mediated rescue from cerebellar ataxia in a mouse model of spinocerebellar ataxia." EMBO reports **9**: 393-399.

Trottier, Y., Y. Lutz, G. Stevanin, G. Imbert, D. Devys, G. Cancel, F. Saudou, C. Weber, G. David, L. Tora and et al. (1995). "Polyglutamine expansion as a pathological epitope in Huntington's disease and four dominant cerebellar ataxias." Nature **378**(6555): 403-406.

Tsai, N. P., Y. L. Lin and L. N. Wei (2009). "MicroRNA mir-346 targets the 5'-untranslated region of receptor-interacting protein 140 (RIP140) mRNA and up-regulates its protein expression." Biochem J **424**(3): 411-418.

van de Warrenburg, B. P. C., R. J. Sinke, C. C. Verschuuren-Bemelmans, H. Scheffer, E. R. Brunt, P. F. Ippel, J. A. Maat-Kievit, D. Dooijes, N. C. Notermans, D. Lindhout, N. V. A. M. Knoers and H. P. H. Kremer (2002). "Spinocerebellar ataxias in the Netherlands: prevalence and age at onset variance analysis." Neurology **58**: 702-708.

van Rooij, E. and S. Kauppinen (2014). "Development of microRNA therapeutics is coming of age." EMBO Mol Med **6**(7): 851-864.

Varkonyi-Gasic, E., R. Wu, M. Wood, E. F. Walton and R. P. Hellens (2007). "Protocol: a highly sensitive RT-PCR method for detection and quantification of microRNAs." Plant Methods **3**: 12.

Voinnet, O. (2009). "Origin, biogenesis, and activity of plant microRNAs." Cell **136**(4): 669-687.

Wati, H., T. Kawarabayashi, E. Matsubara, A. Kasai, T. Hirasawa, T. Kubota, Y. Harigaya, M. Shoji and S. Maeda (2009). "Transthyretin accelerates vascular Abeta deposition in a mouse model of Alzheimer's disease." Brain Pathol **19**(1): 48-57.

Wellington, C. L., L. M. Ellerby, A. S. Hackam, R. L. Margolis, M. A. Trifiro, R. Singaraja, K. McCutcheon, G. S. Salvesen, S. S. Propp, M. Bromm, K. J. Rowland, T. Zhang, D. Rasper, S. Roy, N. Thornberry, L. Pinsky, A. Kakizuka, C. A. Ross, D. W. Nicholson, D. E. Bredesen and M. R. Hayden (1998). "Caspase cleavage of gene products associated with triplet expansion disorders generates truncated fragments containing the polyglutamine tract." J Biol Chem **273**(15): 9158-9167.

Wienholds, E., M. J. Koudijs, F. J. van Eeden, E. Cuppen and R. H. Plasterk (2003). "The microRNA-producing enzyme Dicer1 is essential for zebrafish development." Nat Genet **35**(3): 217-218.

Winborn, B. J., S. M. Travis, S. V. Todi, K. M. Scaglione, P. Xu, A. J. Williams, R. E. Cohen, J. Peng and H. L. Paulson (2008). "The deubiquitinating enzyme ataxin-3, a polyglutamine disease protein, edits Lys63 linkages in mixed linkage ubiquitin chains." Journal of Biological Chemistry **283**: 26436-26443.

Wu, C., J. So, B. N. Davis-Dusenbery, H. H. Qi, D. B. Bloch, Y. Shi, G. Lagna and A. Hata (2011). "Hypoxia potentiates microRNA-mediated gene silencing through posttranslational modification of Argonaute2." Mol Cell Biol **31**(23): 4760-4774.

Xie, X., J. Lu, E. J. Kulbokas, T. R. Golub, V. Mootha, K. Lindblad-Toh, E. S. Lander and M. Kellis (2005). "Systematic discovery of regulatory motifs in human promoters and 3' UTRs by comparison of several mammals." Nature **434**(7031): 338-345.

Yamada, M., T. Sato, S. Tsuji and H. Takahashi (2008). CAG repeat disorder models and human neuropathology: Similarities and differences. Acta Neuropathologica. **115:** 71-86.

Yamada, M., C. F. Tan, C. Inenaga, S. Tsuji and H. Takahashi (2004). "Sharing of polyglutamine localization by the neuronal nucleus and cytoplasm in CAG-repeat diseases." Neuropathol Appl Neurobiol **30**(6): 665-675.

Yekta, S., I. H. Shih and D. P. Bartel (2004). "MicroRNA-directed cleavage of HOXB8 mRNA." Science **304**(5670): 594-596.

Yi, J., L. Zhang, B. Tang, W. Han, Y. Zhou, Z. Chen, D. Jia and H. Jiang (2013). "Sodium valproate alleviates neurodegeneration in SCA3/MJD via suppressing apoptosis and rescuing the hypoacetylation levels of histone H3 and H4." PloS one **8**: e54792.

Yi, R., Y. Qin, I. G. Macara and B. R. Cullen (2003). "Exportin-5 mediates the nuclear export of pre-microRNAs and short hairpin RNAs." Genes Dev **17**(24): 3011-3016.

Yoda, M., T. Kawamata, Z. Paroo, X. Ye, S. Iwasaki, Q. Liu and Y. Tomari (2010). "ATP-dependent human RISC assembly pathways." Nat Struct Mol Biol **17**(1): 17-23.

Yoo, S. Y., M. E. Pennesi, E. J. Weeber, B. Xu, R. Atkinson, S. Chen, D. L. Armstrong, S. M. Wu, J. D. Sweatt and H. Y. Zoghbi (2003). "SCA7 knockin mice model human SCA7 and reveal gradual accumulation of mutant ataxin-7 in neurons and abnormalities in short-term plasticity." Neuron **37**(3): 383-401.

Yu, Y.-C., C.-L. Kuo, W.-L. Cheng, C.-S. Liu and M. Hsieh (2009). "Decreased antioxidant enzyme activity and increased mitochondrial DNA damage in cellular models of Machado-Joseph disease." Journal of neuroscience research **87**: 1884-1891.

Yuasa, T., E. Ohama, H. Harayama, M. Yamada, Y. Kawase, M. Wakabayashi, T. Atsumi and T. Miyatake (1986). "Joseph's disease: clinical and pathological studies in a Japanese family." Ann Neurol **19**(2): 152-157.

Yue, D., H. Liu and Y. Huang (2009). "Survey of Computational Algorithms for MicroRNA Target Prediction." Curr Genomics **10**(7): 478-492.

Zeng, Y. and B. R. Cullen (2004). "Structural requirements for pre-microRNA binding and nuclear export by Exportin 5." Nucleic Acids Res **32**(16): 4776-4785.

Zeng, Y., H. Sankala, X. Zhang and P. R. Graves (2008). "Phosphorylation of Argonaute 2 at serine-387 facilitates its localization to processing bodies." Biochem J **413**(3): 429-436.

Zhang, H. L., X. M. Zhang, X. J. Mao, H. Deng, H. F. Li, R. Press, S. Fredrikson and J. Zhu (2012). "Altered cerebrospinal fluid index of prealbumin, fibrinogen, and haptoglobin in patients with Guillain-Barre syndrome and chronic inflammatory demyelinating polyneuropathy." Acta Neurol Scand **125**(2): 129-135.

Zoghbi, H. Y. (2000). "Spinocerebellar ataxias." Neurobiology of disease **7**: 523-527.